X–ray follow–up work on a set of unassociated sources listed in the Palermo *Swift*/BAT 150–month catalogue

Raffaella Landi & Loredana Bassani

(INAF – OAS Bologna)

Introduction

In the following, we provide a report on a preliminary study aimed at searching the X–ray counterpart to a set of still unassociated sources listed as "PBC_NEW" objects in the Palermo *Swift*/BAT 150–month catalogue (available at: `https://science.clemson.edu/ctagn/bat-150-month-catalog/`). By exploiting the capability of the X–ray telescope (XRT, 0.2–10 keV) onboard the Neil Gehrels *Swift* Observatory (Gehrels et al. 2004) to localise the sources with a positional accuracy of few arcseconds, the search for optical/UV, infrared, and radio counterparts is more efficient and reliable. Each source is discussed in a dedicated section in which we report the log of the XRT observations, the likely counterparts detected, their spectral behaviour, and their multi–wavelength properties.

The *Swift*/BAT sources discussed in this report are the following:

- PBC_NEW_027
- PBC_NEW_040
- PBC_NEW_049
- PBC_NEW_081
- PBC_NEW_138
- PBC_NEW_157
- PBC_NEW_175
- PBC_NEW_176
- PBC_NEW_183
- PBC_NEW_186
- PBC_NEW_187
- PBC_NEW_199
- PBC_NEW_212
- PBC_NEW_215
- PBC_NEW_221
- PBC_NEW_229
- PBC_NEW_230
- PBC_NEW_237
- PBC_NEW_238
- PBC_NEW_246

- PBC_NEW_250
- PBC_NEW_257
- PBC_NEW_263
- PBC_NEW_266
- PBC_NEW_269
- PBC_NEW_277
- PBC_NEW_287
- PBC_NEW_306
- PBC_NEW_320
- PBC_NEW_330
- PBC_NEW_342

Swift/XRT data reduction and analysis

XRT data reduction was performed using the standard data pipeline package (*xrtpipeline* v. 0.13.7), in order to produce screened event files. All data were extracted only in the Photon Counting (PC) mode (Hill et al. 2004), adopting the standard grade filtering (0–12 for PC) according to the XRT nomenclature.
We then, in case of multiple observations, summed together all the available XRT pointings using *XSELECT* v. 2.5c to enhance the signal–to–noise ratio and thus facilitate the detection of candidate counterparts. As a following step, we analysed the XRT images in the 0.3–10 keV energy band by means of *XIMAGE* v. 4.5.1 in search of X–ray detections within or nearby the 95% BAT error circles. The position of the brightest X–ray detections were estimated by using the task *xrtcentroid* v. 0.2.9; for weaker sources we made use of the *XIMAGE* command *detect*. In the XRT images, the black circles depict the 95% BAT positional uncertainties as reported in the 150–month Palermo *Swift*/BAT catalogue. The black–dotted circles represent instead the 90% positional uncertainty of the BAT source as reported in the 157–month catalogue (Lien et al. 2025), while the black ellipse depicts the 95% positional uncertainty of the *Fermi* source as listed in the *Fermi*/LAT DR4 Catalogue (Ballet et al. 2024; Abdollahi et al. 2022).
To visualise better the X–ray counterparts, we smoothed the images. Therefore, the presence of grains and/or features inside the XRT field of view is undoubtedly spurious; in some cases the poor quality of the XRT images is due to the low exposure.
Source events were extracted from the corresponding event file within a circular region with a radius of 20 pixels (1 pixel corresponding to 2.36 arcseconds) centred on the source position, while background events were extracted from a source–free region close to the X–ray source of interest. Then, the source spectra were extracted using the *XSELECT* v. 2.4m software and generally binned using *grppha* to 20 counts per energy bin so that the χ^2 statistic could be applied. For sources with fewer counts (typically lower than 50), data were binned to 1 count per energy bin and the Cash statistic (Cash 1979) was adopted. We used version v. 016 of the response matrices and created individual ancillary response files arf using *xrtmkarf* v. 0.6.4. The spectral analysis was performed using *XSPEC* v. 12.15.0d.

In the first instance, we adopted a basic model consisting of a simple power law passing through Galactic absorption in the source direction (Kalberla et al. 2005). If this baseline model was not adequate to fit the data, we then introduced extra spectral components as required.

The multi–wavelength properties of the objects analysed in this work were collected by exploiting various catalogues and databases reported in the following list:

- The United States Naval Observatory B–1.0 Catalogue (USNO B–1.0, Monet et al. 2003);
- The United States Naval Observatory A–2.0 Catalogue (USNO A–2.0, Monet 1998);
- The Two Micron All–Sky Survey (2MASS, Skrutskie et al. 2006);
- The Two Micron All–Sky Survey Extended Source Survey (2MASX, Skrutskie et al. 2006);
- The Third *Gaia* Data Release, *Gaia* EDR3 (Gaia Collaboration 2021);
- The Wide–field Infrared Survey Explorer (WISE, Wright et al. 2010);
- The AllWISE Source Catalogue (Cutri et al. 2013);
- The DEep Near Infrared Survey of the Southern Sky (DENIS, Epchtein et al. 1994);
- The Galaxy Evolution Explorer All–Sky Survey (GALEX, Bianchi et al. (2011);
- The Sloan Digital Sky Survey (SDSS) DR9 (Ahn et al. 2012);
- The Six–degree Field Galaxy Survey (6dFGS, Jones et al. 2009);
- The Dark Energy Spectroscopic Instrument (DESI) Legacy Imaging Survey (Dey et al. 2019);
- The Dark Energy Spectroscopic Instrument (DESI) Legacy Imaging Surveys DR8 photometric redshifts (Duncan 2022);
- The Beijing–Arizona Sky Survey (BASS, Zou et al. 2017);
- The Dark Energy Camera Plane Survey (DECaPS, Schlafly et al. 2018);
- The Panoramic Survey Telescope and Rapid Response System (Pan–STARRS, Chambers et al. 2016);
- The *XMM–Newton* Slew Survey Full Source Catalogue (XMMSL1, Saxton et al. 2008 and relative updates);
- The Specktr–RG (SRG)/*eROSITA* All–Sky Survey (eRASS1) (Merloni et al. 2024);
- The *ROSAT* All–Sky Survey Bright/Faint Source Catalogues (Voges et al. 1999);
- The Second *ROSAT* All–Sky Survey Source Catalogue (Boller et al. 2016);
- The SRG/ART–XC All–Sky X–ray Survey Catalogue (Sazonov et al. 2024);
- The SPECFIND V3.0 Catalogue of radio continuum spectra (Stein et al. 2021);

- The National Radio Astronomy Observatory (NRAO) Very Large Array (VLA) Sky Survey (NVSS, Condon et al. 1998);
- The Very Large Array (VLA) Faint Images of the Radio Sky at Twenty–centimeters (FIRST) Survey (Helfand et al. 2015);
- The Giant Metrewave Radio Telescope All–Sky 150 MHz Radio Source Catalogue (Intema et al. 2017);
- The Rapid Australian SKA Pathfinder (ASKAP) Continuum Survey (RACS). V. RACS–mid 1367.5 MHz Catalogue (Duchesne et al. 2024);
- The Rapid Australian SKA Pathfinder (ASKAP) Continuum Survey (RACS). VI. RACS–high 1655.5 MHz Catalogue (Duchesne et al. 2025);
- The LOFAR Two–metre Sky Survey (LoTSS) DR2 (Shimwell et al. 2022);
- The Karl G. Jansky Very Large Array Sky Survey (VLASS, Lacy et al. 2020);
- The Very Large Array Sky Survey (VLASS) QL Ep.1 Catalogue, CIRADA version (Gordon et al. 2021);
- The GaLactic and Extragalactic All–Sky Murchison Widefield Array eXtended (GLEAM–X, Ross et al. 2024);
- The NASA/IPAC Extra Database (NED), available at: `https://ned.ipac.caltech.edu/`;
- The VizieR Catalogue Service, available at: `https://vizier.cds.unistra.fr/viz-bin/VizieR`;
- The High–Energy Astrophysics Science Archive Research Center provided by NASA's Goddard Space Flight Center (HEASARC), available at: `http://heasarc.gsfc.nasa.gov/`;
- The SIMBAD Astronomical Database, available at: `http://simbad.u-strasbg.fr/simbad/`.

The method we adopted to pinpoint the unidentified sources that are likely to be Active Galactic Nuclei (AGNs) is based on diagnostic indicators such as *WISE* colours, radio emission, and indication of extension in the optical images (see details in Malizia et al. 2023).

PBC_NEW_027

Source position:

- R.A.(J2000) = $19^h17^m13'.72$
- Dec.(J2000) = $-28°35'22''.70$
- Positional uncertainty = $5'.5059$

One XRT observation available:

1. obscode: 00096610001
   observation date: 17/05/2022
   exposure: 2069 s

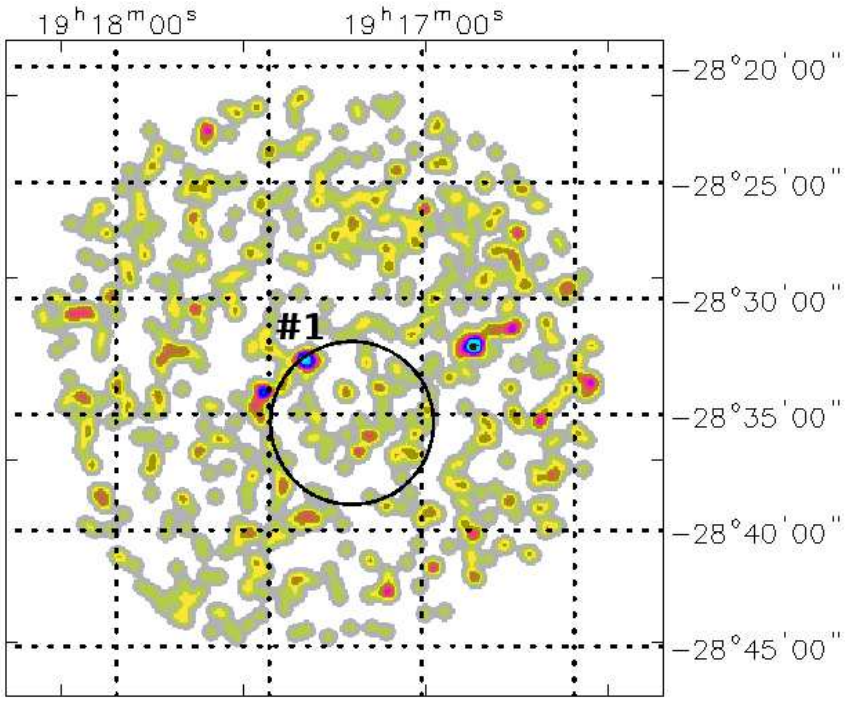

Figure 1: 0.3–10 keV XRT image of the PBC_NEW_027 field.

XRT detects only one source, whose position is compatible with the BAT positional uncertainty (see Figure 1), which is located at:

R.A.(J2000) = $19^h17^m22'.80$

Dec.(J2000) = $-28^\circ 32' 38''.50$

error box = $6''.00$

It is detected at 3.2σ c.l. in the 0.3–10 keV energy band and is not visible above 3 keV.

Multi–wavelength counterparts to this XRT detection:

- AllWISE J191723.06–283237.2 with magnitudes $W1 = (15.254 \pm 0.037)$, $W2 = (14.049 \pm 0.049)$, $W3 = (11.495 \pm 0.262)$, $W4 = (8.271 \pm 0.000)$, and colours ($W1 - W2 = 1.205$, $W2 - W3 = 2.554$) typical of an AGN candidate;
- GALEX J191723.0–283238 with magnitude $NUV = (20.986 \pm 0.272)$;
- TGSSADR J191723.1–283238 with flux density $S(150\ \mathrm{MHz}) = (2522.4 \pm 252.9)$ mJy;
- RACS–MID J191723.1–283235 with flux Ftot(1367.5 MHz) = 350 mJy;
- RACS–HIGH J191723–28323 with flux Ftot(1655.5 MHz) = 330 mJy.

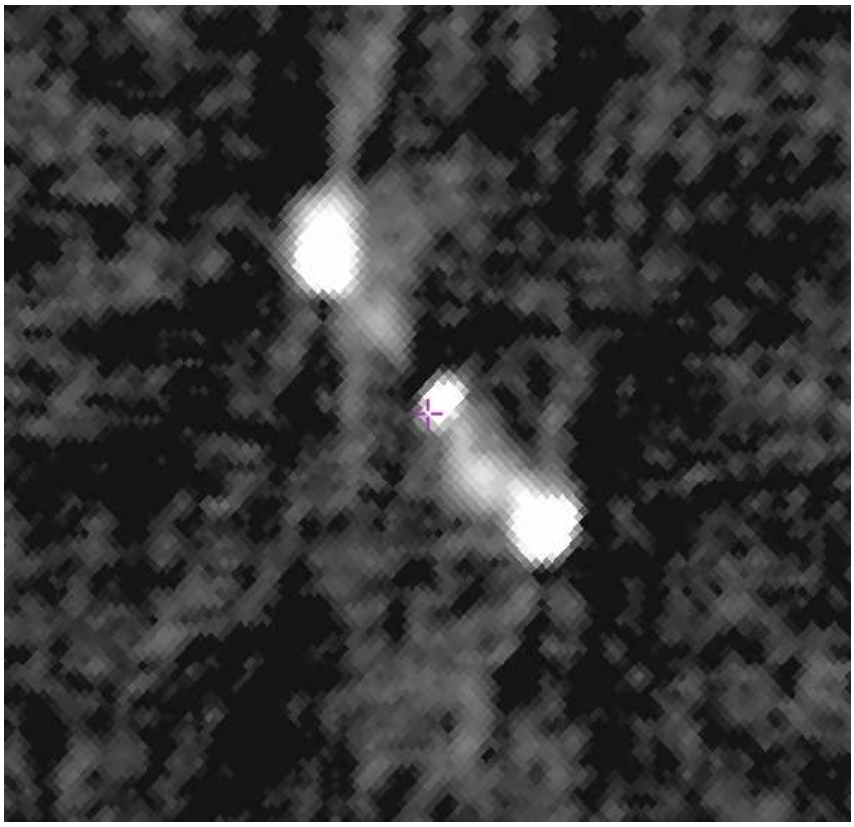

Figure 2: Radio image of source #1 from VLASS.

The fit with a power law passing through Galactic absorption ($N_{\mathrm{H(Gal)}} = 8.55 \times 10^{20}$ cm^{-2}) yields a photon index $\Gamma = \left(2.05^{+1.28}_{-1.60}\right)$ and a 2–10 keV flux of $\sim$1.76 $\times$ 10^{-13} erg cm^{-2} s^{-1}.

The source is radio extended (see Figure 2 from VLASS), is polarised in radio (Farnes et al. 2014), and is also variable when comparing NVSS and FIRST data sets (Ofek et al. 2011). The radio spectral index is –0.8 from the SPECFIND V3.0 Catalogue.

We conclude that the source is a radio galaxy with an active nucleus at the centre and, as such, a likely counterpart to the BAT object.

PBC_NEW_040

Source position:

- R.A.(J2000) = $21^{\mathrm{h}}59^{\mathrm{m}}10'.90$
- Dec.(J2000) = $-54^{\circ}53'21''.80$
- Positional uncertainty = $3'.898$

Seven XRT observations available:

1. obscode: 00096611001
   observation date: 27/06/2022
   exposure: 1635 s
2. obscode: 03111995001
   observation date: 20/03/2023
   exposure: 4794 s
3. obscode: 03111995003
   observation date: 04/05/2023
   exposure: 251 s
4. obscode: 03111995005
   observation date: 03/07/2023
   exposure: 572 s
5. obscode: 03111995007
   observation date: 10/08/2023
   exposure: 60 s
6. obscode: 03111995009
   observation date: 12/08/2023
   exposure: 1165 s
7. obscode: 03111995011
   observation date: 13/08/2023
   exposure: 1885 s

This source is also listed in the *Swift*/BAT 157–month catalogue as SWIFT J2159.3–5455, whose coordinates are:

- R.A.(J2000) = $21^{\mathrm{h}}59^{\mathrm{m}}20'.64$
- Dec.(J2000) = $-54^{\circ}55'29''.30$

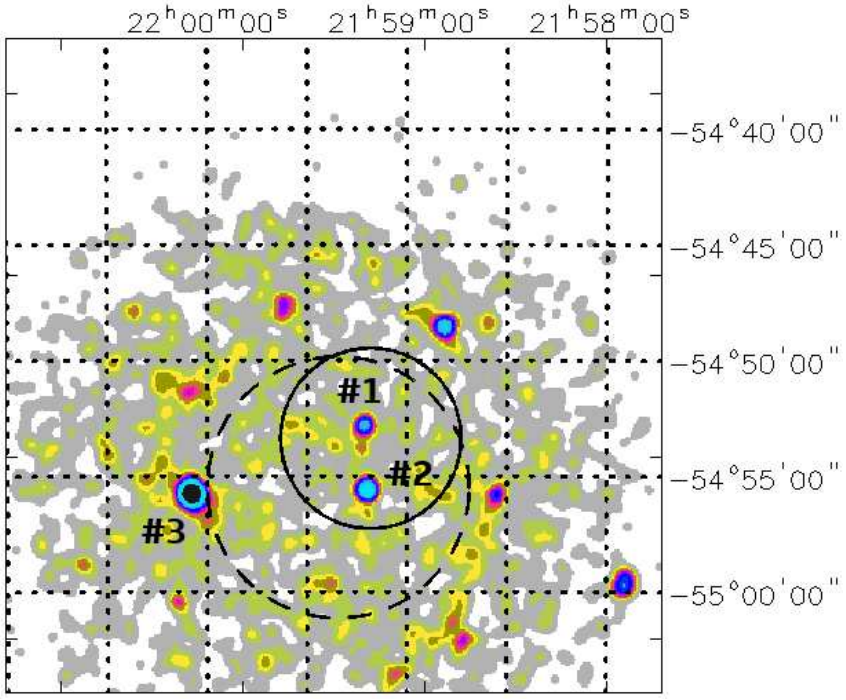

Figure 3: 0.3–10 keV XRT image of the PBC_NEW_040 field.

- Positional uncertainty = 5′.65

It is associated with 2MASS J22000495–5455445, classified as a BL Lac (source #3 in Figure 3), which is located at:

R.A.(J2000) = $22^{\rm h}00^{\rm m}04'.70$

Dec.(J2000) = $-54^{\circ}55'44''.42$

error box = $3''.73$

It is detected at 17.7σ c.l. in the 0.3–10 keV energy band and at 6.7σ c.l. above 3 keV.

The source X–ray spectrum is well modelled with a simple power law ($N_{\rm H(Gal)} = 1.94 \times 10^{20}$ cm^{-2}) having a photon index $\Gamma = (1.69 \pm 0.15)$ and a 2–10 keV flux of $\sim 1.2 \times 10^{-12}$ erg cm^{-2} s^{-1}.

However, XRT detects other two X–ray sources within the positional uncertainties of both PBC_NEW_040 and SWIFT J2159.3–5455 (see Figure 3):

➢ Source #1 is located at:

R.A.(J2000) = $21^{\rm h}59^{\rm m}12'.79$

Dec.(J2000) = $-54^{\circ}52'48''.58$

error box = $4''.67$

It is detected at 5.8σ c.l. in the 0.3–10 keV energy band and at 5.4σ c.l. above 3 keV.

Multi–wavelength counterparts to this XRT detection:

- USNO–A2.0 0300–37448642 with magnitudes $B = 17.7$ and $R = 16.1$;
- 2MASS J21591299–5452461 with magnitudes $J = (16.090 \pm 0.000)$, $H = (15.161 \pm 0.000)$, and $K = (15.026 \pm 0.158)$;
- AllWISE J215912.99–545246.2 with magnitudes $W1 = (14.152 \pm 0.037)$, $W2 = (13.251 \pm 0.034)$, $W3 = (10.233 \pm 0.105)$, $W4 = (7.317 \pm 0.213)$, and colours ($W1 - W2 = 0.901$, $W2 - W3 = 3.018$) typical of an AGN;
- *Gaia* source 6413085707138052992 with magnitudes $G = (20.754 \pm 0.014)$, $BP = (19.505 \pm 0.036)$, and $RP = (18.098 \pm 0.021)$
  ($BP - RP = 1.407$);
- RACS–MID J215913.1–545246 with flux Ftot(1367.5 MHz) = 1.22 mJy.

By modelling the source spectrum with a power law passing through Galactic absorption ($N_{\rm H(Gal)} = 2.01 \times 10^{20}$ cm^{-2}), we find a photon index $\Gamma = \left(1.57^{+0.40}_{-0.48}\right)$ and a 2–10 keV flux of $\sim 1.9 \times 10^{-13}$ erg cm^{-2} s^{-1}.

This source is most likely an AGN/QSO (quasi–stellar object) candidate due to its *AllWISE* colours and radio detection.

➢ Source #2 is located at:

R.A.(J2000) = $21^{\rm h}59^{\rm m}11'.98$

Dec.(J2000) = $-54^\circ 55' 33''.52$

error box = $4''.80$

It is detected at 8.6σ c.l. in the 0.3–10 keV energy range and at 2.7σ c.l. above 3 keV.

Multi–wavelength counterparts to this XRT detection:

- USNO–A2.0 0300–37448543 with magnitudes $B = 17.80$ and $R = 17.90$;
- AllWISE J215912.13–545535.4 with magnitudes $W1 = (14.480 \pm 0.029)$, $W2 = (13.507 \pm 0.031)$, $W3 = (10.975 \pm 0.184)$, $W4 = (8.103 \pm 0.000)$, and colours ($W1 - W2 = 0.973$, $W2 - W3 = 2.532$) as expected from an AGN candidate;
- *Gaia* source 6413085462323877376 with magnitudes $G = (18.339 \pm 0.004)$, $BP = (18.421 \pm 0.018)$, and $RP = (18.066 \pm 0.017)$
  ($BP - RP = 0.356$);

- 1eRASS J215912.3–545533 with flux F(0.2–2.3 keV) $\sim 2.9 \times 10^{-13}$ erg cm^{-2} s^{-1}.

  Also in this case a power law passing through Galactic absorption ($N_{\mathrm{H(Gal)}} = 1.99 \times 10^{20}$ cm^{-2}), with a photon index $\Gamma = \left(2.10^{+0.39}_{-0.40}\right)$ and a 2–10 keV flux of $\sim 1.7 \times 10^{-13}$ erg cm^{-2} s^{-1}, provides a good fit to the data.

  Also this source is most likely a QSO candidate at redshift $z = 0.54$ due its IR colours and *Gaia* properties (Wu et al. 2023; Flesch 2024).

The BL Lac is most likely the best association with PBC_NEW_040, although we notice that object #1 is quite hard in X–rays, making it a potential contender at higher energies.

PBC_NEW_049

Source position:

- R.A.(J2000) = $03^{h}29^{m}03'.83$
- Dec.(J2000) = $+40°46'24''.60$
- Positional uncertainty = $3'.8716$

One XRT observation available:

1. obscode: 00096615001
   observation date: 20/09/2022
   exposure: 1630 s

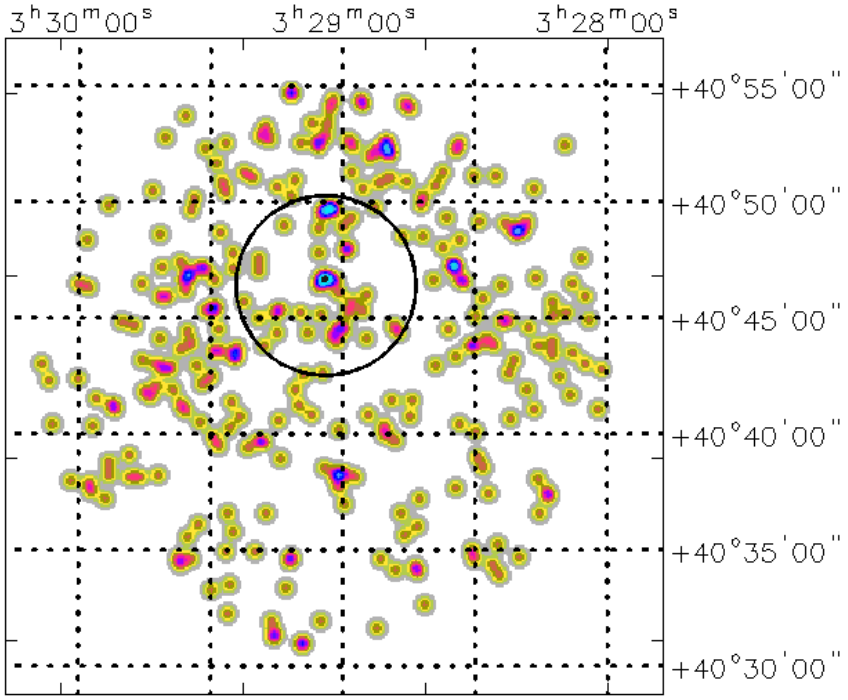

Figure 4: 0.3–10 keV XRT image of the PBC_NEW_049 field.

No X–ray counterpart is detected by XRT in the region surrounding PBC_NEW_049, as shown in Figure 4.

However, from the multi–band archival data, we find that inside the BAT error circle there is an X–ray source (2RXS J032905.9+404650) belonging to the Second *ROSAT* All–Sky Survey Source

Catalogue, which is located at:

R.A.(J2000) = $03^{\rm h}29^{\rm m}05'.96$

Dec.(J2000) = $+40^{\circ}46'50''.45$

It is detected at 2.4σ c.l. in the 0.1–2.4 keV energy range; the flux F(0.2–2.4 keV) is $\sim 4.6 \times 10^{-13}$ erg cm^{-2} s^{-1}.

This source has not been optically classified yet.

PBC_NEW_081

Source position:

- R.A.(J2000) = $15^{\rm h}04^{\rm m}57'.40$
- Dec.(J2000) = $+37^{\circ}12'18''.40$
- Positional uncertainty = $3'.9774$

Four XRT observations available:

1. obscode: 03109614001
   observation date: 23/03/2019
   exposure: 562 s
2. obscode: 03109614003
   observation date: 19/04/2019
   exposure: 2410 s
3. obscode: 03109614004
   observation date: 22/04/2019
   exposure: 191 s
4. obscode: 03109614005
   observation date: 24/04/2019
   exposure: 1444 s

XRT detects two X–ray sources whose positions are compatible with the BAT positional uncertainty (see Figure 5):

➢ Source #1 is located at:

R.A.(J2000) = $15^{\rm h}05^{\rm m}01'.48$

Dec.(J2000) = $+37^{\circ}13'13''.18$

error box = $5''.05$

It is detected at 5.5σ c.l. in the 0.3–10 keV energy band and at 4.4σ c.l. above 3 keV.

Multi–wavelength counterparts to this XRT detection:

- USNO–A2.0 1200–07458734 with magnitudes $B = 16.9$ and $R = 15.4$;

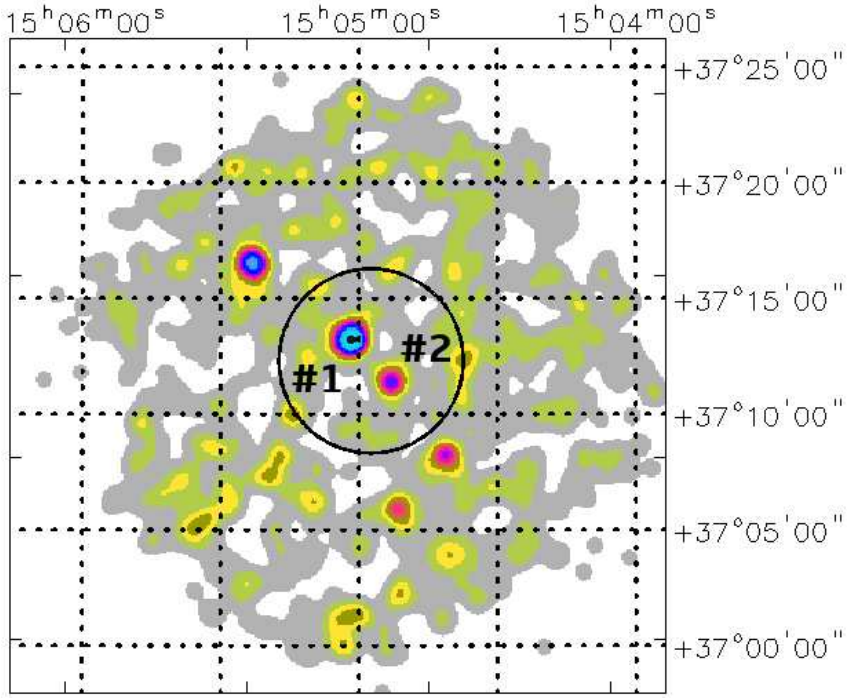

Figure 5: 0.3–10 keV XRT image of the PBC_NEW_081 field.

- 2MASS J15050155+3713115 with magnitudes $J = (14.596 \pm 0.040)$, $H = (13.803 \pm 0.043)$, and $K = (13.247 \pm 0.041)$;
- 2MASX J15050154+3713112 with magnitudes $J = (14.233 \pm 0.075)$, $H = (13.419 \pm 0.080)$, and $K = (13.005 \pm 0.102)$;
- AllWISE J150501.55+371311.5 with magnitudes $W1 = (12.230 \pm 0.023)$, $W2 = (11.407 \pm 0.021)$, $W3 = (8.514 \pm 0.022)$, $W4 = (6.114 \pm 0.037)$, and AGN colours ($W1 - W2 = 0.823$, $W2 - W3 = 2.893$);
- *Gaia* 1294976383987364480 with magnitudes $G = (19.293 \pm 0.028)$, $BP = (17.372 \pm 0.011)$, and $RP = (16.038 \pm 0.010)$
  ($BP - RP = 1.333$);
- GALEX J150501.5+371310 with magnitudes $FUV = (21.093 \pm 0.273)$ and $NUV = (19.933 \pm 0.083)$;
- ILTJ150501.53+371311.1 with flux Ftot(144 MHz) = 2.365 mJy.

A power law passing through Galactic absorption ($N_{\mathrm{H(Gal)}} = 1.20 \times 10^{20}$ cm^{-2}), with a photon index $\Gamma = \left(-0.25^{+0.49}_{-0.58}\right)$ and a 2–10 keV flux of $\sim 1.2 \times 10^{-12}$ erg cm^{-2} s^{-1}, provides a good fit to the data. However, if we fix the photon index to 1.8, the data seem to require intrinsic absorption $N_{\mathrm{H(int)}} = \left(3.20^{+2.75}_{-1.25}\right) \times 10^{22}$ cm^{-2}, which is more typical of an absorbed AGN; the 2–10 keV flux is $\sim 7 \times 10^{-13}$ erg cm^{-2} s^{-1}.

Indeed, this source is classified as a Seyfert 2 galaxy at redshift $z = (0.06517 \pm 0.00002)$; the optical source morphology is peculiar, with the nucleus location north of the galaxy extended emission, as shown in Figure 6 from SDSS.

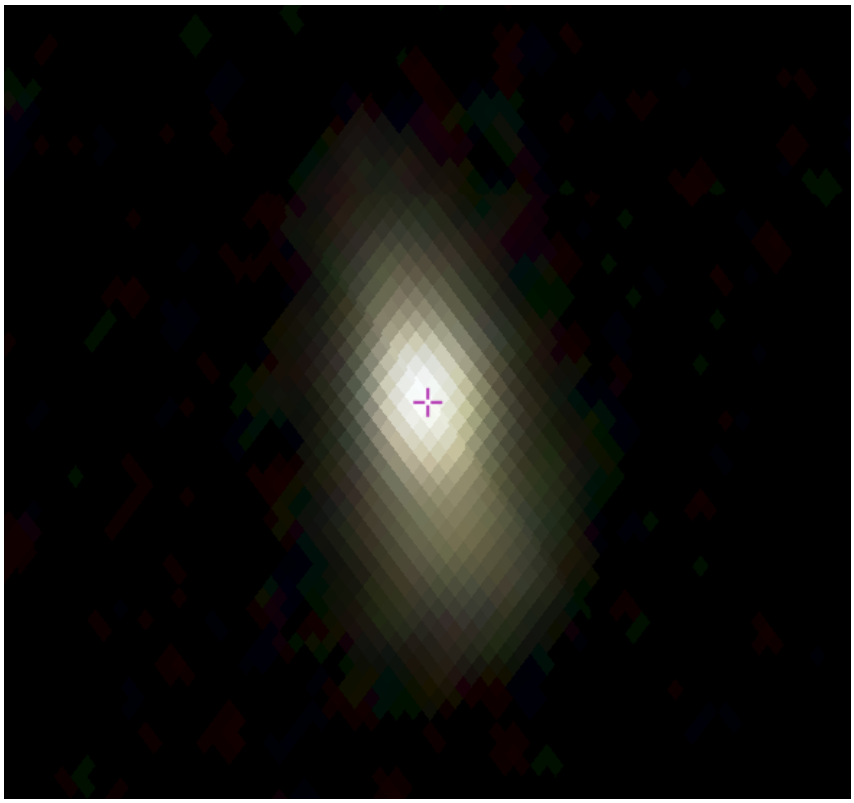

Figure 6: Optical image of source #1 from SDSS.

➢ Source #2 is located at:

R.A.(J2000) = $15^{\rm h}04^{\rm m}53'.07$

Dec.(J2000) = $+37°11'22''.37$

error box = $6''.00$

It is detected at 3.1σ c.l. in the 0.3–10 keV energy range, but not above 3 keV.

Multi–wavelength counterparts to this XRT detection:

- USNO–A2.0 1200–07458188 with magnitudes $B = 19.6$ and $R = 18.8$;
- *Gaia* 1294976276612376064 with magnitudes $G = (20.906 \pm 0.026)$, $BP = (20.737 \pm 0.245)$, and $RP = (19.632 \pm 0.189)$
  $(BP - RP = 1.105)$;
- GALEX J150453.1+371119 with magnitudes $FUV = (21.177 \pm 0.282)$ and $NUV = (20.529 \pm 0.112)$.

A simple power law plus Galactic absorption ($N_{\rm H(Gal)} = 1.20 \times 10^{20}$ cm^{-2}) provides a photon index $\Gamma \sim$1.2 and a 2–10 keV flux of $\sim 1.4 \times 10^{-13}$ erg cm^{-2} s^{-1}. If we freeze the photon index to 1.8, we estimate a 2–10 keV flux of $\sim 8.3 \times 10^{-14}$ erg cm^{-2} s^{-1}.

Given the lower X–ray flux and the relative soft spectrum (no detection above 3 keV) of source #2, we can conclude that this detection is an unlikely counterpart to the BAT source, thus pointing to the Seyfert 2 galaxy as the real association.

PBC_NEW_138

Source position:

- R.A.(J2000) = $17^h56^m59'.47$
- Dec.(J2000) = $-45°19'32''.10$
- Positional uncertainty = $4'.2920$

Two XRT observations available:

1. obscode: 00096628001
   observation date: 17/10/2022
   exposure: 945 s
2. obscode: 00096628002
   observation date: 24/10/2022
   exposure: 800 s

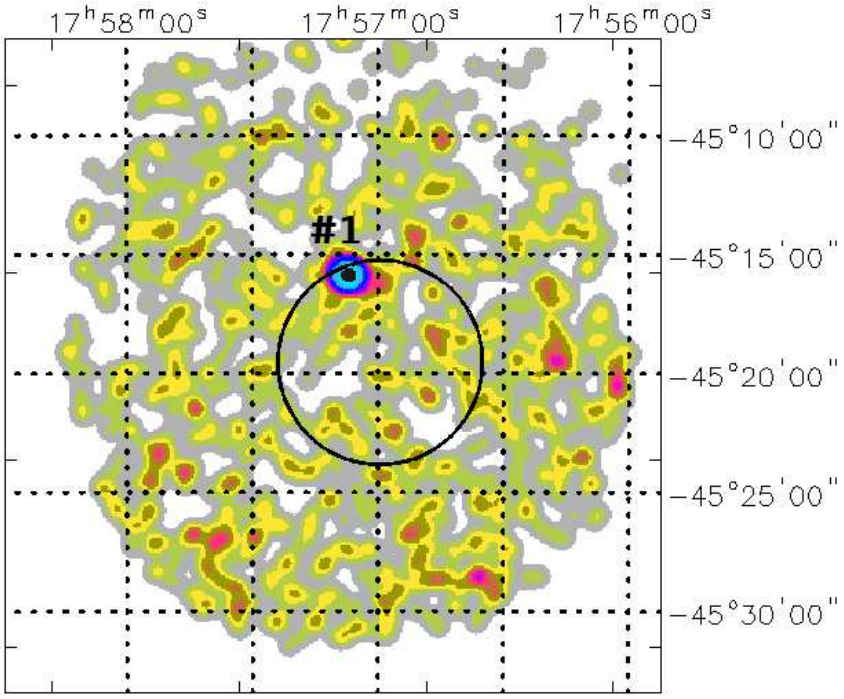

Figure 7: 0.3–10 keV XRT image of the PBC_NEW_138 field.

The only X–ray source detected by XRT inside the BAT positional uncertainty (see Figure 7) is located at:

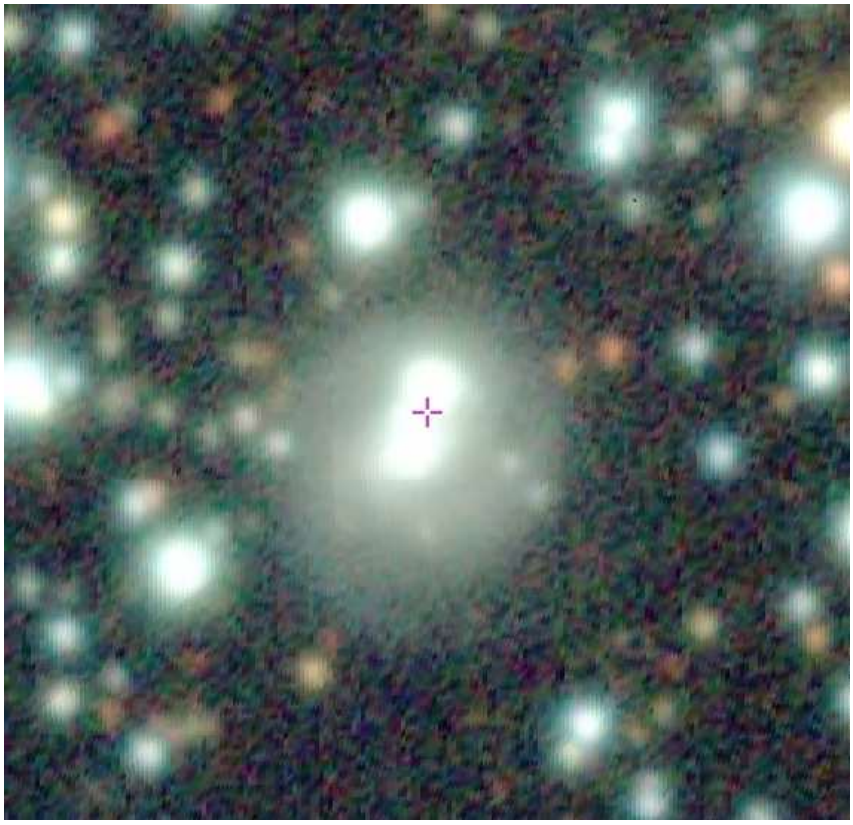

Figure 8: Optical image of source #1 from DECaPS.

R.A.(J2000) = $17^{\rm h}57^{\rm m}07'.01$

Dec.(J2000) = $-45^{\circ}15'52''.91$

error box = $4''.19$

It is detected at 9.2σ and at 4.7σ c.l. in the 0.3–10 keV energy range and above 3 keV, respectively.

Multi–wavelength counterparts to this XRT detection:

- USNO–A2.0 0375–33824485 with magnitudes $B = 13.5$ and $R = 13.1$;
- 2MASS J17570698–4515515 with magnitudes $J = (13.349 \pm 0.000)$, $H = (13.001 \pm 0.080)$, and $K = (12.793 \pm 0.079)$;
- 2MASS J17570705–4515547 with magnitudes $J = (13.4639 \pm 0.000)$, $H = (13.519 \pm 0.076)$, and $K = (12.811 \pm 0.043)$;
- AllWISE J175707.05–451554.2 with magnitudes $W1 = (11.138 \pm 0.023)$, $W2 = (10.365 \pm 0.019)$, $W3 = (7.330 \pm 0.017)$, $W4 = (4.955 \pm 0.027)$, and colours typical of an AGN ($W1 - W2 = 0.773$, $W2 - W3 = 3.335$);
- *Gaia* 5954488134567739776 with magnitude $G = (18.664 \pm 0.004)$;

- *Gaia* 5954488134593659392 with magnitudes $G = (15.515 \pm 0.003)$, $BP = (16.097 \pm 0.006)$, and $RP = (14.703 \pm 0.004)$
  $(BP - RP = 1.394)$;
- *Gaia* 5954488134593658752 with magnitudes $G = (17.591 \pm 0.019)$, $BP = (17.200 \pm 0.058)$, and $RP = (15.898 \pm 0.045)$
  $(BP - RP = 1.302)$;
- 1RXS J175706.6–451556 (also 6dFGS J1757070–451554) with flux F(0.2–2.4 keV) $= (2.68 \pm 0.69) \times 10^{-12}$ erg cm^{-2} s^{-1};
- 1eRASS J175707.1–451556 with flux F(0.2–2.3 keV) $\sim 1.9 \times 10^{-12}$ erg cm^{-2} s^{-1};
- RACS–MID J175707.1–451545 with flux Ftot(1367.5 MHz) = 8.07 mJy;
- RACS–HIGH J175707–45154 with flux Ftot(1655.5 MHz) = 6.01 mJy.

A simple power law passing through Galactic absorption ($N_{\mathrm{H(Gal)}} = 1.10 \times 10^{21}$ cm^{-2}) provides a photon index $\Gamma = (1.58 \pm 0.38)$ and a 2–10 keV flux of $\sim 2.7 \times 10^{-12}$ erg cm^{-2} s^{-1}.

All source characteristics (radio detection, *AllWISE* colours, and optical extension, as shown in Figure 8 from DECaPS) point to an AGN candidate.

PBC_NEW_157

Source position:

- R.A.(J2000) = $01^{h}15^{m}18'.24$
- Dec.(J2000) = $-38°07'11''.70$
- Positional uncertainty = $4'.4208$

One XRT observation available:

1. obscode: 00096635001
   observation date: 29/11/2022
   exposure: 1622 s

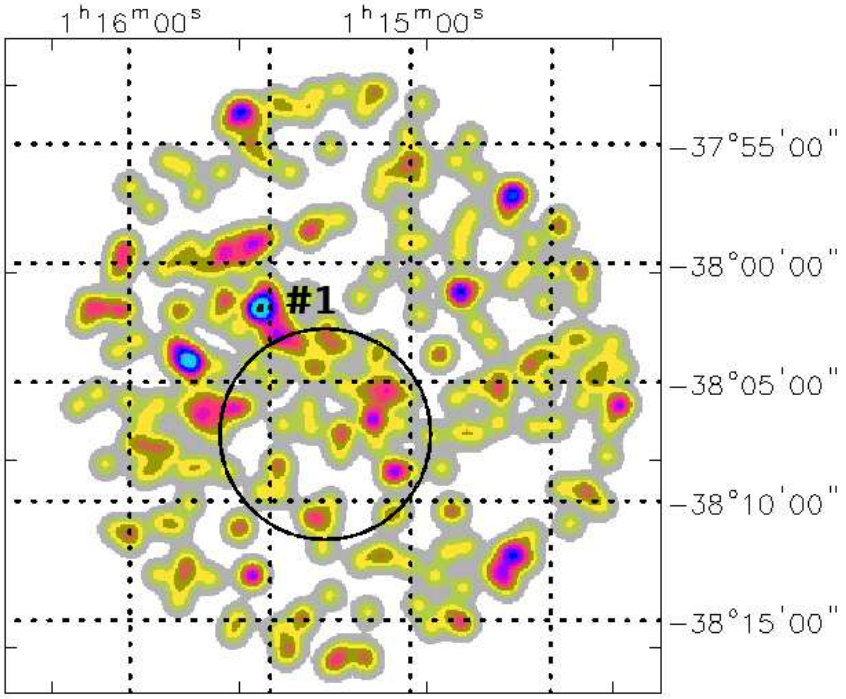

Figure 9: 0.3–10 keV XRT image of the PBC_NEW_157 field.

The only X–ray source detected by XRT in the region surrounding PBC_NEW_157 lies outside the BAT positional uncertainty (see Figure 9) and is located at:

R.A.(J2000) = $01^{h}15^{m}32'.82$

Dec.(J2000) = $-38^{\circ}01'50''.50$

error box = $7''.00$

It is detected at 2.4σ c.l. in the 0.3–10 keV energy range; no detection is found above 3 keV.

Multi–wavelength counterparts to this XRT detection:

- USNO–A2.0 0450–00440174 with magnitudes $B = 19.1$ and $R = 17.6$;
- AllWISE J011532.64–380156.8 with magnitudes $W1 = (15.398 \pm 0.038)$, $W2 = (14.638 \pm 0.053)$, $W3 = (12.081 \pm 0.000)$, $W4 = (9.167 \pm 0.000)$, and colours that point to an AGN candidate ($W1 - W2 = 0.760$, $W2 - W3 = 2.557$);
- *Gaia* 4988578744500378240 with magnitudes $G = (20.207 \pm 0.021)$, $BP = (20.104 \pm 0.076)$, and $RP = (19.517 \pm 0.068)$
  ($BP - RP = 0.587$).

Due to the low quality of the X–ray data, we can only infer a 2–10 keV flux of $\sim 1.4 \times 10^{-13}$ erg cm^{-2} s^{-1} by assuming a power law continuum (photon index frozen to 1.8) passing through Galactic absorption ($N_{\rm H(Gal)} = 1.20 \times 10^{20}$ cm^{-2}).

Although no radio emission is reported for this source, its extragalactic/AGN nature is indicated by its four infrared colours, as well as its properties with respect to various catalogues: i.e., the "Large Quasar Astrometric Catalogue 6, LQAC–6" (Souchay et al. 2024) and the "*Gaia* DR3 quasar and galaxy classification" (Hughes et al. 2022). The suggested photometric redshift is $z = (0.697 \pm 0.217)$ (Duncan 2022).

PBC_NEW_175

Source position:

- R.A.(J2000) = $19^h49^m14'.83$
- Dec.(J2000) = $+48°49'26''.00$
- Positional uncertainty = $4'.6236$

One XRT observation available:

1. obscode: 00096643001
   observation date: 23/11/2022
   exposure: 1715 s

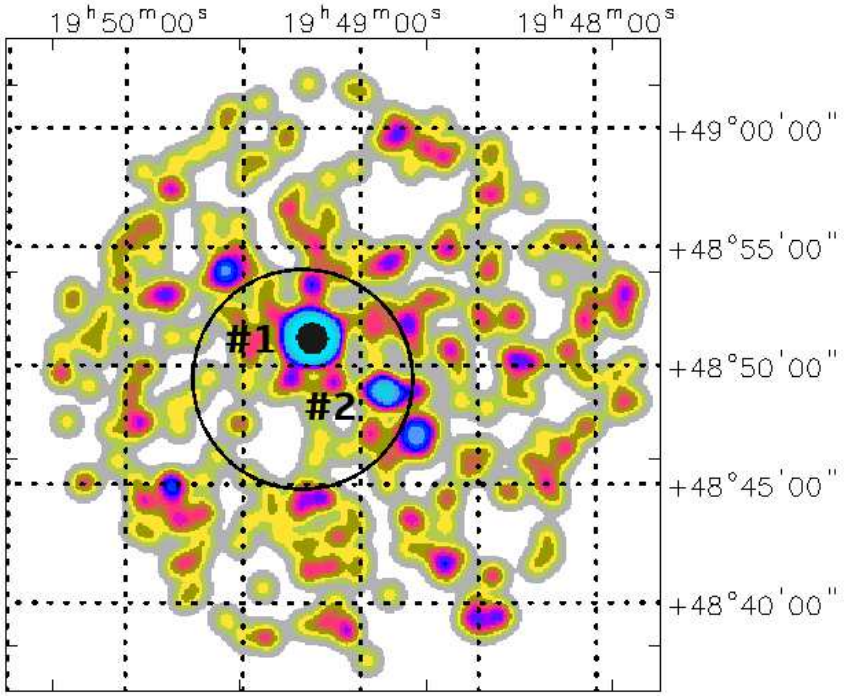

Figure 10: 0.3–10 keV XRT image of the PBC_NEW_175 field.

XRT detects two X–ray sources within the BAT positional uncertainty (see Figure 10):

➢ Source #1 is located at:

R.A.(J2000) = $19^h49^m12'.29$

Dec.(J2000) = $+48^{\circ}51'08''.54$

error box = $4''.06$

It is detected at 11.0σ and 4.8σ c.l. in the 0.3–10 keV energy range and above 3 keV, respectively.

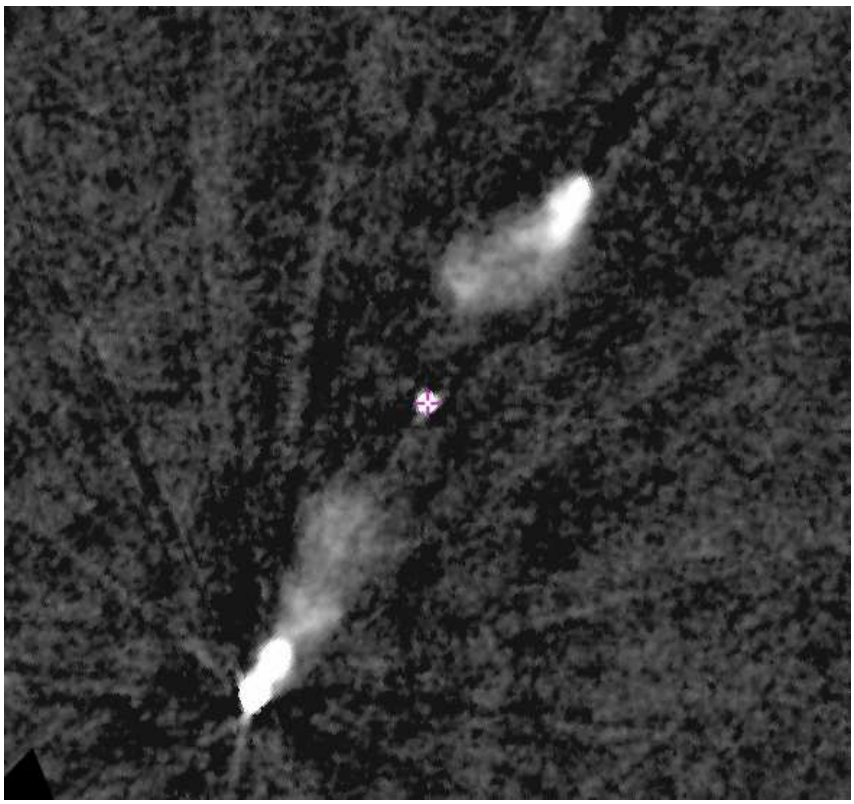

Figure 11: Radio image of source #1 from VLASS.

Multi–wavelength counterparts to this XRT detection:

- USNO–A2.0 1350–11119311 with magnitudes $B = 17.8$ and $R = 17.00$;
- 2MASS J19491217+4851058 with magnitudes $J = (16.453 \pm 0.124)$, $H = (15.752 \pm 0.129)$, and $K = (14.569 \pm 0.121)$;
- AllWISE J194912.16+485106.1 with magnitudes $W1 = (12.767 \pm 0.023)$, $W2 = (11.534 \pm 0.021)$, $W3 = (8.607 \pm 0.023)$, $W4 = (6.131 \pm 0.042)$, and AGN colours ($W1 - W2 = 1.233$, $W2 - W3 = 2.927$);
- *Gaia* 2086768512837469184 with magnitudes $G = (18.140 \pm 0.012)$, $BP = (18.547 \pm 0.037)$, and $RP = (17.099 \pm 0.030)$
  ($BP - RP = 1.448$);
- GALEX J194912.1+485106 with magnitude $NUV = (21.506 \pm 0.338)$;

- 2RXS J194912.2+485105 with flux F(0.2–2.4 keV) $\sim 7.3 \times 10^{-13}$ erg cm^{-2} s^{-1};
- VLASS1QLCIR J194912.15+485106.0 with flux Ftot(2000–4000 MHz) $= (33.449 \pm 0.332)$ mJy;
- RACS–MID J194914.9+485021 with flux Ftot(1367.5 MHz) = 1103 mJy.

The fit with a power law passing through Galactic absorption ($N_{\rm H(Gal)} = 1.29 \times 10^{21}$ cm^{-2}) does not provide a good fit to the data, as a hint of the presence of extra absorption is evident in the residuals to the data. The addition of this component is required at 99% c.l. and yields an intrinsic column density $N_{\rm H(int)} = \left(0.26^{+0.36}_{-0.17}\right) \times 10^{22}$ cm^{-2}; the photon index is $\Gamma = \left(2.29^{+0.60}_{-0.50}\right)$, while the 2–10 keV flux is $\sim 2.2 \times 10^{-12}$ erg cm^{-2} s^{-1}.

The source is clearly an AGN candidate due to its *AllWISE* colours and radio detection. Furthermore, the VLASS image of the source (see Figure 11) shows a clear extended morphology with a central nucleus and two distant radio lobes. Fu et al. (2021) provide a photometric redshift $z = 0.423$. If confirmed, this would imply a source radio size of $\sim$1 Mpc with largest angular size (LAS) of 3′, thus making this object a giant radio galaxy (GRG) candidate.

➢ Source #2 is located at:

R.A.(J2000) = $19^{\rm h}48^{\rm m}53'.60$

Dec.(J2000) = $+48^{\circ}48'54''.20$

error box = $6''.00$

It is detected at 2.9σ c.l. in the 0.3–10 keV energy range and is not revealed above 3 keV.

Multi–wavelength counterparts to this XRT detection:

- USNO–B1.0 1388–0320338 with magnitudes $B2 = 19.77$ and $R2 = 19.45$;
- AllWISE J194853.78+484854.9 with magnitudes $W1 = (15.946 \pm 0.045)$, $W2 = (14.874 \pm 0.051)$, $W3 = (11.962 \pm 0.198)$, $W4 = (8.684 \pm 0.000)$, and AGN colours ($W1 - W2 = 1.072$, $W2 - W3 = 2.912$).

In this case, from the X–ray data we can infer a 2–10 keV flux of $\sim 1.2 \times 10^{-13}$ erg cm^{-2} s^{-1} by assuming a power law continuum ($\Gamma \sim 2$) passing through Galactic absorption ($N_{\rm H(Gal)} = 1.29 \times 10^{21}$ cm^{-2}).

Optically, it is most likely a QSO candidate (Flesch 2024; Liao et al. 2019) of unknown redshift.

Considering that source #2 is much weaker and softer than source #1, we can conclude that it is an unlikely candidate counterpart to PBC_NEW_175.

PBC_NEW_176

Source position:

- R.A.(J2000) = $03^h58^m24'.40$
- Dec.(J2000) = $-05°34'03''.20$
- Positional uncertainty = $4'.5389$

Two XRT observations available:

1. obscode: 00096644001
   observation date: 22/03/2023
   exposure: 2184 s
2. obscode: 00096644002
   observation date: 23/07/2023
   exposure: 1304 s

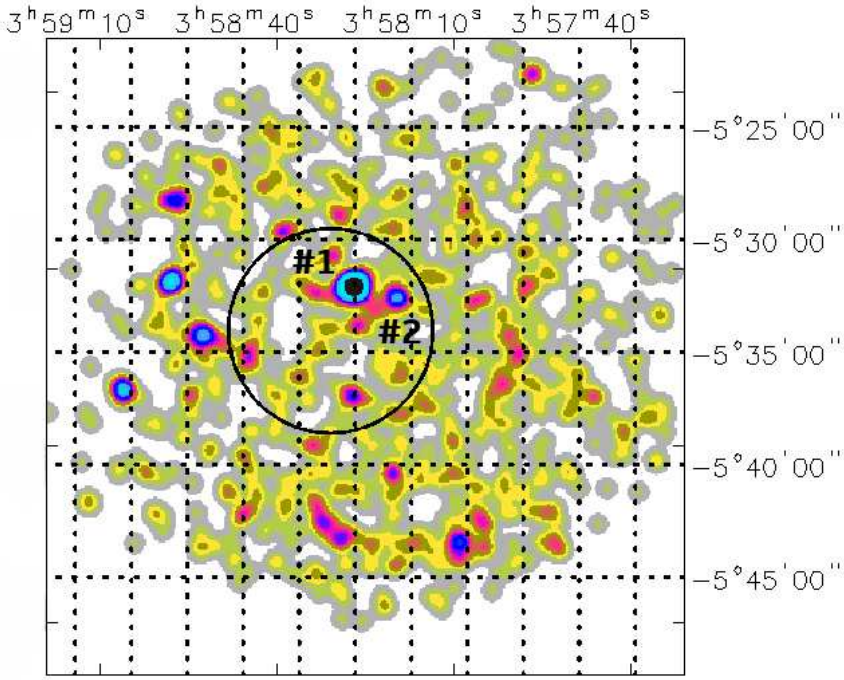

Figure 12: 0.3–10 keV XRT image of the PBC_NEW_176 field.

XRT detects two X–ray sources within the BAT positional uncertainty (see Figure 12):

➢ Source #1 is located at:

R.A.(J2000) = $03^{h}58^{m}20'.25$

Dec.(J2000) = $-05^{\circ}32'04''.95$

error box = $4''.46$

It is detected at 7.4σ and 5.3σ c.l. in the 0.3–10 keV energy range and above 3 keV, respectively.

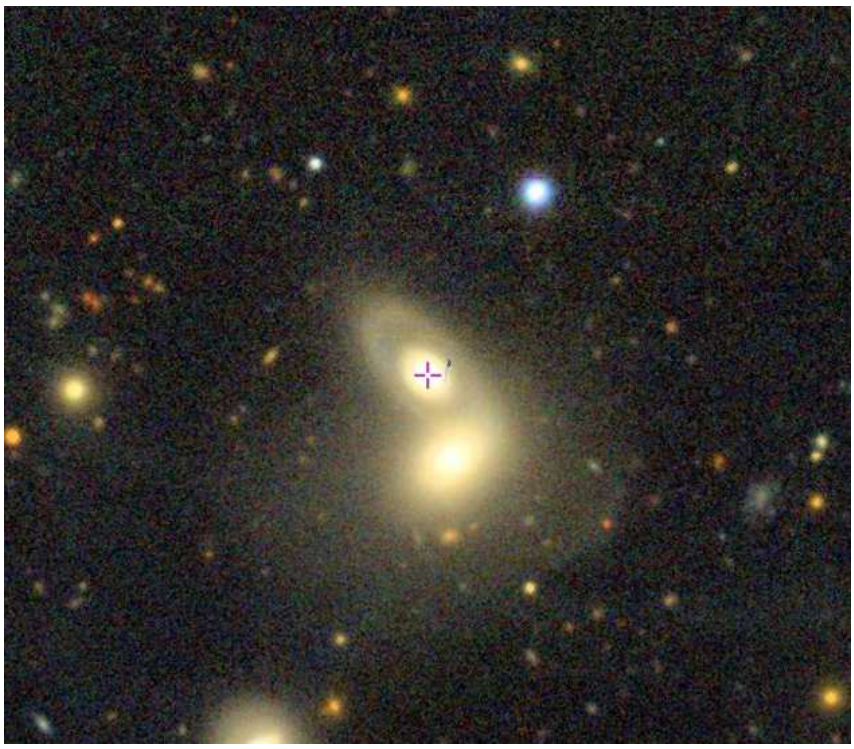

Figure 13: Optical image of source #1 from the DESI Legacy Imaging Survey.

Multi–wavelength counterparts to this XRT detection:

- USNO–A2.0 0825–00895647 with magnitudes $B = 15.5$ and $R = 13.9$;
- 2MASS J03582008–0532066 with magnitudes $J = (14.228 \pm 0.058)$, $H = (13.325 \pm 0.065)$, and $K = (12.655 \pm 0.045)$;
- 2MASX J0825–00895647 with magnitudes $J = (12.749 \pm 0.144)$, $H = (12.039 \pm 0.027)$, and $K = (11.560 \pm 0.069)$;

- AllWISE J035820.08–053206.6 with magnitudes $W1 = (11.446 \pm 0.021)$, $W2 = (10.741 \pm 0.021)$, $W3 = (7.598 \pm 0.018)$, $W4 = (4.930 \pm 0.027)$, and colours of an active galaxy ($W1 - W2 = 0.705$, $W2 - W3 = 3.143$);
- *Gaia* 3245116180341183744 with magnitudes $G = (16.869 \pm 0.006)$, $BP = (16.616 \pm 0.013)$, and $RP = (15.302 \pm 0.009)$
  ($BP - RP = 1.314$);
- 1eRASS J035820.0–053205 with flux F(0.2–2.3 keV) $\sim 3.8 \times 10^{-13}$ erg cm^{-2} s^{-1};
- VLASS1QLCIR J035820.13–053205.9 with no information about the flux;
- RACS–MID J035820.1–053206 with flux Ftot(1367.5 MHz) = 4.26 mJy;
- RACS–HIGH J035820–05320 with flux Ftot(1665.5 MHz) = 4.38 mJy.

By fitting the data with a simple power law ($N_{\rm H(Gal)} = 5.37 \times 10^{20}$ cm^{-2}), we find a flat photon index $\Gamma = \left(0.50^{+0.42}_{-0.44}\right)$ and a 2–10 keV flux of $\sim 2.1 \times 10^{-12}$ erg cm^{-2} s^{-1}. However, if we fix the photon index to 1.8, the residuals to the data show evidence of intrinsic absorption $N_{\rm H(int)} = \left(0.97^{+1.55}_{-0.65}\right) \times 10^{22}$ cm^{-2}; the 2–10 keV flux is $\sim 1.1 \times 10^{-12}$ erg cm^{-2} s^{-1}.

The source is identified with LEDA 1043483, a Seyfert 1 galaxy at redshift $z = (0.06231 \pm 0.00015)$. It is an interacting system with LEDA 1043429, at a similar redshift, as portrayed in Figure 13 from the DESI Legacy Imaging Survey.

➢ Source #2 is located at:

R.A.(J2000) = $03^{\rm h}58^{\rm m}12'.60$

Dec.(J2000) = $-05^{\circ}32'35''.50$

error box = $6''.00$

It is detected at 2.9σ c.l. in the 0.3–10 keV energy range and is not revealed above 3 keV.

Multi–wavelength counterparts to this XRT detection:

- USNO–B1.0 0844–0037362 with magnitudes $R1 = 19.51$ and $R2 = 19.26$);
- AllWISE J035812.52–053239.6 with magnitudes $W1 = (15.946 \pm 0.055)$, $W2 = (14.726 \pm 0.061)$, $W3 = (12.127 \pm 0.000)$, $W4 = (8.472 \pm 0.000)$, and colours of an active galaxy ($W1 - W2 = 1.22$, $W2 - W3 = 2.599$);
- *Gaia* 3245303711496428928 with magnitudes $G = (20.407 \pm 0.011)$, $BP = (20.686 \pm 0.074)$, and $RP = (19.894 \pm 0.112)$
  ($BP - RP = 0.791$).

For this source, due to the poor statistical quality of the data, from the X–ray data we can only infer a 2–10 keV flux of $\sim 8 \times 10^{-14}$ erg cm^{-2} s^{-1} by assuming a power law continuum (photon index frozen to 1.8) passing through Galactic absorption ($N_{\rm H(Gal)} = 6.56 \times 10^{20}$

cm^{-2}).

This source is probably a background QSO (Wu et al. 2023) at redshift $z = 1.211$ (Duncan 2022). However, given its X–ray spectral properties (weak flux and soft spectrum), it is an unlikely counterpart to PBC_NEW_176.

PBC_NEW_183

Source position:

- R.A.(J2000) = $23^h29^m00'.91$
- Dec.(J2000) = $-35°10'53''.10$
- Positional uncertainty = $4'.2677$

One XRT observation available:

1. obscode: 00096646001
   observation date: 12/01/2023
   exposure: 2066 s

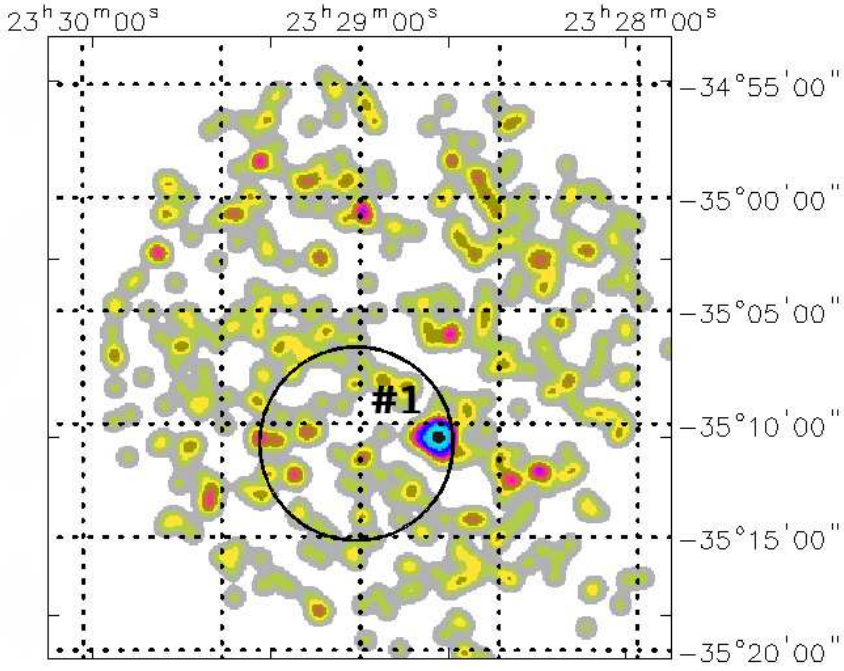

Figure 14: 0.3–10 keV XRT image of the PBC_NEW_183 field.

The only X–ray source detected by XRT within the BAT positional uncertainty (see Figure 14) is located at:

R.A.(J2000) = $23^h28^m43'.03$

Dec.(J2000) = $-35°10'35''.46$

error box = $4''.88$

It is detected at 6.2σ and 6.1σ c.l. in the 0.3–10 keV energy range and above 3 keV, respectively.

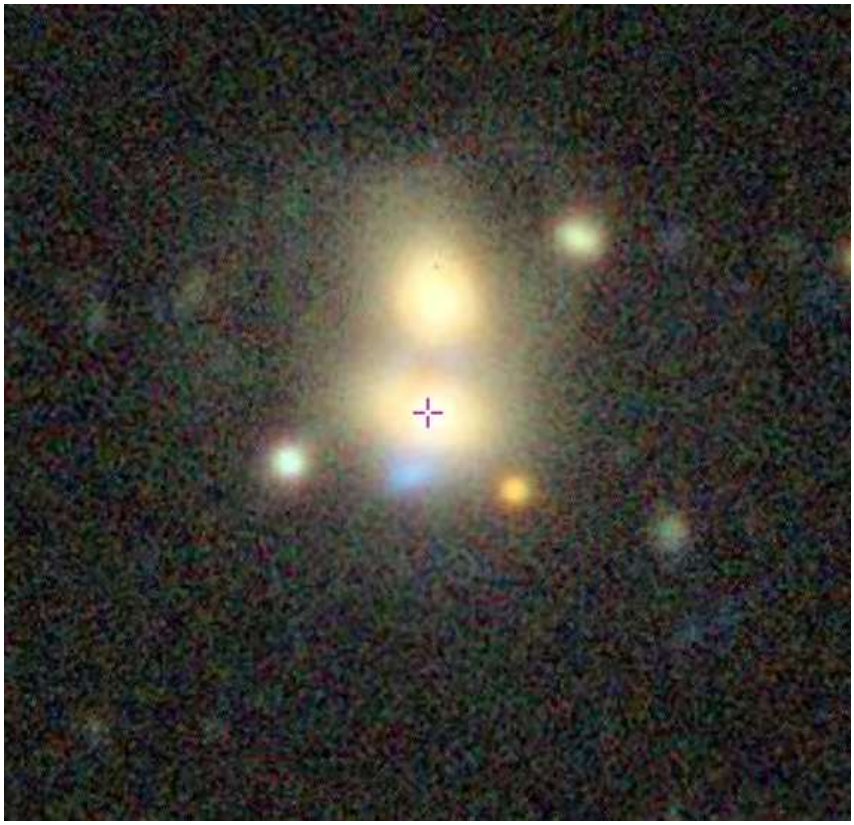

Figure 15: Optical image of source #1 from the DESI Legacy Imaging Survey.

Multi–wavelength counterparts to this XRT detection:

- 2MASS J23284287–3510324 with magnitudes $J = (14.985 \pm 0.088)$, $H = (14.279 \pm 0.091)$, and $K = (13.630 \pm 0.060)$;
- 2MASX J23284284–3510323 with magnitudes $J = (13.751 \pm 0.068)$, $H = (12.983 \pm 0.078)$, and $K = (13.038 \pm 0.141)$;
- AllWISE J232842.88–351032.3 with magnitudes $W1 = (12.508 \pm 0.025)$, $W2 = (11.930 \pm 0.023)$, $W3 = (9.606 \pm 0.041)$, $W4 = (7.270 \pm 0.122)$, and colours ($W1 - W2 = 0.578$, $W2 - W3 = 2.324$) that point to an AGN candidate;
- *Gaia* 6551466838994709376 with magnitudes $G = (19.746 \pm 0.013)$, $BP = (17.924 \pm 0.033)$, and $RP = (16.414 \pm 0.015)$
  ($BP - RP = 1.510$);
- GALEX J232842.9–351034 with magnitudes $FUV = (19.736 \pm 0.195)$ and $NUV = (19.408 \pm 0.104)$;

- GLEAM–X J232843.1–351034;
- VLASS1QLCIR J232842.90–351031.9 with flux Ftot(2000–4000 MHz) $= (3.734 \pm 0.406)$ mJy;
- VLASS1QLCIR J232842.90–351031.8 with flux Ftot(2000–4000 MHz) $= (4.052 \pm 0.443)$ mJy;
- RACS–MID J232842.8–351030 with flux Ftot(1367.5 MHz) = 5.57 mJy;
- RACS–HIGH J232842–35103 with flux Ftot(1655.5 MHz) = 4.01 mJy.

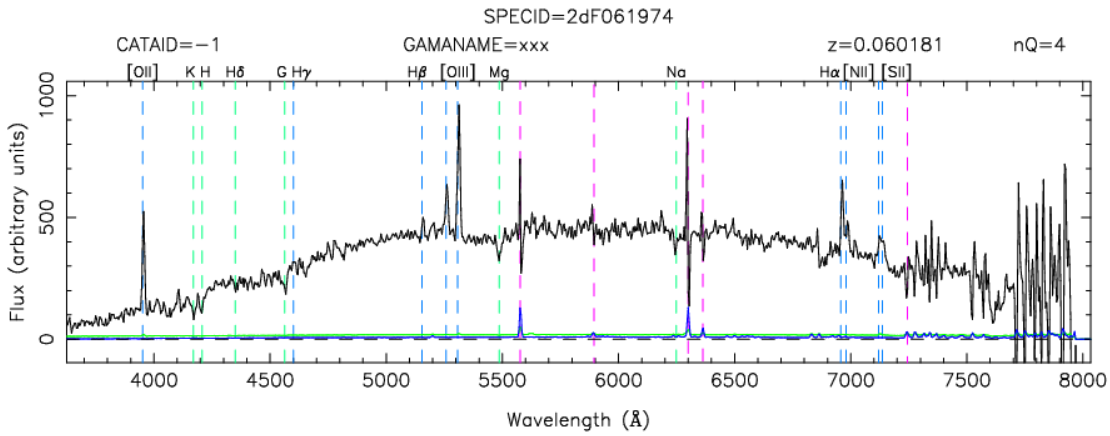

Figure 16: Optical spectrum of source #1 from the 6dF Galaxy Survey.

The fit with a power law passing through Galactic absorption ($N_{\mathrm{H(Gal)}} = 1.40 \times 10^{20}$ cm^{-2}) indicates a photon index $\Gamma \sim$–1.8 and a 2–10 keV flux of $\sim 1 \times 10^{-11}$ erg cm^{-2} s^{-1}. If we fix the photon index to 1.8, the data require (at $> 99.99\%$ c.l.) extra absorption $N_{\mathrm{H(int)}} = \left(19.3^{+11.4}_{-8.9}\right) \times 10^{22}$ cm^{-2}, while the 2–10 keV flux is $\sim 4.4 \times 10^{-12}$ erg cm^{-2} s^{-1}.

This source is identified with a galaxy at redshift $z = (0.0602 \pm 0.0003)$; it is interesting to note that the source seems to be in interaction with another object (see Figure 15 from the DESI Legacy Imaging Survey). Its *AllWISE* colours and radio detection point to an active galaxy. The optical spectrum of the source from the 6dF Galaxy Survey is shown in Figure 16; it suggests a type 2 AGN, as confirmed by the absorption measured in X–rays.

PBC_NEW_186

Source position:

- R.A.(J2000) = $16^h26^m37'.64$
- Dec.(J2000) = $-33°08'53''.60$
- Positional uncertainty = $4'.3837$

Two XRT observations available:

1. obscode: 00015479001
   observation date: 20/01/2023
   exposure: 2076 s
2. obscode: 00096647001
   observation date: 21/01/2023
   exposure: 1841 s

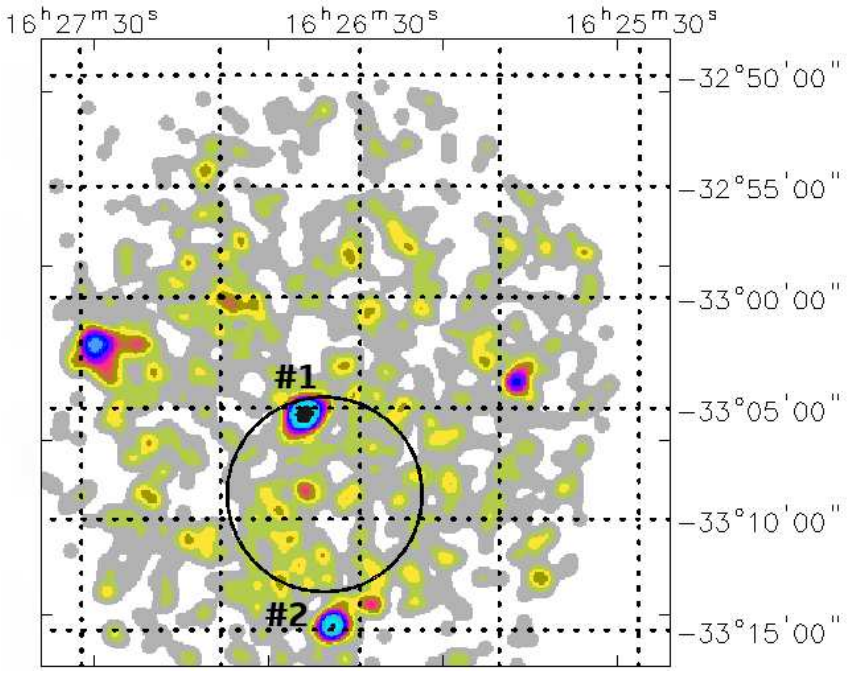

Figure 17: 0.3–10 keV XRT image of the PBC_NEW_186 field.

XRT detects two X–ray sources in the region surrounding PBC_NEW_186 (see Figure 17):

➢ Source #1 is located at:

R.A.(J2000) = $16^{\rm h}26^{\rm m}41'.88$

Dec.(J2000) = $-33°05'19''.20$

error box = $4''.15$

It is detected at 10.0σ and 8.9σ c.l. in the 0.3–10 keV energy range and above 3 keV, respectively.

Multi–wavelength counterparts to this XRT detection:

- *Gaia* 6024855916679317632 with magnitudes $G = (21.000 \pm 0.031)$ and $BP = (11.462 \pm 0.006)$;
- 1eRASS J162642.0–330519 with flux F(0.2–2.3 keV) $\sim 7.2 \times 10^{-13}$ erg cm^{-2} s^{-1}.

By fitting the X–ray data with a simple power law ($N_{\rm H(Gal)} = 1.58 \times 10^{21}$ cm^{-2}), we find a photon index $\Gamma = \left(-0.35^{+0.37}_{-0.43}\right)$ and a 2–10 keV flux of $\sim 5.8 \times 10^{-12}$ erg cm^{-2} s^{-1}. If we fix the photon index to 1.8, the data require a double power law model: one passing through Galactic absorption, the other through intrinsic absorption $N_{\rm H(int)} = \left(7.40^{+7.8}_{-3.2}\right) \times 10^{20}$ cm^{-2}; the 2–10 keV flux turnes out to be $\sim 3.1 \times 10^{-12}$ erg cm^{-2} s^{-1}.

Within the positional uncertainty of the X–ray detection we find an association with the source DENIS J162642.2–330522, with magnitudes $I = (16.827 \pm 0.100)$, $J = (14.994 \pm 0.140)$, $H = (13.169 \pm 0.160)$, $R = 15.6$, and $B = 17.5$, which is suggested as possible AGN by Edelson & Malkan (2012); however, the sky region is very crowded making the optical association difficult.

➢ Source #2 is located at:

R.A.(J2000) = $16^{\rm h}26^{\rm m}36'.04$

Dec.(J2000) = $-33°14'48''.46$

error box = $4''.61$

It is detected at 6.5σ c.l. in the 0.3–10 keV energy range and is not revealed above 3 keV.

Multi–wavelength counterparts to this XRT detection:

- USNO–A2.0 0525–22695287 with magnitudes $B = 11.8$ and $R = 10.4$;

- 2MASS J16263591–3314481 with magnitudes $J = (9.486 \pm 0.035)$, $H = (8.958 \pm 0.036)$, and $K = (8.838 \pm 0.035)$;
- AllWISE J162635.90–331448.3 with magnitudes $W1 = (8.736 \pm 0.025)$, $W2 = (8.722 \pm 0.024)$, $W3 = (8.620 \pm 0.029)$, $W4 = (8.219 \pm 0.000)$, and colours ($W1 - W2 = 0.014$, $W2 - W3 = 0.102$);
- *Gaia* 6024849594490361856 with magnitudes $G = (10.975 \pm 0.031)$, $BP = (11.462 \pm 0.006)$, and $RP = (10.312 \pm 0.005)$
  ($BP - RP = 1.150$);
- *Gaia* 6024849594478514304 with magnitudes $G = (18.810 \pm 0.007)$, $BP = (18.005 \pm 0.161)$, and $RP = (16.597 \pm 0.088)$
  ($BP - RP = 1.408$);
- *Gaia* 6024849594478514176 with magnitudes $G = (19.534 \pm 0.006)$;
- 2RXS J162635.4–331519 with flux F(0.2–2.4 keV) $\sim 8.9 \times 10^{-13}$ erg cm^{-2} s^{-1};
- 1eRASS J162635.8–331449 with flux F(0.2–2.3 keV) $\sim 7.2 \times 10^{-13}$ erg cm^{-2} s^{-1}.

The fit with a simple power law ($N_{\rm H(Gal)} = 1.67 \times 10^{21}$ cm^{-2}) shows a photon index $\Gamma = (1.38 \pm 0.31)$ and a 2–10 keV flux of $\sim 3 \times 10^{-13}$ erg cm^{-2} s^{-1}. The fit is equally good if we adopt the *apec* model (an emission spectrum from collisionally–ionized diffuse gas), which provides a temperature $kT_{\rm apec} = \left(0.42^{+0.36}_{-0.12}\right)$ keV and a 2–10 keV flux of $\sim 1 \times 10^{-14}$ erg cm^{-2} s^{-1}.

Source #2 is however too weak and soft in X–rays to be a likely association, living object #1 as the only possible counterpart to PBC_NEW_186.

PBC_NEW_187

Source position:

- R.A.(J2000) = $09^{h}18^{m}24'.13$
- Dec.(J2000) = $-12°57'18''.10$
- Positional uncertainty = $4'.4595$

Two XRT observations available:

1. obscode: 00096648001
   observation date: 14/12/2022
   exposure: 1522 s
2. obscode: 00096648002
   observation date: 15/12/2022
   exposure: 742 s

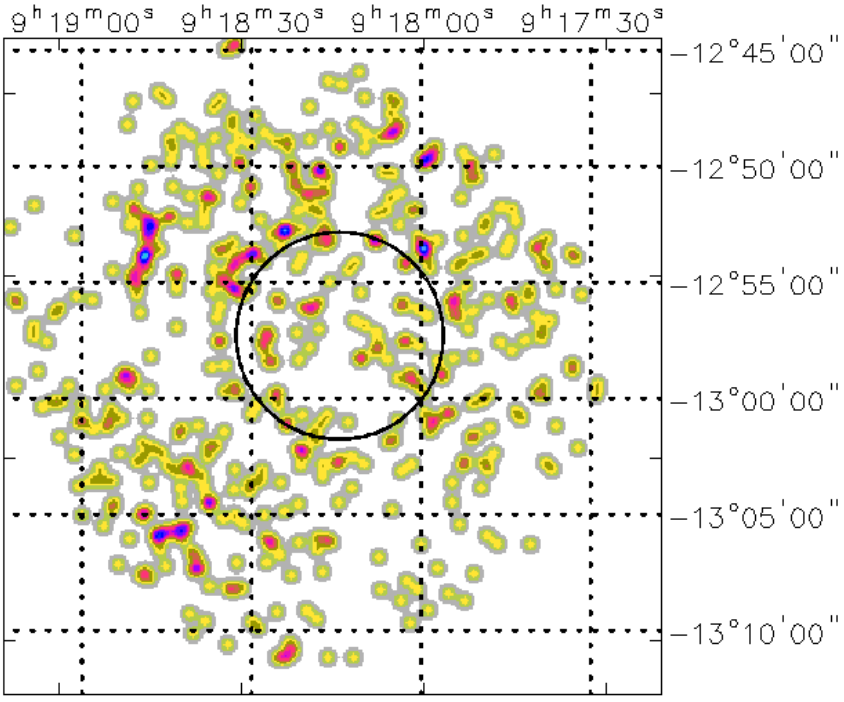

Figure 18: 0.3–10 keV XRT image of the PBC_NEW_187 field.

No X–ray source is detected by XRT within the region surrounding PBC_NEW_187 (see Figure 18), nor other X–ray sources are reported in the archives.

PBC_NEW_199

Source position:

- R.A.(J2000) = $21^{h}23^{m}23'.22$
- Dec.(J2000) = $+29^{\circ}41'41''.50$
- Positional uncertainty = $4'.4939$

Two XRT observations available:

1. obscode: 00096655001
   observation date: 14/12/2022
   exposure: 1778 s
2. obscode: 00096655002
   observation date: 16/12/2022
   exposure: 359 s

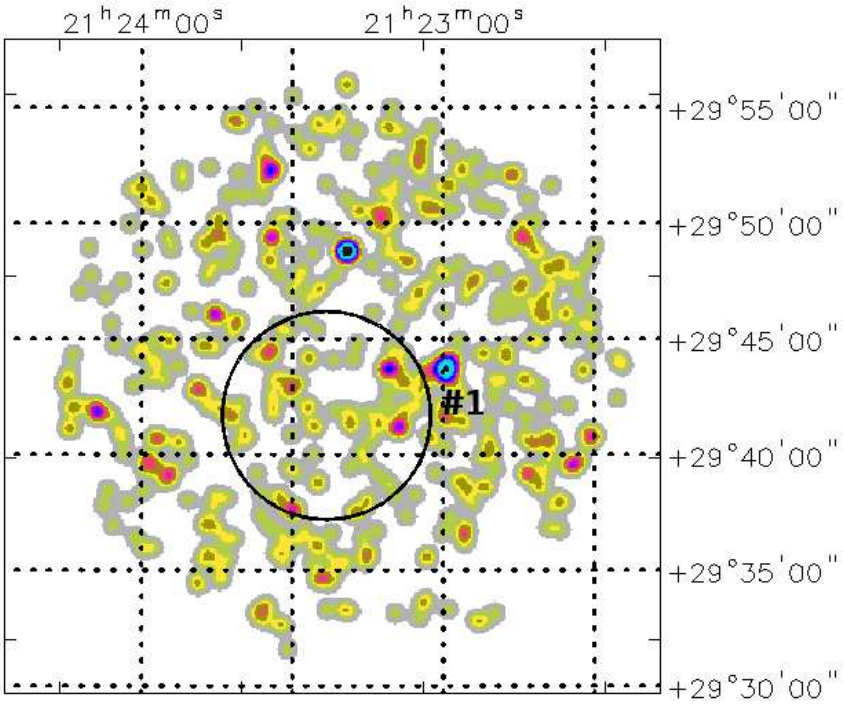

Figure 19: 0.3–10 keV XRT image of the PBC_NEW_199 field.

XRT detects an X–ray source just outside the BAT positional uncertainty (see Figure 19), which is located at:

R.A.(J2000) = $21^{\rm h}22^{\rm m}59'.30$

Dec.(J2000) = $+29^{\circ}43'44''.50$

error box = $6''.00$

It is detected at 3.9σ c.l. in the 0.3–10 keV energy range; no detection is found above 3 keV.

Multi–wavelength counterparts to this XRT detection:

- USNO–A2.0 1125–18296178 with magnitudes $B = 19.8$ and $R = 19.5$;
- AllWISE J212259.24+294341.9 with magnitudes $W1 = (15.356 \pm 0.040)$, $W2 = (14.460 \pm 0.052)$, $W3 = (11.723 \pm 0.211)$, $W4 = (8.925 \pm 0.000)$, and colours ($W1 - W2 = 0.896$, $W2 - W3 = 2.737$) typical of an active galaxy;
- *Gaia* 1848709024059091328 with magnitudes $G = (20.581 \pm 0.011)$, $BP = (20.779 \pm 0.104)$, and $RP = (19.736 \pm 0.065)$
  ($BP - RP = 1.043$).

The fit with a simple power law ($N_{\rm H(Gal)} = 1.23 \times 10^{21}$ cm^{-2}) provides a photon index $\Gamma = (1.87 \pm 0.99)$ and a 2–10 keV flux of $\sim 2.3 \times 10^{-13}$ erg cm^{-2} s^{-1}.

The source is likely a QSO candidate, since it is listed as such in a number of catalogues: i.e., the "Finding QSOs behind the Galactic Plane. I. The GPQ catalogue" (Fu et al. 2021), the "Catalogue of QSO candidates with *Gaia* EDR3" (Wu et al. 2023), and "The *WISE* AGN candidates catalogues" (Assef et al. 2018). The photometric redshift is $z = 0.637$ (Fu et al. 2021). No radio detection has been reported so far.

PBC_NEW_212

Source position:

- R.A.(J2000) = $14^h52^m44'.37$
- Dec.(J2000) = $-13°16'35''.20$
- Positional uncertainty = $4'.646$

One XRT observation available:

1. obscode: 00096662001
   observation date: 25/12/2022
   exposure: 2211 s

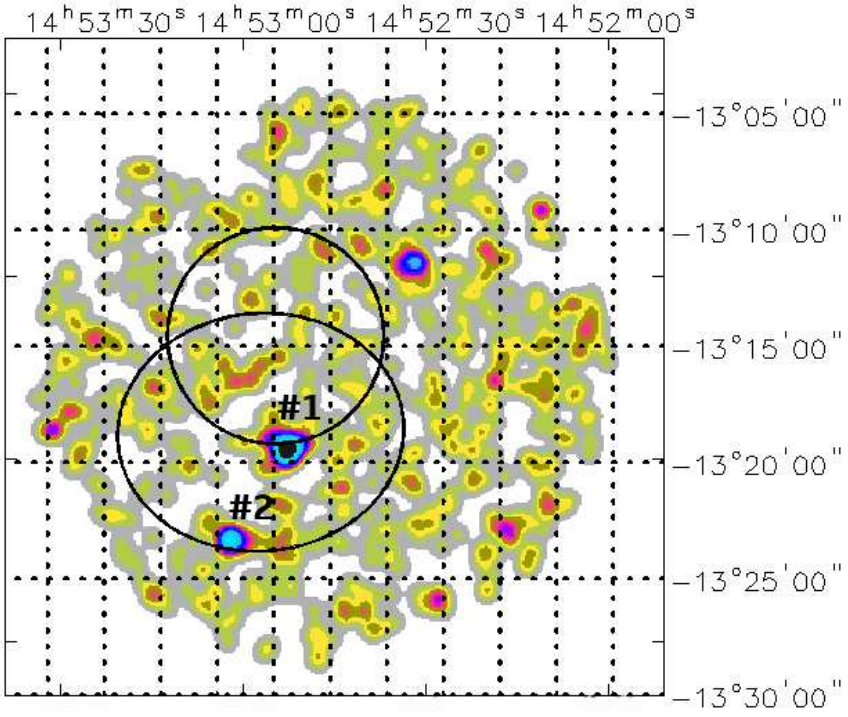

Figure 20: 0.3–10 keV XRT image of the PBC_NEW_212 field.

As shown in Figure 20, the BAT positional uncertainty partially overlaps the error ellipse of the *Fermi* source 4FGL J1453.0–1318 that was associated with the radio source TXS 1450–131 (source #1). Its X–ray position is:

R.A.(J2000) = $14^h52^m57'.46$

Dec.(J2000) = $-13^{\circ}19'26''.37$

error box = $4''.72$

It is detected at 6.7σ and 3.3σ c.l. in the 0.3–10 keV energy range and above 3 keV, respectively.

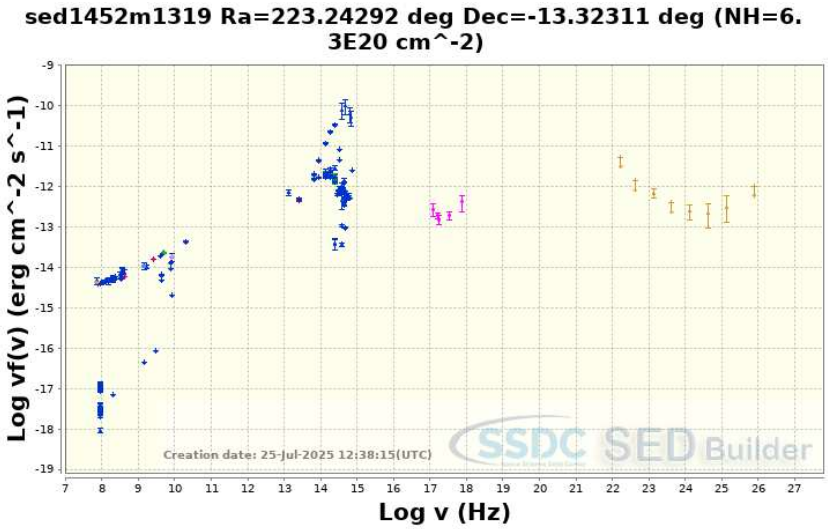

Figure 21: SED of TXS 1450–131. See text for details.

Its X–ray spectrum is consistent with a power law passing through Galactic absorption ($N_{\rm H(Gal)} = 6.26 \times 10^{20}$ cm^{-2}) characterised by a photon index $\Gamma = \left(1.61^{+0.48}_{-0.46}\right)$ and a 2–10 keV flux of $\sim$7.8 $\times$ 10^{-13} erg cm^{-2} s^{-1}.

Optically, it is still unclassified since it has been studied only at radio frequencies. Most likely, it is a blazar of the flat–spectrum QSO type (Healey et al. 2007). Its broad–band Spectral Energy Distribution (SED), from ASI/SSDC builder (available at: `https://tools.ssdc.asi.it/SED/`) and depicted in Figure 21, suggests a Compton peak in the MeV region as expected in FSRQs. Alternatively, the source may be a radio galaxy, as the VLASS image (see Figure 22) suggests some extention in the radio morphology. Indeed, recently, Paliya et al. (2024) suggest the source to be a FRII radio galaxy with LAS of $12''.1$ and a low core dominance of 0.038.

Within the positional uncertainty of the *Fermi* source there is another X–ray source (source #2 in Figure 20), which is located at:

R.A.(J2000) = $14^{\rm h}53^{\rm m}07'.70$

Dec.(J2000) = $-13^{\circ}23'18''.20$

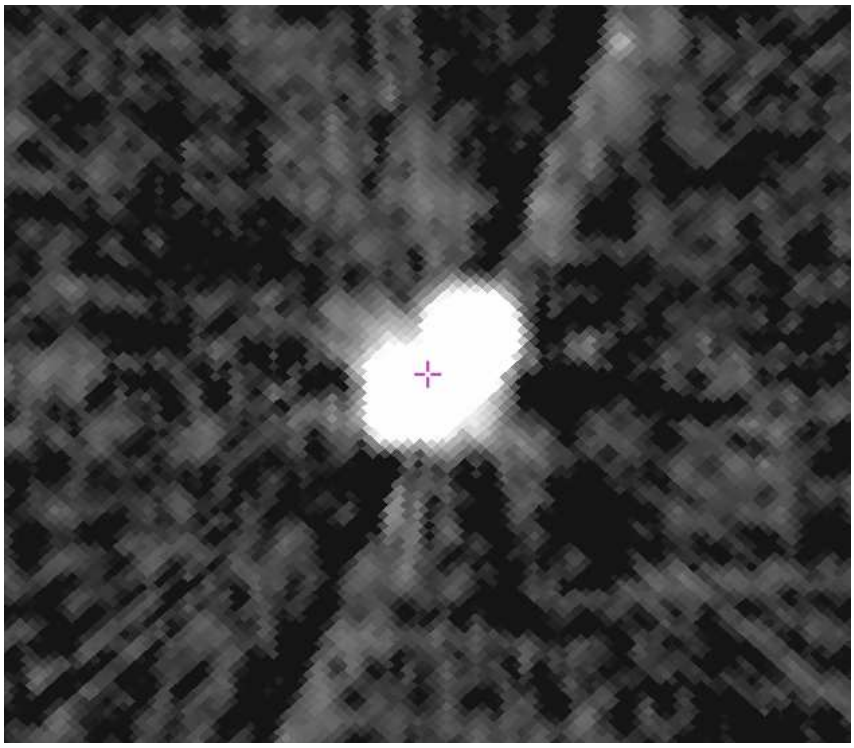

Figure 22: Radio image of TXS 1450–131 from VLASS.

error box = $5''.70$

It is detected at 4.4σ and at 2.5σ c.l. in the 0.3–10 keV energy range and above 3 keV, respectively.

Multi–wavelength counterparts to this XRT detection:

- USNO–B1.0 0766–0306818 with magnitudes $B2 = 20.66$, $R1 = 18.65$, and $R2 = 18.67$;
- USNO–B1.0 0766–0306824 with magnitudes $B2 = 19.90$ and $R1 = 19.17$;
- 2MASS J14530752–1323195 with magnitudes $J = (16.126 \pm 0.107)$, $H = (15.491 \pm 0.104)$, and $K = (15.301 \pm 0.185)$;
- AllWISE J145307.51–132319.1 with magnitudes $W1 = (15.083 \pm 0.037)$, $W2 = (15.121 \pm 0.105)$, $W3 = (12.301 \pm 0.000)$, $W4 = (9.071 \pm 0.000)$, and colours ($W1 - W2 = -0.038$, $W2 - W3 = 2.820$);
- *Gaia* 6311411560519677184 with magnitudes $G = (18.636 \pm 0.004)$, $BP = (19.842 \pm 0.100)$, and $RP = (17.693 \pm 0.028)$
  ($BP - RP = 2.150$).

In this case, from the X–ray data we find a 2–10 keV flux of $\sim 1.9 \times 10^{-12}$ erg cm^{-2} s^{-1} by assuming a power law continuum, with a flat photon index $\Gamma = \left(0.29^{+0.93}_{-0.87}\right)$, passing through Galactic absorption ($N_{\rm H(Gal)} = 6.26 \times 10^{20}$ cm^{-2}). If we fix the photon index to 1.8, the data, although of low statistical quality, show the presence of an intrinsic absorber $N_{\rm H(int)} = \left(1.36^{+2.56}_{-0.89}\right) \times 10^{20}$ cm^{-2};

the 2–10 keV flux is $\sim 8 \times 10^{-13}$ erg cm^{-2} s^{-1}.

This source is probably unrelated to PBC_NEW_212, as well as to the *Fermi* object, pointing to TXS 1450–131 as the most likely counterpart to both high–energy emitters.

PBC_NEW_215

Source position:

- R.A.(J2000) = $23^h44^m10'.33$
- Dec.(J2000) = $+11°44'13''.40$
- Positional uncertainty = $4'.6114$

One XRT observation available:

1. obscode: 00096663001
   observation date: 18/11/2022
   exposure: 1592 s

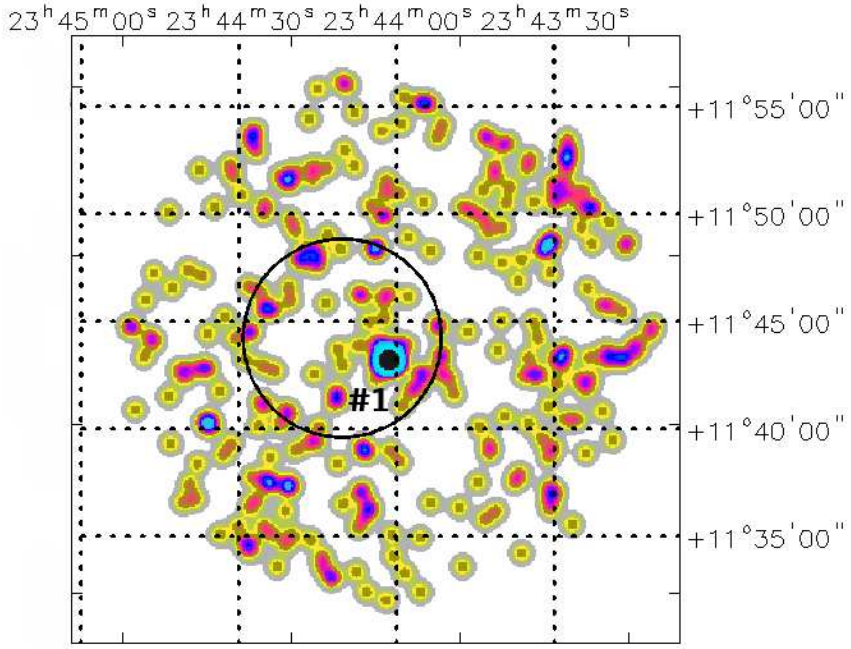

Figure 23: 0.3–10 keV XRT image of the PBC_NEW_215 field.

The only X–ray source detected by XRT within the BAT error circle (see Figure 23) is located at:

R.A.(J2000) = $23^h44^m01'.39$

Dec.(J2000) = $+11°43'10''.35$

error box = $5''.02$

It is detected at 6.3σ and 3.9σ c.l. in the 0.3–10 keV energy range and above 3 keV, respectively.

Multi–wavelength counterparts to this XRT detection:

- USNO–B1.0 1017–0692925 with magnitudes $B2 = 20.62$, $R1 = 19.10$, and $R2 = 19.03$;
- AllWISE J234401.32+114311.5 with magnitudes $W1 = (13.470 \pm 0.025)$, $W2 = (12.479 \pm 0.024)$, $W3 = (10.037 \pm 0.077)$, $W4 = (7.866 \pm 0.171)$, and colours ($W1 - W2 = 0.991$, $W2 - W3 = 2.442$) typical of an AGN;

The XRT data modelled with a simple power law ($N_{\rm H(Gal)} = 4.58 \times 10^{20}$ cm^{-2}) provide a flat photon index $\Gamma = (0.46 \pm 0.42)$ and a 2–10 keV flux of $\sim 3.3 \times 10^{-12}$ erg cm^{-2} s^{-1}. If the photon index is frozen to 1.8, we can estimate an intrinsic absorption $N_{\rm H(int)} = \left(1.00^{+0.71}_{-0.46}\right) \times 10^{22}$ cm^{-2} and a 2–10 keV flux of $\sim 1.8 \times 10^{-12}$ erg cm^{-2} s^{-1}.

The source is likely an AGN/QSO candidate at photometric redshift $z = (0.409 \pm 0.056)$ (Duncan 2022); however, no radio emission has been reported so far.

PBC_NEW_221

Source position:

- R.A.(J2000) = $18^h21^m11'.94$
- Dec.(J2000) = $+76°57'49''.90$
- Positional uncertainty = $4'.7380$

One XRT observation available:

1. obscode: 00096669001
   observation date: 26/03/2023
   exposure: 1720 s

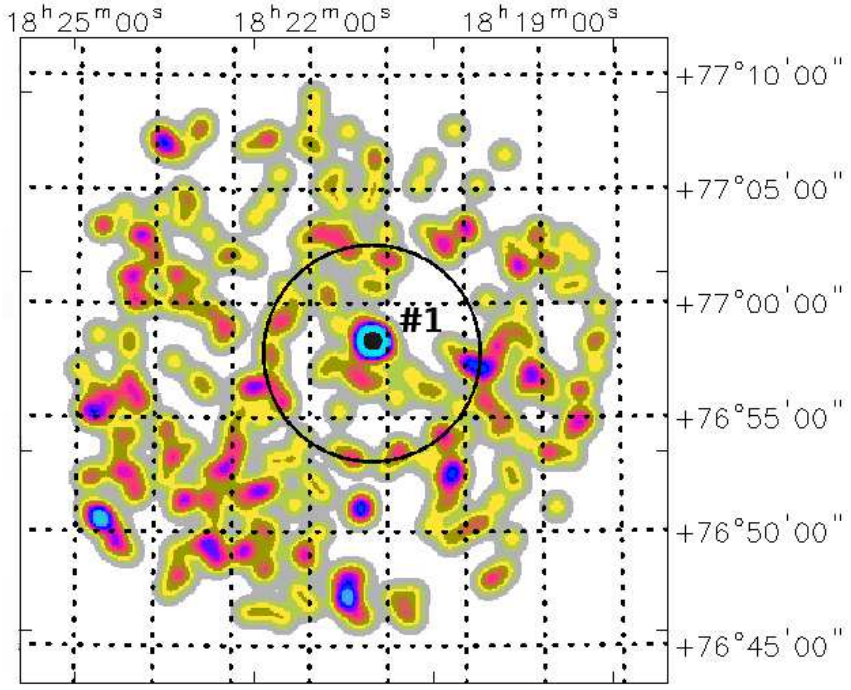

Figure 24: 0.3–10 keV XRT image of the PBC_NEW_221 field.

XRT detects only one X–ray source within the BAT positional uncertainty (see Figure 24), which is located at:

R.A.(J2000) = $18^h21^m10'.46$

Dec.(J2000) = $+76^{\circ}58'22''.42$

error box = $6''.41$

It is detected at 3.8σ and 3.4σ c.l. in the 0.3–10 keV energy range and above 3 keV, respectively.

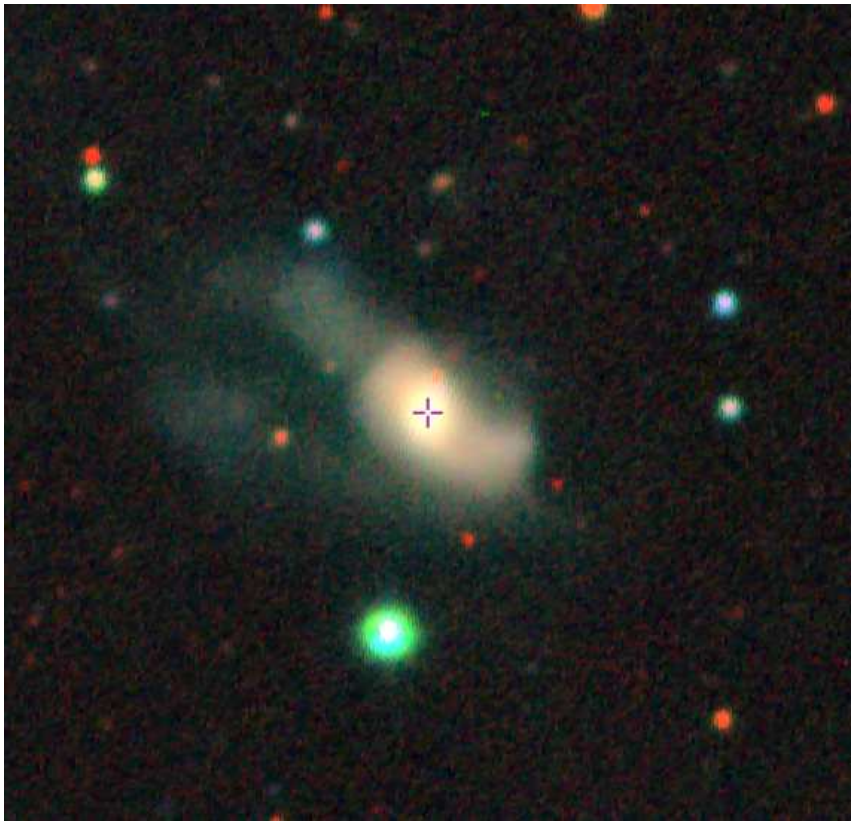

Figure 25: Optical image of source #1 from BASS.

Multi–wavelength counterparts to this XRT detection:

- USNO–A2.0 1650–02029482 with magnitudes $B = 15.1$ and $R2 = 12.0$;
- 2MASS J18211160+7658170 with magnitudes $J = (14.617 \pm 0.094)$, $H = (13.968 \pm 0.106)$, and $K = (13.252 \pm 0.071)$;
- 2MASX J18211166+7658168 with magnitudes $J = (13.201 \pm 0.063)$, $H = (12.571 \pm 0.091)$, and $K = (12.086 \pm 0.079)$;
- AllWISE J182111.63+765817.0 with magnitudes $W1 = (11.658 \pm 0.023)$, $W2 = (10.745 \pm 0.020)$, $W3 = (7.902 \pm 0.018)$, $W4 = (5.412 \pm 0.032)$, and colours ($W1 - W2 = 0.913$, $W2 - W3 = 2.843$) typical of an AGN candidate;

- *Gaia* 2269494258608614144 with magnitudes $G = (19.781 \pm 0.016)$, $BP = (17.943 \pm 0.057)$, and $RP = (16.480 \pm 0.051)$
  $(BP - RP = 1.463)$;
- GALEX J182111.2+765817 with magnitude $NUV = (20.203 \pm 0.209)$;
- SRGA J18211+765816 with a flux F(4–12 keV) $\sim 1.7 \times 10^{-12}$ erg cm^{-2} s^{-1};
- VLASS1QLCIR J182111.52+765816.6 with Ftot(2000–4000 MHz) $= (1.116 \pm 0.306)$ mJy.

By fitting the X–ray data with a power law passing through Galactic absorption ($N_{\rm H(Gal)} = 4.92 \times 10^{20}$ cm^{-2}), we find a photon index $\Gamma = \left(-0.17^{+0.71}_{-0.82}\right)$ and a 2–10 keV flux of $\sim 2 \times 10^{-12}$ erg cm^{-2} s^{-1}. If we fix the photon index to 1.8, we measure an intrinsic column density $N_{\rm H(int)} = \left(3.84^{+4.25}_{-1.89}\right) \times 10^{22}$ cm^{-2} and a 2–10 keV flux of $\sim 1.1 \times 10^{-12}$ erg cm^{-2} s^{-1}.

The source is classified as a galaxy (LEDA 2772547) at photometric redshift $z = 0.063$ (Flesch 2024). It has an unusual optical morphology, as shown in Figure 25 from BASS.
All source characteristics point to a type 1 AGN.

PBC_NEW_229

Source position:

- R.A.(J2000) = $08^h18^m03'.90$
- Dec.(J2000) = $+35°16'13''.30$
- Positional uncertainty = $4'.4058$

One XRT observation available:

1. obscode: 00096675001
   observation date: 20/01/2023
   exposure: 2090 s

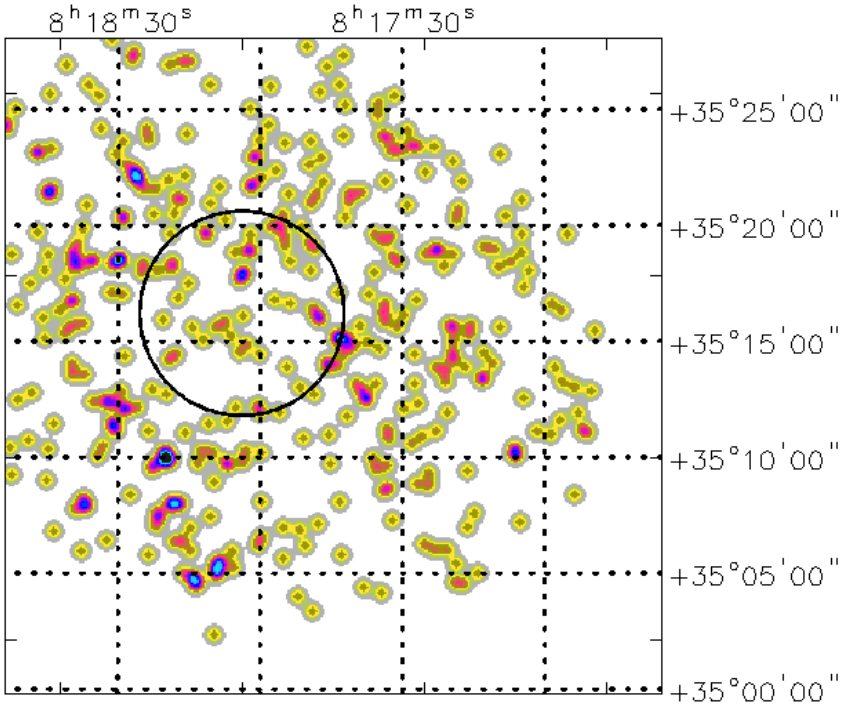

Figure 26: 0.3–10 keV XRT image of the PBC_NEW_229 field.

No X–ray source is detected by XRT in the region surrounding PBC_NEW_229 (see Figure 26), nor other X–ray sources are reported in the archives.

PBC_NEW_230

Source position:

- R.A.(J2000) = $04^{h}30^{m}46'.05$
- Dec.(J2000) = $+28^{\circ}03'31''.00$
- Positional uncertainty = $4'.3982$

Nineteen XRT observations available:

1. obscode: 03111950001
   observation date: 20/07/2022
   exposure: 364 s
2. obscode: 0311950003
   observation date: 16/19/2022
   exposure: 173 s
3. obscode: 03111950005
   observation date: 31/10/2022
   exposure: 493 s
4. obscode: 03111950007
   observation date: 04/11/2022
   exposure: 386 s
5. obscode: 00096676001
   observation date: 13/12/2022
   exposure: 1577 s
6. obscode: 03111950009
   observation date: 21/12/2022
   exposure: 118 s
7. obscode: 00096676002
   observation date: 25/12/2022
   exposure: 401 s
8. obscode: 03111950011
   observation date: 08/01/2023
   exposure: 822 s
9. obscode: 03111950013
   observation date: 13/01/2023
   exposure: 213 s

10. obscode: 03111950015
    observation date: 21/01/2023
    exposure: 115 s
11. obscode: 03111950017
    observation date: 18/02/2023
    exposure: 1038 s
12. obscode: 03111950019
    observation date: 24/02/2023
    exposure: 1657 s
13. obscode: 03111950021
    observation date: 02/04/2023
    exposure: 3789 s
14. obscode: 03111950023
    observation date: 04/04/2023
    exposure: 945 s
15. obscode: 0311195025
    observation date: 05/04/2023
    exposure: 1301 s
16. obscode: 03111950027
    observation date: 06/04/2023
    exposure: 2287 s
17. obscode: 03111950029
    observation date: 07/04/2023
    exposure: 598.0
18. obscode: 03111950031
    observation date: 09/04/2023
    exposure: 2071. s
19. obscode: 03111950032
    observation date: 28/07/2023
    exposure: 1635 s

This source is also listed in the *Swift*/BAT 157–month catalogue as SWIFT J0430.7+2809, whose coordinates are:

- R.A.(J2000) = $04^{\rm h}30^{\rm m}43'.25$
- Dec.(J2000) = $+28^{\circ}09'28''.10$
- Positional uncertainty = $5'.54$

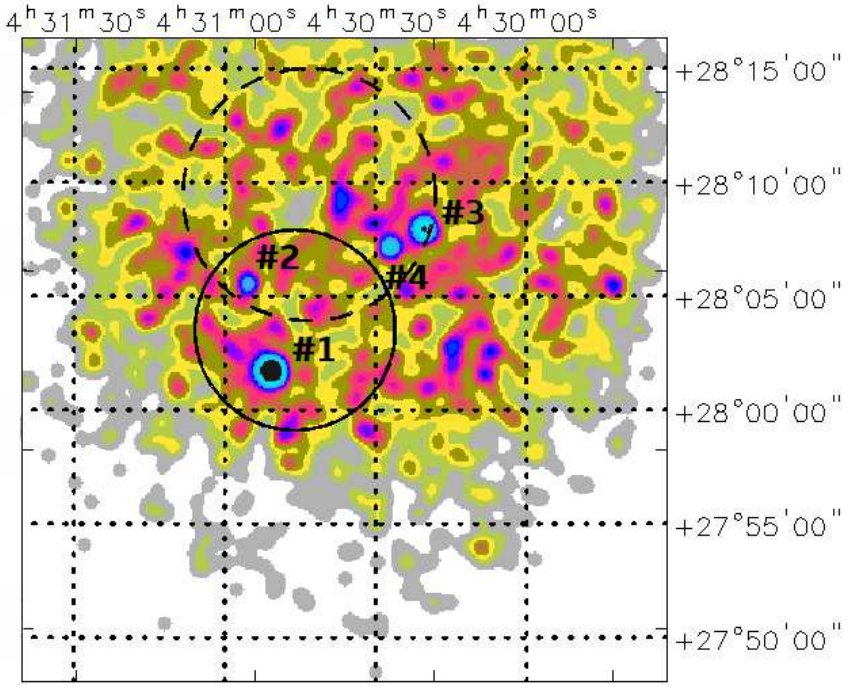

Figure 27: 0.3–10 keV XRT image of the PBC_NEW_230 field.

As shown in Figure 27, XRT detects four X–ray sources in the region surrounding PBC_NEW_230:

➢ Source #1 lies within the PBC_NEW_230 error circle and is located at:

R.A.(J2000) = $04^{h}30^{m}50'.67$

Dec.(J2000) = $+28^{\circ}01'43''.05$

error box = $4''.01$

It is detected at 10.4σ and 5.5σ c.l. in the 0.3–10 keV energy range and above 3 keV, respectively.

➢ Source #2 falls inside both the PBC_NEW_230 and SWIFT J0430.7+2809 error circles and is located at:

R.A.(J2000) = $04^{h}30^{m}55'.30$

Dec.(J2000) = $+28^{\circ}05'31''.70$

error box = $6''.00$

It is detected at 3.7σ c.l. in the 0.3–10 keV energy range and is not revealed above 3 keV.

➢ Source #3 is located inside the error circle of SWIFT J0430.7+2809 at:

R.A.(J2000) = $04^{h}30^{m}20'.48$

Dec.(J2000) = $+28°07'53''.64$

error box = $4''.19$

It is detected at 6.3σ c.l. in the 0.3–10 keV energy range, but not above 3 keV.

➢ Source #4 lies within the error circle of SWIFT J0430.7+2809 and is located at:

R.A.(J2000) = $04^{h}30^{m}27'.00$

Dec.(J2000) = $+28°07'11''.03$

error box = $6''.0$

It is detected at 4.5σ and 3.4σ c.l. in the 0.3–10 keV energy range and above 3 keV, respectively.

To discriminate which of these X–ray detections might be the likely counterpart to the BAT high–energy emitter, we extracted the XRT image above 3 keV (see Figure 28). As can be seen in the Figure, only two sources are still detected above 3 keV: source #1 and source #4.

Multi–wavelength counterparts to these XRT detections are:

➢ Source #1

- USNO–A2.0 1125–01665573 with magnitudes $B = 19.3$ and $R = 18.7$;
- AllWISE J043050.70+280142.8 with magnitudes $W1 = (14.112 \pm 0.029)$, $W2 = (13.021 \pm 0.031)$, $W3 = (10.343 \pm 0.106)$, $W4 = (8.087 \pm 0.348)$, and colours of an AGN candidate ($W1 - W2 = 1.091$, $W2 - W3 = 2.678$);
- *Gaia* 152619463841036544 with magnitudes $G = (18.817 \pm 0.008)$, $BP = (19.494 \pm 0.058)$, and $RP = (17.978 \pm 0.037)$
  ($BP - RP = 1.516$);
- *Gaia* 152619669999467776 with magnitudes $G = (19.611 \pm 0.005)$, $BP = (20.593 \pm 0.140)$, and $RP = (18.672 \pm 0.052)$
  ($BP - RP = 1.921$).

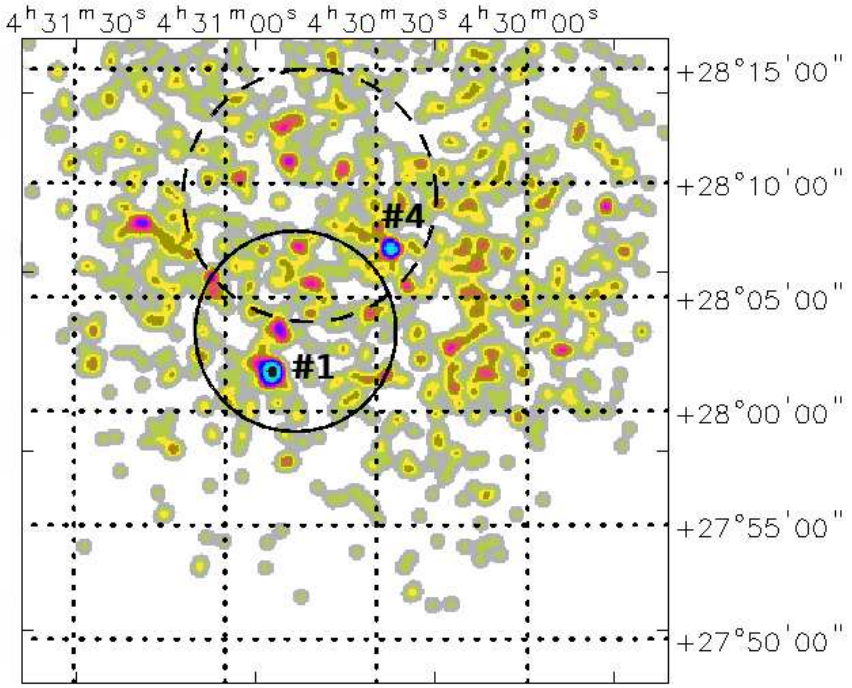

Figure 28: XRT image of the PBC_NEW_230 field above 3 keV.

The fit with a simple power law ($N_{\mathrm{H(Gal)}} = 1.65 \times 10^{21}$ cm^{-2}) shows a photon index $\Gamma = (1.38 \pm 0.31)$ and a 2–10 keV flux of $\sim 3 \times 10^{-13}$ erg cm^{-2} s^{-1}.

This source is probably a QSO candidate, as it is listed, for example, in the "Catalogue of QSO candidates with *Gaia* EDR3" (Wu et al. 2023) and the "Large Quasar Astrometric Catalogue 6, LQAC–6" (Souchay et al. 2024); its photometric redshift is $z = 1.39$ (Fu et al. 2021).

➢ Source #4

- USNO–A2.0 1125–01662903 with magnitudes $B = 19.5$ and $R = 15.9$;
- 2MASS J04302710+2807073 with magnitudes $J = (14.572 \pm 0.069)$, $H = (13.699 \pm 0.080)$, and $K = (12.853 \pm 0.064)$;
- 2MASX J04302705+2807071 with magnitudes $J = (13.108 \pm 0.059)$, $H = (12.055 \pm 0.058)$, and $K = (11.571 \pm 0.058)$;
- AllWISE J043027.10+280707.3 with magnitudes $W1 = (11.142 \pm 0.022)$, $W2 = (9.787 \pm 0.020)$, $W3 = (6.402 \pm 0.016)$, $W4 = (3.738 \pm 0.0030)$, and colours typical of an active nucleus ($W1 - W2 = 1.355$, $W2 - W3 = 3.385$);
- *Gaia* 152668018447579392 with magnitudes $G = (20.836 \pm 0.028)$, $BP = (19.532 \pm 0.085)$, and $RP = (17.060 \pm 0.089)$
  ($BP - RP = 2.472$);
- NVSS J043027+280707 with flux density $S(1.4\ \mathrm{GHz}) = (48.8 \pm 4.5)$ mJy;
- GLEAM–X J043027.1+280707;

- VLASS1QLCIR J043027.06+280707.4 with flux Ftot(2000–4000 MHz) $= (23.324 \pm 0.451)$ mJy;
- TGSSADR J043027.1+280708 with flux density $S(150\ \mathrm{MHz}) = (180.8 \pm 23.2)$ mJy;
- RACS–MID J043027.0+280706 with flux Ftot(1367.5 MHz)= 49.9 mJy;
- RACS–HIGH J043027+280 with flux Ftot(1655.5 MHz)= 41.2 mJy.

From the XRT data we infer a 2–10 keV flux of $\sim 7 \times 10^{-13}$ erg cm^{-2} s^{-1} by assuming a power law continuum (photon index Γ $\sim$–1.7) passing through Galactic absorption ($N_{\mathrm{H(Gal)}} = 1.63 \times 10^{21}$ cm^{-2}). If we freeze the photon index to 1.8, tha data show evidence, although the poor statistics, of extra absorption $N_{\mathrm{H(int)}} = \left(51.8^{+37.0}_{-25.0}\right) \times 10^{21}$ cm^{-2}; the 2–10 keV flux is $\sim 4.5 \times 10^{-13}$ erg cm^{-2} s^{-1}.

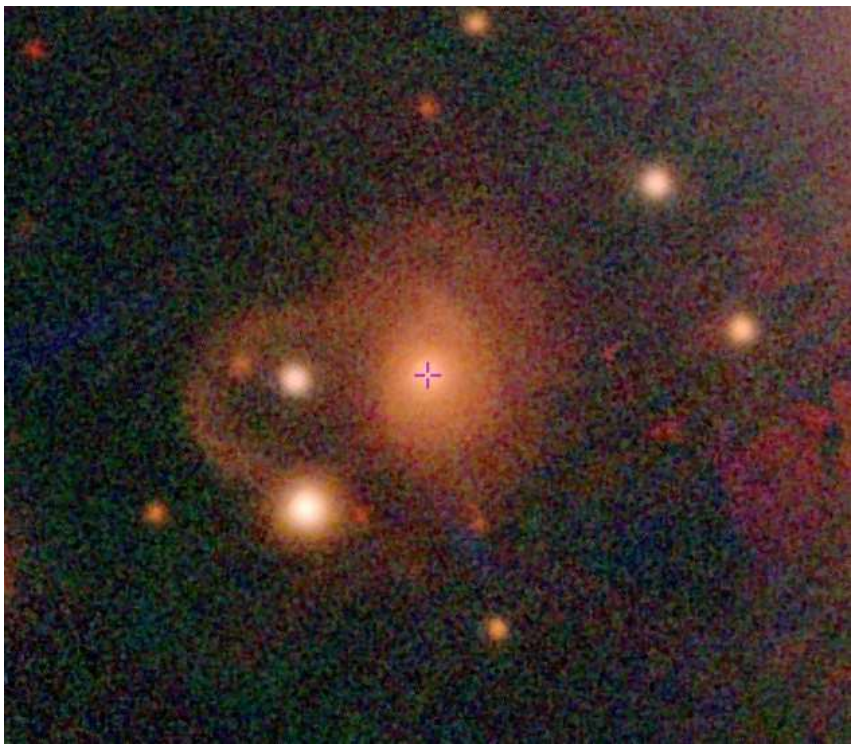

Figure 29: Optical image of source #4 from Pan–STARRS.

The source is identified with the galaxy LEDA 5060720/IRAS F04273+2800 at redshift $z = (0.05953 \pm 0.00007)$. It is a relatively strong radio source, variable at 1.4 GHz (Ofek et al. 2011); optically, it is most likely a type 1 AGN (Zaw et al. 2019) with a peculiar morphology (see Figure 29).

Both source #1 and #4 have the characteristics to be likely counterparts to this high–energy emitter and we cannot exclude, at this stage, that both contribute to the emission above 10 keV; ideally, a *NuSTAR* observation could discriminate among the two.

PBC_NEW_237

Source position:

- R.A.(J2000) = $20^{h}03^{m}08'.26$
- Dec.(J2000) = $-22^{\circ}26'26''.80$
- Positional uncertainty = $4'.24$

Sixteen XRT observations available:

1. obscode: 00096677001
   observation date: 08/03/2023
   exposure: 1978 s
2. obscode: 03111991004
   observation date: 10/07/2024
   exposure: 167 s
3. obscode: 03111991005
   observation date: 21/08/2024
   exposure: 182 s
4. obscode: 03111991006
   observation date: 11/09/2024
   exposure: 552 s
5. obscode: 03111991007
   observation date: 21/09/2024
   exposure: 540 s
6. obscode: 03111991008
   observation date: 26/10/2024
   exposure: 529 s
7. obscode: 03111991009
   observation date: 14/11/2024
   exposure: 631 s
8. obscode: 03111991010
   observation date: 16/11/2024
   exposure: 1892 s
9. obscode: 03111991011
   observation date: 18/11/2024
   exposure: 1681 s

10. obscode: 03111991012
    observation date: 21/11/2024
    exposure: 145 s

11. obscode: 03111991013
    observation date: 25/11/2024
    exposure: 1227 s

12. obscode: 03111991014
    observation date: 27/11/2024
    exposure: 534 s

13. obscode: 03111991016
    observation date: 06/03/2025
    exposure: 606 s

14. obscode: 03111991017
    observation date: 08/03/2025
    exposure: 127 s

15. obscode: 03111991018
    observation date: 30/04/2025
    exposure: 394 s

16. obscode: 03111991019
    observation date: 09/05/2025
    exposure: 172 s

This source is also listed in the *Swift*/BAT 157–month catalogue as SWIFT J2003.2–2225, whose coordinates are:

- R.A.(J2000) = $20^{\rm h}03^{\rm m}09'.26$
- Dec.(J2000) = $-22^\circ25'25''.00$
- Positional uncertainty = $5'.69$

As can be seen from Figure 30, XRT detects two X–ray sources in the region surrounding PBC_NEW_237:

➢ Source #1 lies within both the PBC_NEW_237 and SWIFT J2003.2–2225 error circles and is located at:

R.A.(J2000) = $20^{\rm h}03^{\rm m}17'.51$

Dec.(J2000) = $-22^\circ25'49''.91$

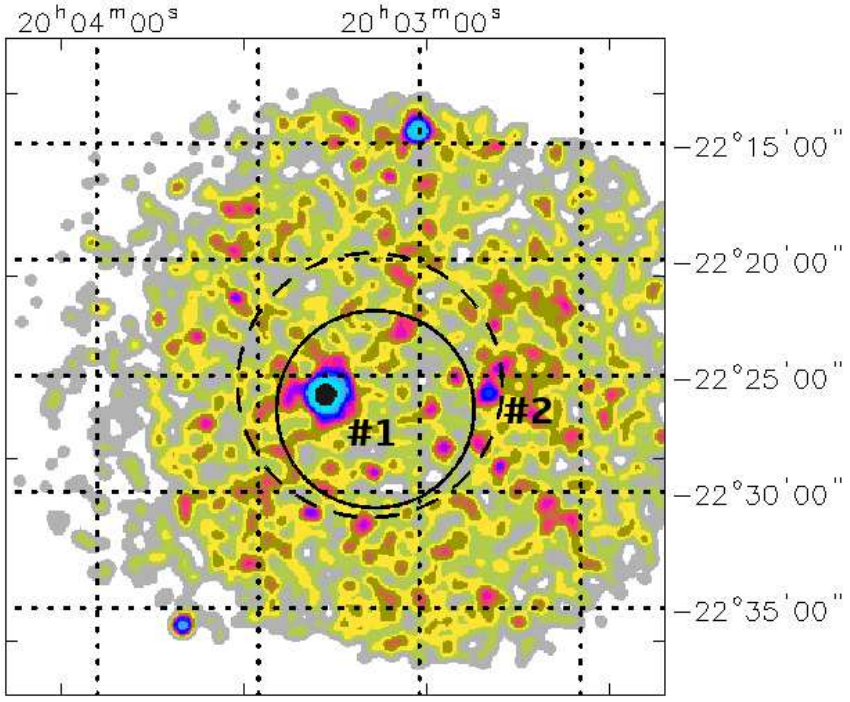

Figure 30: 0.3–10 keV XRT image of the PBC_NEW_237 field.

error box = $3''.61$

It is detected at 25.3σ and 14.1σ c.l. in the 0.3–10 keV energy range and above 3 keV, respectively.

Multi–wavelength counterparts to this XRT detection:

- USNO–A2.0 0675–34797159 with magnitudes $B = 17.2$ and $R = 18.0$;
- 2MASS J20031748–2225486 with magnitudes $J = (16.354 \pm 0.106)$, $H = (16.052 \pm 0.141)$, and $K = (15.432 \pm 0.000)$;
- AllWISE J200317.48–222549.4 with magnitudes $W1 = (15.212 \pm 0.042)$, $W2 = (14.835 \pm 0.082)$, $W3 = (11.860 \pm 0.000)$, $W4 = (8.775 \pm 0.000)$, and borderline AGN colours ($W1 - W2 = 0.377$, $W2 - W3 = 2.975$), more typical of a low–luminosity or absorbed galaxy;
- *Gaia* 6852210001071552512 with magnitudes $G = (17.046 \pm 0.006)$, $BP = (17.169 \pm 0.022)$, and $RP = (16.777 \pm 0.018)$
  ($BP - RP = 0.392$);
- GALEX J200317.4–222548 with magnitudes $FUV = (18.402 \pm 0.065)$ and $NUV = (18.158 \pm 0.039)$;
- 1RXS J200317.6–222603 (also 6dFGS J2003175–222549) with flux F(0.2–2.4 keV) $= (2.08 \pm 0.46) \times 10^{-12}$ erg cm^{-2} s^{-1};
- XMMSL3 J200317.2–222545 with flux F(0.2–12 keV) $= (3.32 \pm 1.35) \times 10^{-12}$ erg cm^{-2} s^{-1}.

The fit with a power law passing through Galactic absorption ($N_{\rm H(Gal)} = 7.62 \times 10^{20}$ cm^{-2}) does not provide a good fit to the data, as a hint of the presence of extra absorption and an excess below 1 keV is evident in the residuals to the data. We then modelled the data by adopting a primary absorbed power law component plus a power law, having the same photon index and absorbed only by Galactic column density. This model, required at a c.l. higher than 99.99%, provides an intrinsic column density $N_{\rm H(int)} = \left(5.60^{+3.78}_{-2.00}\right) \times 10^{22}$ cm^{-2} and a photon index $\Gamma = \left(1.95^{+0.23}_{-0.24}\right)$; the 2–10 keV flux is $\sim$3.5 $\times$ 10^{-12} erg cm^{-2} s^{-1}.

Although no radio detection is reported, this source is probably an absorbed extragalactic source (QSO?), possibly at redshift $z = 0.8$ (Flesch 2024; see also Mahony et al. 2010).

➢ Source #2, which lies just outside the PBC_NEW_237 error circle but inside the SWIFT J2003.2–2225 one, is located at:

R.A.(J2000) = $20^{\rm h}02^{\rm m}47'.10$

Dec.(J2000) = $-22^\circ25'43''.00$

error box = $7''.00$

It is detected at 3.4σ in the 0.3–10 keV energy range; no detection is found above 3 keV.

Multi–wavelength counterparts to this XRT detection:

- AllWISE J200247.22–222543.7 with magnitudes $W1 = (16.971 \pm 0.133)$, $W2 = (15.942 \pm 0.224)$, $W3 = (12.396 \pm 0.000)$, $W4 = (8.470 \pm 0.000)$, suggesting a distant (likely extragalactic) object.

A power law passing through Galactic absorption ($N_{\rm H(Gal)} = 7.51 \times 10^{20}$ cm^{-2}) indicates a photon index $\Gamma = \left(1.53^{+1.00}_{-0.91}\right)$ and a 2–10 keV flux of $\sim$1 $\times$ 10^{-13} erg cm^{-2} s^{-1}.

Based on the overall properties of source #1, we can conclude that this X–ray detection is the likely counterpart to the BAT object, being source #2 dimmer and softer.

PBC_NEW_238

Source position:

- R.A.(J2000) = $08^{h}49^{m}52'.23$
- Dec.(J2000) = $-17°25'48''.30$
- Positional uncertainty = $4'.6464$

Two XRT observations available:

1. obscode: 00096678002
   observation date: 19/01/2023
   exposure: 1607 s
2. obscode: 00096678003
   observation date: 20/01/2023
   exposure: 647 s

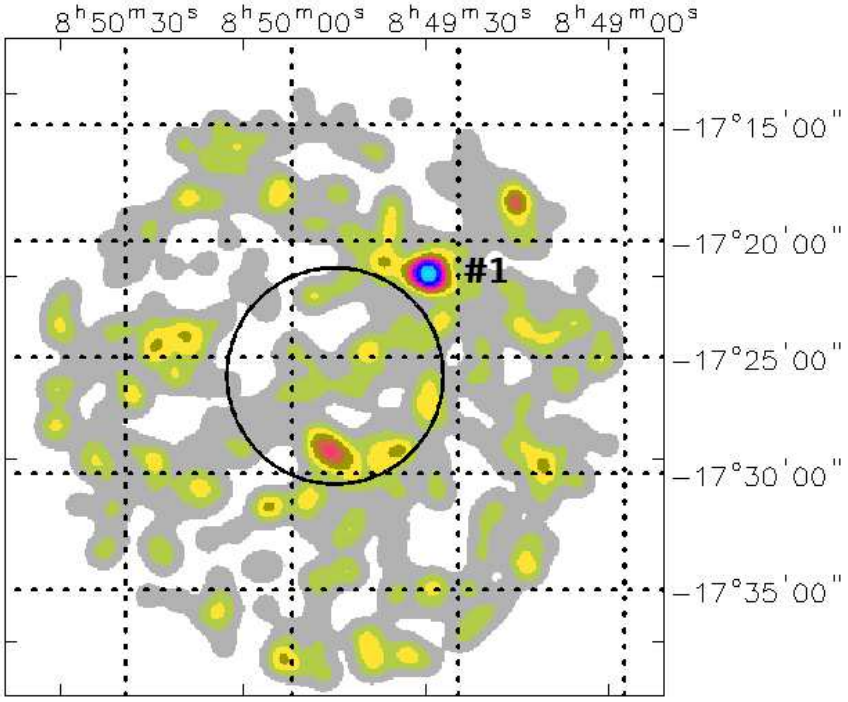

Figure 31: 0.3–10 keV XRT image of the PBC_NEW_238 field.

The only X–ray detection lies just outside the BAT positional uncertainty (see Figure 31) and is located at:

R.A.(J2000) = $08^{\rm h}49^{\rm m}35'.29$

Dec.(J2000) = $-17^{\circ}21'23''.39$

error box = $6''.21$

It is detected at 4.0σ and 2.5σ c.l. in the 0.3–10 keV energy range and above 3 keV, respectively.

Multi–wavelength counterparts to this XRT detection:

- USNO–B1.0 0726–0262165 with magnitude $R2 = 17.80$;
- USNO–B1.0 0726–0262157 with magnitudes $B2 = 18.33$, $R1 = 18.21$, and $R2 = 17.76$;
- 2MASS J08493501–1721218 with magnitudes $J = (16.171 \pm 0.085)$, $H = (15.498 \pm 0.105)$, and $K = (14.771 \pm 0.109)$;
- AllWISE J084935.02–172121.8 with magnitudes $W1 = (13.137 \pm 0.024)$, $W2 = (12.193 \pm 0.022)$, $W3 = (9.866 \pm 0.047)$, $W4 = (7.620 \pm 0.137)$, and typical AGN colours ($W1 - W2 = 0.944$, $W2 - W3 = 2.327$);
- *Gaia* 5706035198594239744 with magnitudes $G = (18.928 \pm 0.012)$, $BP = (18.811 \pm 0.040)$, and $RP = (17.523 \pm 0.020)$
  ($BP - RP = 1.288$);
- 2RXS J084935.4–172117 with flux F(0.2–2.4 keV) $\sim 1.1 \times 10^{-12}$ erg cm^{-2} s^{-1};
- 1eRASS J084934.9–172121 with flux F(0.2–2.3 keV) $\sim 3 \times 10^{-13}$ erg cm^{-2} s^{-1};
- NVSS J084934–172120 with flux density S(1.4 GHz) $= (148.9 \pm 4.5)$ mJy;
- VLASS1QLCIR J084934.98–172120.5 with flux Ftot(2000–4000 MHz) $= (81.936 \pm 0.991)$ mJy;
- RACS–MID J084934.9–172121 with flux Ftot(1367.5 MHz) = 149.3 mJy;
- RACS–HIGH J084934–17212 with flux Ftot(1655.5 MHz) = 123.0 mJy.

A power law passing through Galactic absorption ($N_{\rm H(Gal)} = 6.65 \times 10^{20}$ cm^{-2}) indicates a flat photon index $\Gamma = (0.67 \pm 0.81)$ and a 2–10 keV flux of $\sim 8.2 \times 10^{-13}$ erg cm^{-2} s^{-1}. If the photon index is frozen to 1.8, we find evidence of intrinsic absorption $N_{\rm H(int)} = \left(0.57^{+1.88}_{-0.51}\right) \times 10^{22}$ cm^{-2}; the 2–10 keV flux is $\sim 4.5 \times 10^{-13}$ erg cm^{-2} s^{-1}.

As AGN/QSO candidate, this source is listed in many catalogues such as the "Large Quasar Astrometric Catalogue 6, LQAC–6" (Souchay et al. 2024) and the "*Gaia* DR3. Cross–match with known variable objects" (Gavras et al. 2023). It is a strong radio source reported in many radio catalogues and variable at 1.4 GHz, as evident from a comparison between NVSS and FIRST data sets (Ofek et al. 2011). It is also listed as GLEAM J084935–172120, a blazar of the BL Lac type (in Simbad) following D'Abrusco et al. (2019); the photometric redshift is quoted by Fu et al. (2021) to be $z = 0.47$.

PBC_NEW_246

Source position:

- R.A.(J2000) = $20^{h}52^{m}32'.04$
- Dec.(J2000) = $-28^{\circ}08'24''.30$
- Positional uncertainty = $3'.6578$

Twentyone XRT observations available:

1. obscode: 03111993001
   observation date: 19/03/2023
   exposure: 647 s
2. obscode: 00015930001
   observation date: 20/03/2023
   exposure: 2482 s
3. obscode: 00096680001
   observation date: 22/03/2023
   exposure: 2196 s
4. obscode: 03111993003
   observation date: 02/09/2023
   exposure: 241 s
5. obscode: 03111993004
   observation date: 09/06/2024
   exposure: 421 s
6. obscode: 03111993005
   observation date: 20/06/2024
   exposure: 1223 s
7. obscode: 03111993006
   observation date: 18/09/2024
   exposure: 138 s
8. obscode: 03111993007
   observation date: 18/09/2024
   exposure: 215 s
9. obscode: 03111993008
   observation date: 11/11/2024
   exposure: 625 s

10. obscode: 03111993009
    observation date: 13/11/2024
    exposure: 347 s

11. obscode: 03111993010
    observation date: 14/11/2024
    exposure: 1491 s

12. obscode: 03111993011
    observation date: 17/11/2024
    exposure: 215 s

13. obscode: 03111993012
    observation date: 19/11/2024
    exposure: 521 s

14. obscode: 03111993013
    observation date: 20/11/2024
    exposure: 1181 s

15. obscode: 03111993014
    observation date: 21/11/2024
    exposure: 184 s

16. obscode: 03111993015
    observation date: 24/11/2024
    exposure: 564 s

17. obscode: 03111993016
    observation date: 01/12/2024
    exposure: 896 s

18. obscode: 03111993017
    observation date: 07/12/2024
    exposure: 355 s

19. obscode: 03111993018
    observation date: 09/12/2024
    exposure: 6664 s

20. obscode: 03111993019
    observation date: 10/12/2024
    exposure: 106 s

21. obscode: 03111993020
    observation date: 11/12/2024
    exposure: 4584 s

This source is also listed in the *Swift*/BAT 157–month catalogue as SWIFT J2052.3–2806, whose coordinates are:

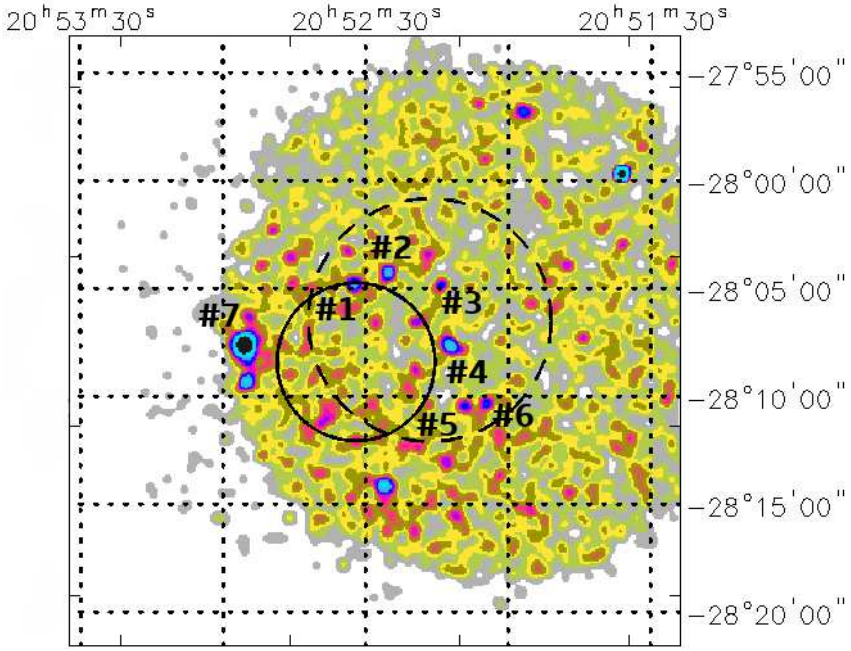

Figure 32: 0.3–10 keV XRT image of the PBC_NEW_246 field.

- R.A.(J2000) = $20^{h}52^{m}16'.54$
- Dec.(J2000) = $-28^{\circ}06'28''.10$
- Positional uncertainty = $5'.63$

As can be seen from Figure 32, XRT detects only one source located at the border of the PBC_NEW_246 positional uncertainty, which also lies within the error circle of SWIFT J2052.3–2806; this object (source #1) is located at:

R.A.(J2000) = $20^{h}52^{m}32'.20$

Dec.(J2000) = $-28^{\circ}04'45''.10$

error box = $6''.90$

It is detected at 4.0σ c.l. in the 0.3–10 keV energy range; no detection is observed above 3 keV.

Nevertheless, there are other five detections that are instead located within the error circle of SWIFT J2052.3–2806 plus a bright object (source #7 in Figure 32) that lies outside both the PBC_NEW_246 and SWIFT J2052.3–2806 positional uncertainties. These X–ray detections are located at:

➢ Source #2:

R.A.(J2000) = $20^{h}52^{m}25'.10$

Dec.(J2000) = $-28^{\circ}04'14''.50$

error box = $6''.00$

It is detected at 4.2σ c.l. in the 0.3–10 keV energy range, but is not observed above 3 keV.

➢ Source #3:

R.A.(J2000) = $20^{h}52^{m}14'.00$

Dec.(J2000) = $-28^{\circ}04'48''.90$

error box = $6''.00$

It is detected at 2.9σ c.l. in the 0.3–10 keV energy range and is not revealed above 3 keV.

➢ Source #4:

R.A.(J2000) = $20^{h}52^{m}12'.10$

Dec.(J2000) = $-28^{\circ}07'37''.50$

error box = $6''.00$

It is detected at 5.2σ and at 3.2σ c.l. in the 0.3–10 keV energy range and above 3 keV, respectively.

➢ Source #5:

R.A.(J2000) = $20^{h}52^{m}08'.90$

Dec.(J2000) = $-28^{\circ}10'26''.10$

error box = $6''.00$

It is detected at 3.0σ c.l. in the 0.3–10 keV energy range and is not revealed above 3 keV.

➢ Source #6:

R.A.(J2000) = $20^h52^m04'.30$

Dec.(J2000) = $-28^\circ10'19''.70$

error box = $6''.00$

It is detected at 2.9σ c.l. in the 0.3–10 keV energy range and is not revealed above 3 keV.

➢ Source #7:

R.A.(J2000) = $20^h52^m55'.46$

Dec.(J2000) = $-28^\circ07'38''.17$

error box = $3''.67$

It is detected at 18.0σ c.l. in the 0.3–10 keV energy range and at 11.7σ c.l. above 3 keV.

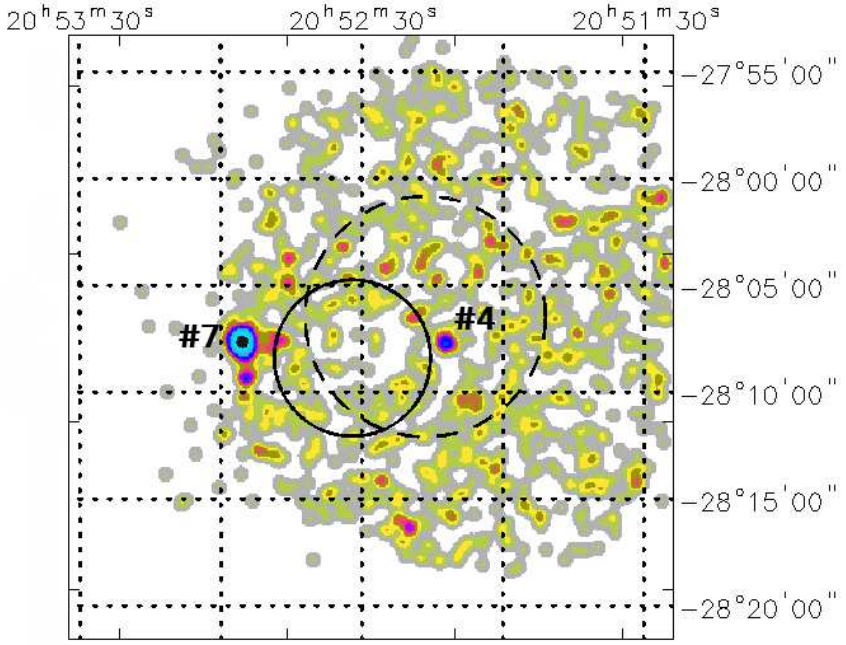

Figure 33: XRT image of the PBC_NEW_246 field above 3 keV.

We then extracted the XRT image above 3 keV (see Figure 33) to investigate which of these detections might be the likely counterpart to the BAT high–energy emitter. As can be seen in the Figure,

only two sources are still detected above 3 keV: source #4 and source #7.

Multi–wavelength counterparts to these XRT detections are:

➢ Source #4

- USNO–A2.0 0600–43097841 with magnitudes $B = 20.3$ and $R = 18.1$;
- AllWISE J205212.06–280740.9 with magnitudes $W1 = (15.235 \pm 0.039)$, $W2 = (14.476 \pm 0.054)$, $W3 = (11.898 \pm 0.343)$, $W4 = (8.313 \pm 0.000)$, and colours of an AGN candidate ($W1 - W2 = 0.759$, $W2 - W3 = 2.578$);
- *Gaia* 6795644457148836608 with magnitudes $G = (20.578 \pm 0.012)$, $BP = (20.356 \pm 0.068)$, and $RP = (19.252 \pm 0.058)$
  ($BP - RP = 1.104$);
- GALEX J205211.9–280740 with magnitude $NUV = (21.634 \pm 0.372)$.

From the X–ray data we can only infer a 2–10 keV flux of $\sim 4.8 \times 10^{-13}$ erg cm^{-2} s^{-1} by assuming a power law continuum, with photon index $\Gamma = (1.72^{+0.83}_{-1.15})$, passing through Galactic absorption ($N_{\rm H(Gal)} = 7.37 \times 10^{20}$ cm^{-2}).

Also this source is likely an AGN/QSO candidate listed in the "Large Quasar Astrometric Catalogue 6, LQAC–6" (Souchay et al. 2024); its photometric redshift is $z = 0.42$ (Barrows et al. 2021).

➢ Source #7

- USNO–A2.0 0600–43108843 with magnitudes $B = 16.4$ and $R = 15.3$;
- 2MASS J20525549–2807397 with magnitudes $J = (15.015 \pm 0.049)$, $H = (14.226 \pm 0.057)$, and $K = (13.398 \pm 0.046)$;
- 2MASX J20525548–2807400 with magnitudes $J = (14.577 \pm 0.085)$, $H = (13.733 \pm 0.087)$, and $K = (13.198 \pm 0.112)$;
- AllWISE J205255.50–280739.6 with magnitudes $W1 = (12.547 \pm 0.024)$, $W2 = (11.792 \pm 0.022)$, $W3 = (9.208 \pm 0.045)$, $W4 = (6.537 \pm 0.077)$, and colours typical of an AGN ($W1 - W2 = 0.755$, $W2 - W3 = 2.774$);
- *Gaia* 6801636829880596352 with magnitudes $G = (16.697 \pm 0.011)$, $BP = (16.732 \pm 0.028)$, and $RP = (15.741 \pm 0.020)$
  ($BP - RP = 1.288$);
- RACS–HIGH J205255–28073 with flux Ftot(1655.5 MHz) = 1.07 mJy.

The X–ray data are consistent with a power law continuum passing through Galactic absorption ($N_{\rm H(Gal)} = 7.15 \times 10^{20}$ cm^{-2}) and characterised by a flat photon index $\Gamma = (0.91 \pm 0.13)$ and a 2–10 keV flux $\sim 1.7 \times 10^{-12}$ erg cm^{-2} s^{-1}.

This source is likely a QSO candidate (Souchay et al. 2024; Liao et al. 2019) of unknown redshift; the AGN nature is also suggested by the *AllWISE* colours and radio detection.

Given its higher X–ray flux and detection significance above 3 keV, we consider source #7 as the most likely association.

PBC_NEW_250

Source position:

- R.A.(J2000) = $20^h33^m11'.52$
- Dec.(J2000) = $-17°53'54''.00$
- Positional uncertainty = $4'.6104$

One XRT observation available:

1. obscode: 00096681001
   observation date: 03/12/2022
   exposure: 1813 s

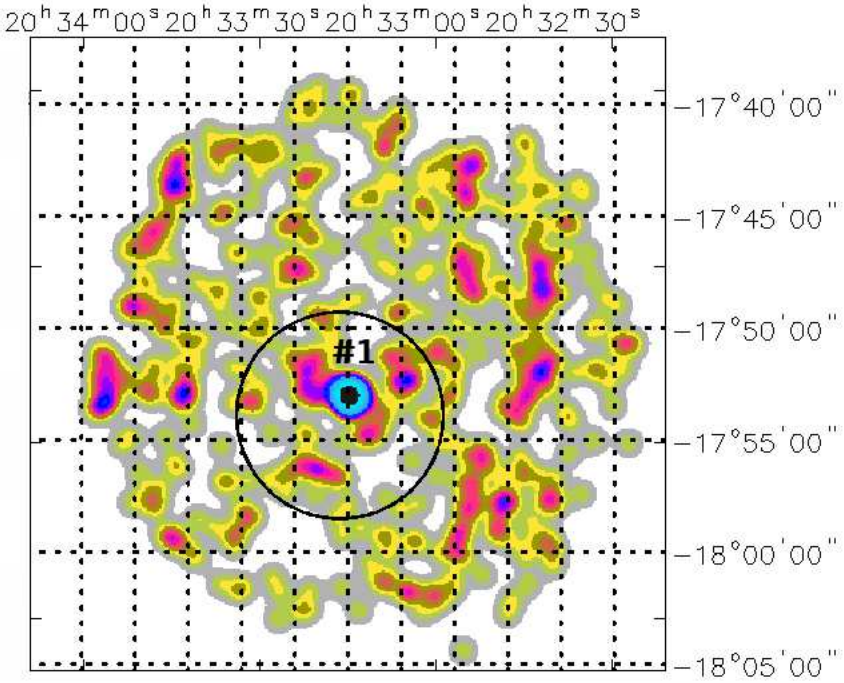

Figure 34: 0.3–10 keV XRT image of the PBC_NEW_250 field.

XRT detects only one X–ray source within the BAT positional uncertainty (see Figure 34), which is located at:

R.A.(J2000) = $20^h33^m09'.72$

Dec.(J2000) = $-17°53'01''.56$

error box = $4''.72$

It is detected at 7.2σ and 7.0σ c.l. in the 0.3–10 keV energy range and above 3 keV, respectively.

Multi–wavelength counterparts to this XRT detection:

- USNO–A2.0 0675–35567451 with magnitudes $B = 13.0$ and $R = 14.8$;
- 2MASS J20330963–1753001 with magnitudes $J = (15.063 \pm 0.071)$, $H = (14.331 \pm 0.099)$, and $K = (13.822 \pm 0.072)$;
- 2MASX J20330961–1753001 with magnitudes $J = (14.168 \pm 0.109)$, $H = (13.474 \pm 0.159)$, and $K = (12.694 \pm 0.107)$;
- AllWISE J203309.64–175300.0 with magnitudes $W1 = (12.812 \pm 0.024)$, $W2 = (12.008 \pm 0.024)$, $W3 = (8.423 \pm 0.023)$, $W4 = (5.541 \pm 0.038)$, and AGN colours ($W1 - W2 = 0.804$, $W2 - W3 = 3.585$);
- *Gaia* 6862371928052033408 with magnitudes $G = (19.750 \pm 0.009)$, $BP = (17.848 \pm 0.024)$, and $RP = (16.422 \pm 0.006)$
  ($BP - RP = 1.426$);
- GALEX J203309.6–175301 with magnitudes $FUV = (20.700 \pm 0.209)$ and $NUV = (20.155 \pm 0.153)$;
- NVSS J203309–175302 with flux density $S(1.4\ \mathrm{GHz}) = (8.9 \pm 0.5)$ mJy;
- VLASS1QLCIR J203309.66–175300.0 with flux $F\mathrm{tot}(2000\text{–}4000\ \mathrm{MHz}) = (3.180 \pm 0.504)$ mJy;
- TGSSADR J203309.8–175258 with flux density $S(150\ \mathrm{MHz}) = (38.2 \pm 8.5)$ mJy;
- RACS–MID J203309.6–175300 with flux $F\mathrm{tot}(1367.5\ \mathrm{MHz}) = 9.4$ mJy;
- RACS–HIGH J203309–17525 with flux $F\mathrm{tot}(1655.5\ \mathrm{MHz}) = 7.72$ mJy.

The fit with a power law passing through Galactic absorption ($N_{\mathrm{H(Gal)}} = 4.58 \times 10^{20}$ cm^{-2}) shows a flat photon index $\Gamma = \left(-0.85^{+0.48}_{-0.57}\right)$ and a 2–10 keV flux of $\sim 7 \times 10^{-12}$ erg cm^{-2} s^{-1}. If we freeze the photon index to 1.8, the residuals to the data indicate, although the poor statistics, the presence of extra absorption $N_{\mathrm{H(int)}} = \left(12.4^{+10.7}_{-7.0}\right) \times 10^{20}$ cm^{-2}; the 2–10 keV flux is $\sim 3.8 \times 10^{-12}$ erg cm^{-2} s^{-1}.

This source is identified with LEDA 875940, classified as a spiral galaxy with no redshift measuremets so far, although a photometric redshift $z = (0.0655 \pm 0.015)$ is available in Alam et al. (2015). The source is variable in radio at 1.4 GHz from NVSS and FIRST data sets (Ofek et al. 2011). All properties (optical extension, *AllWISE* colours, and radio detection) point to an AGN candidate.

PBC_NEW_257

Source position:

- R.A.(J2000) = $16^h58^m25'.73$
- Dec.(J2000) = $+68°51'03''.70$
- Positional uncertainty = $4'.7327$

One XRT observation available:

1. obscode: 00096683001
   observation date: 28/10/2022
   exposure: 1720 s

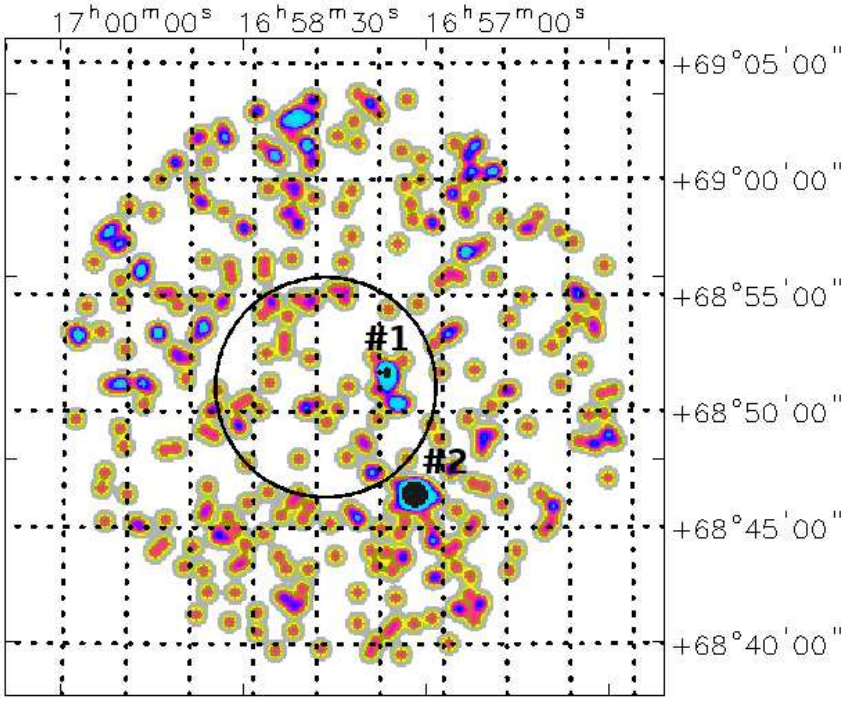

Figure 35: 0.3–10 keV XRT image of the PBC_NEW_257 field.

XRT detects two X–ray sources within the BAT positional uncertainty (see Figure 35):

➢ Source #1 is located at:

R.A.(J2000) = $16^h57^m56'.20$

Dec.(J2000) = $+68^{\circ}51'40''.00$

error box = $6''.00$

It is detected at 2.9σ c.l. in the 0.3–10 keV energy range and is not revealed above 3 keV.

Multi–wavelength counterparts to this XRT detection:

- USNO–B1.0 1588–0137997 with magnitudes $B1 = 20.23$, $B2 = 20.15$, and $R2 = 20.40$;
- AllWISE J165756.94+685139.9 with magnitudes $W1 = (15.258 \pm 0.041)$, $W2 = (14.360 \pm 0.032)$, $W3 = (11.254 \pm 0.073)$, $W4 = (8.802 \pm 0.211)$, and AGN colours ($W1 - W2 = 0.898$, $W2 - W3 = 3.106$);
- *Gaia* 1649026786057381632 with magnitudes $G = (20.010 \pm 0.009)$, $BP = (20.193 \pm 0.073)$, and $RP = (19.574 \pm 0.067)$
  ($BP - RP = 0.619$);
- NVSS J165756+685142 with flux density $S(1.4\ \mathrm{GHz}) = (29.4 \pm 1.0)$ mJy;
- VLASS1QLCIR J165756.72+685140.3 with flux Ftot(2000–4000 MHz) $= (7.036 \pm 0.200)$ mJy; this source is very close to anoter VLASS detection (VLASS1QLCIR J165756.09+685145.0). This could be either a nearby object or a feature of the X–ray emission like a jet? (see Figure 36);
- TGSSADR J165756.7+685142 with flux density $S(150\ \mathrm{MHz}) = (240.4 \pm 24.7)$ mJy;
- ILTJ165756.71+685143.1 with flux Ftot(144 MHz) = 265.9 mJy.

From the XRT data we can only infer a 2–10 keV flux of $\sim 1.7 \times 10^{-13}$ erg cm^{-2} s^{-1} by assuming a power law continuum (photon index frozen to 1.8) passing through Galactic absorption ($N_{\mathrm{H(Gal)}} = 4.84 \times 10^{20}$ cm^{-2}).

This source is probably a QSO candidate (Flesch 2024; Guo et al. 2018), very bright at radio frequencies, although its X–ray flux and soft spectrum make it a less probable counterpart to PBC_NEW_257.

➢ Source #2 is located at:

R.A.(J2000) = $16^{\mathrm{h}}57^{\mathrm{m}}43'.38$

Dec.(J2000) = $+68^{\circ}46'29''.20$

error box = $4''.50$

It is detected at 8.2σ and 3.9σ c.l. in the 0.3–10 keV energy range and above 3 keV, respectively.

Multi–wavelength counterparts to this XRT detection:

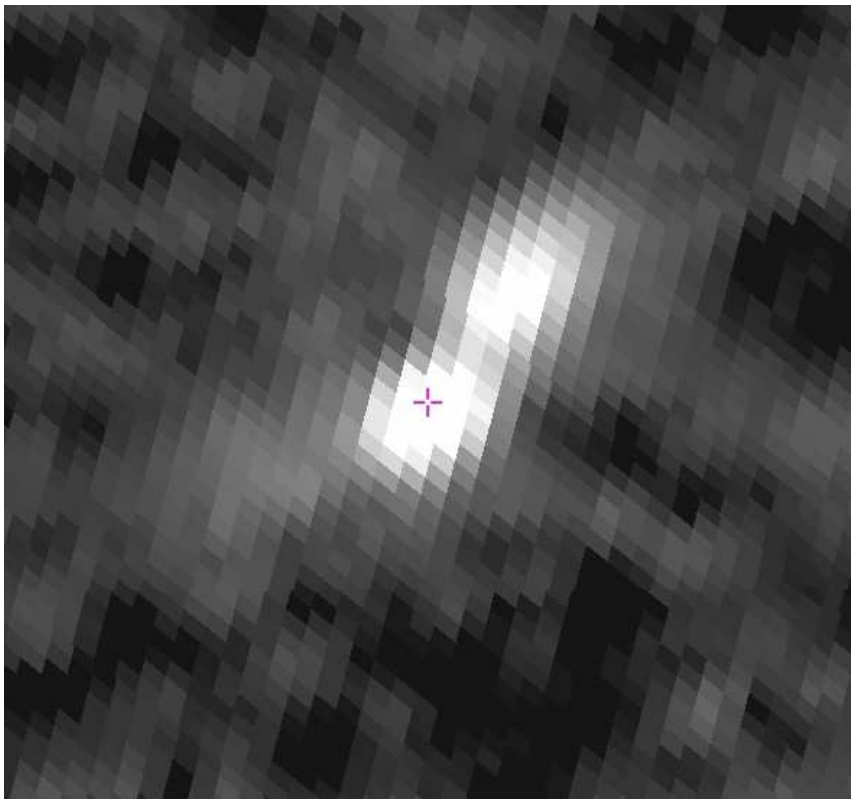

Figure 36: Radio image of source #1 from VLASS.

- USNO–A2.0 1575–03729058 with magnitudes $B = 16.7$ and $R = 15.3$;
- 2MASX J16574368+6846309 with magnitudes $J = (14.655 \pm 0.122)$, $H = (13.614 \pm 0.122)$, and $K = (13.356 \pm 0.125)$;
- WISE J165743.71+684630.8 with magnitudes $W1 = (13.199 \pm 0.023)$, $W2 = (12.795 \pm 0.022)$, $W3 = (10.280 \pm 0.031)$, $W4 = (7.459 \pm 0.063)$, and colours barely compatible with an AGN candidate ($W1 - W2 = 0.404$, $W2 - W3 = 2.515$);
- *Gaia* 1649022594169288448 with magnitudes $G = (19.134 \pm 0.012)$, $BP = (17.864 \pm 0.031)$, and $RP = (16.514 \pm 0.012)$
  ($BP - RP = 1.350$);
- GALEX J165743.6+684630 with magnitudes $FUV = (20.311 \pm 0.173)$ and $NUV = (19.621 \pm 0.085)$;
- 1RXS J165743.1+684626 with flux F(0.2–2.4 keV) $\sim 7.3 \times 10^{-13}$ erg cm^{-2} s^{-1}.

The X–ray data are well modelled with a power law, passing through Galactic absorption ($N_{\mathrm{H(Gal)}} = 4.62 \times 10^{20}$ cm^{-2}), characterised by a photon index $\Gamma = (1.53 \pm 0.39)$ and a 2–10 keV flux of $\sim 1.5 \times 10^{-12}$ erg cm^{-2} s^{-1}.

This source is associated with the galaxy LEDA 2723633; the DESI Legacy Imaging Survey provides a photometric redshift $z = (0.125 \pm 0.03)$ (Duncan 2022) (NED gives $z = 0.105$).

Source #2, being brighter and harder than source #1, is a more likely counterpart to PBC_NEW_257, although it lies outside the error circle and is not a strong radio source.

PBC_NEW_263

Source position:

- R.A.(J2000) = $08^{h}44^{m}13'.10$
- Dec.(J2000) = $-14°07'22''.60$
- Positional uncertainty = $4'.7457$

Two XRT observations available:

1. obscode: 00096685001
   observation date: 06/12/2022
   exposure: 1397 s
2. obscode: 00096685002
   observation date: 12/12/2022
   exposure: 1078 s

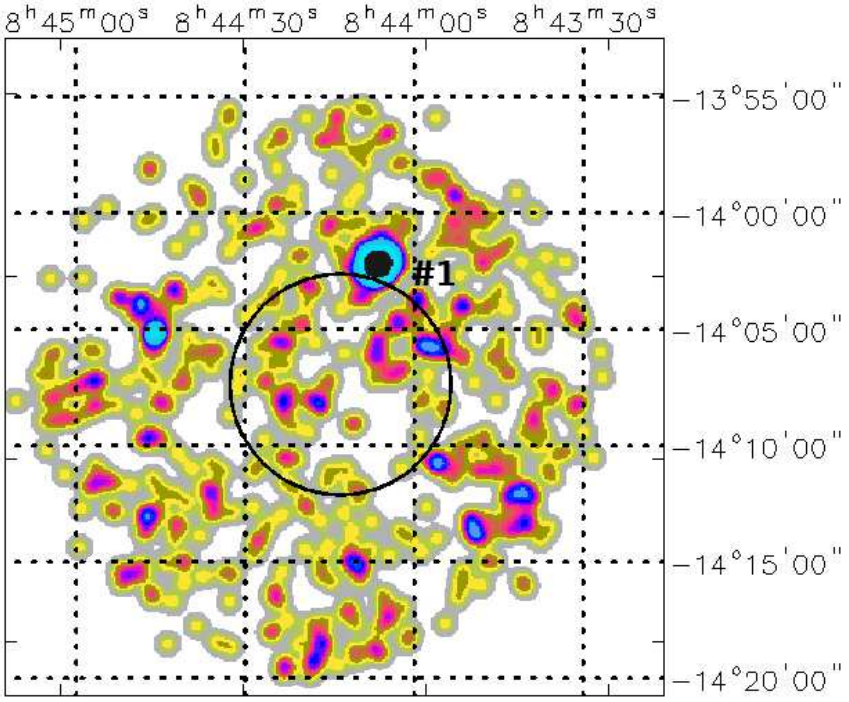

Figure 37: 0.3–10 keV XRT image of the PBC_NEW_263 field.

XRT detects one X–ray source just outside the BAT positional uncertainty (see Figure 37), which is located at:

R.A.(J2000) = $08^{h}44^{m}06'.45$

Dec.(J2000) = $-14^{\circ}02'10''.57$

error box = $4''.03$

It is detected at 12.1σ and 3.9σ c.l. in the 0.3–10 keV energy range and above 3 keV, respectively.

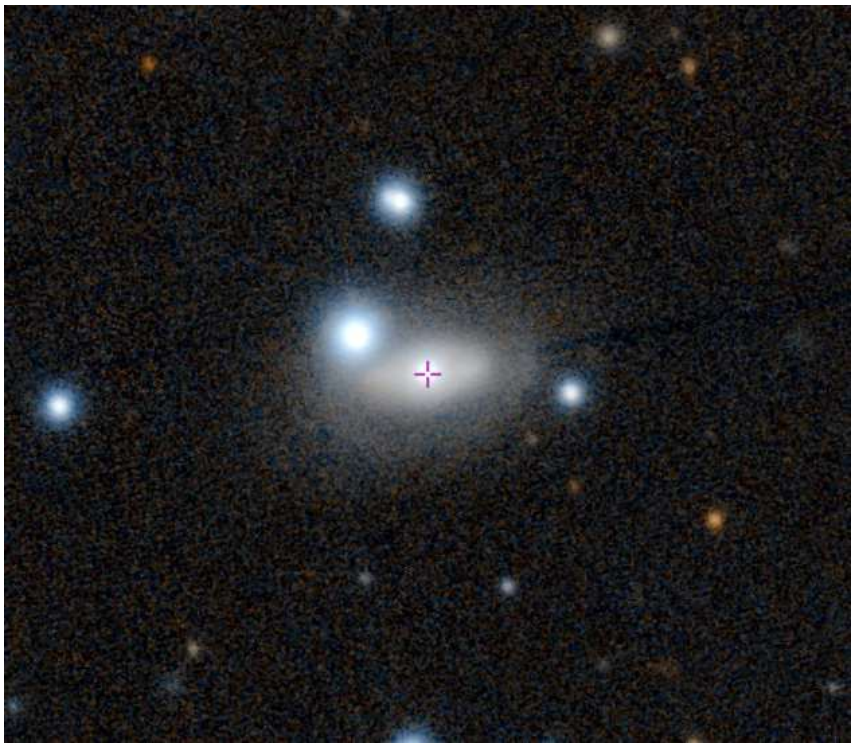

Figure 38: Optical image of source #1 from Pan–STARRS.

Multi–wavelength counterparts to this XRT detection:

- USNO–B1.0 0759–0204843 with magnitudes $B1 = 13.13$, $B2 = 11.14$, $R1 = 11.26$, and $R2 = 11.14$;
- 2MASS J08440645–1402128 with magnitudes $J = (13.385 \pm 0.057)$, $H = (12.589 \pm 0.072)$, and $K = (11.897 \pm 0.042)$;
- 2MASX J08440647–1402130 with magnitudes $J = (12.363 \pm 0.037)$, $H = (11.642 \pm 0.049)$, and $K = (11.192 \pm 0.063)$;
- AllWISE J084406.46–140212.8 with magnitudes $W1 = (10.788 \pm 0.023)$, $W2 = (10.105 \pm 0.021)$, $W3 = (6.946 \pm 0.016)$, $W4 = (4.395 \pm 0.025)$, and AGN colours ($W1 - W2 = 0.683$, $W2 - W3 = 3.159$);

- *Gaia* 5734670505766302592 with magnitudes $G = (16.469 \pm 0.006)$, $BP = (15.998 \pm 0.009)$, and $RP = (14.837 \pm 0.007)$
  $(BP - RP = 1.140)$;
- 2RXS J084406.4–140212 with flux F(0.2–2.4 keV) $\sim 3.2 \times 10^{-12}$ erg cm^{-2} s^{-1};
- 1eRASS J084406.5–140213 with flux F(0.2–2.3 keV) $\sim 2.5 \times 10^{-12}$ erg cm^{-2} s^{-1};
- NVSS J084406–140210 with flux density S(1.4 GHz) $= (7.5 \pm 0.5)$ mJy;
- VLASS1QLCIR J084406.47–140212.8 with flux Ftot(2000–4000 MHz) $= (4.356 \pm 0.330)$ mJy;
- RACS–MID J084406.4–140213 with flux Ftot(1367.5 MHz) $= 8.58$ mJy;
- RACS–HIGH J084406–14021 with flux Ftot(1655.5 MHz) $= 6.58$ mJy.

The fit with a simple power law passing through Galactic absorption does not provide a good fit to the data; the residuals to the data hint at a curvature of the spectrum that we modelled with a broken power law. The best–fit parameters of this model, which improves the fit at 99% c.l., are the following: $\Gamma_1 = \left(3.22^{+2.49}_{-0.78}\right)$, $\Gamma_2 = \left(1.67^{+0.33}_{-0.31}\right)$, and $E_{\rm break} = \left(0.87^{+0.29}_{-0.35}\right)$; the 2–10 keV flux is $\sim 2.3 \times 10^{-12}$ erg cm^{-2} s^{-1}.

This source is associated with LEDA 2816626, classified as a Seyfert 1 galaxy at redshift $z = (0.02796 \pm 0.00015)$; a more refined optical class (AGN 1.5) is given in Hon et al. (2025). The source, which is also named IRAS 08417–1351, seems to be in interaction with a nearby companion, as displayed in Figure 38 from Pan–STARRS.

PBC_NEW_266

Source position:

- R.A.(J2000) = $02^{h}16^{m}26'.78$
- Dec.(J2000) = $+23°37'50''.10$
- Positional uncertainty = $4'.3566$

Fifteen XRT observations available:

1. obscode: 03111941001
   observation date: 23/07/2022
   exposure: 98 s
2. obscode: 03111941003
   observation date: 28/07/2022
   exposure: 2217 s
3. obscode: 03111941005
   observation date: 11/09/2022
   exposure: 120 s
4. obscode: 00096686001
   observation date: 18/10/2022
   exposure: 1709 s
5. obscode: 03111941007
   observation date: 10/12/2022
   exposure: 311 s
6. obscode: 03111941009
   observation date: 14/12/2022
   exposure: 416 s
7. obscode: 03111941011
   observation date: 08/02/2023
   exposure: 980 s
8. obscode: 03111941013
   observation date: 16/02/2023
   exposure: 995 s
9. obscode: 03111941015
   observation date: 17/02/2023
   exposure: 920 s

10. obscode: 03111941017
    observation date: 01/03/2023
    exposure: 637 s
11. obscode: 03111941019
    observation date: 29/06/2023
    exposure: 371 s
12. obscode: 03111941021
    observation date: 02/07/2023
    exposure: 958 s
13. obscode: 03111941023
    observation date: 03/07/2023
    exposure: 680 s
14. obscode: 03111941025
    observation date: 07/07/2023
    exposure: 775 s
15. obscode: 03111941027
    observation date: 09/07/2023
    exposure: 148 s

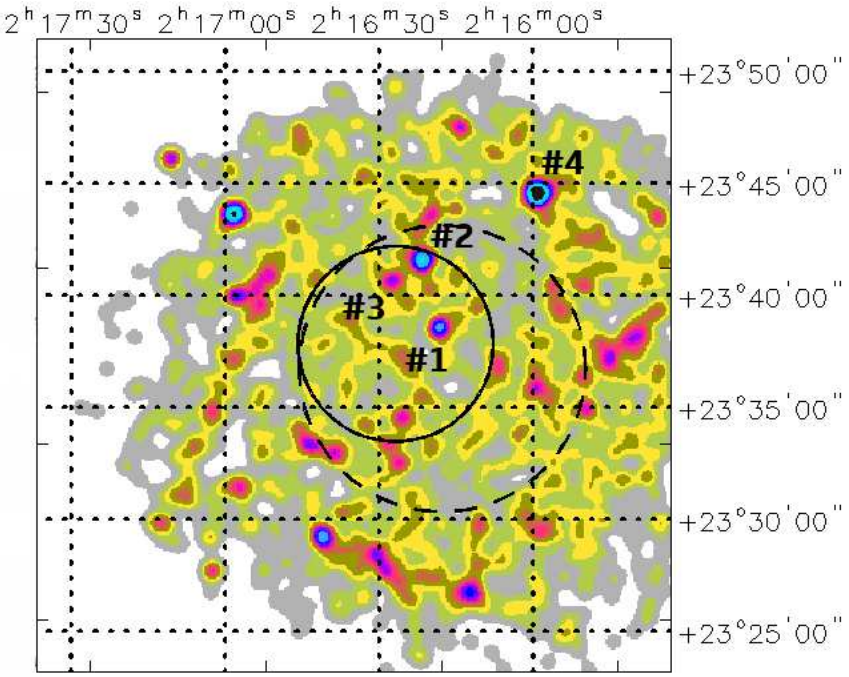

Figure 39: 0.3–10 keV XRT image of the PBC_NEW_266 field.

This source is also listed in the *Swift*/BAT 157–month catalogue as SWIFT J0216.3+2337, whose coordinates are:

- R.A.(J2000) = $02^{h}16^{m}17'.66$
- Dec.(J2000) = $+23^{\circ}36'43''.60$
- Positional uncertainty = $6'.39$

XRT detects three X–ray sources within the PBC_NEW_266 positional uncertainty, which also lie inside the SWIFT J0216.3+2337 error circle (see Figure 39):

➢ Source #1 is located at:

R.A.(J2000) = $02^{h}16^{m}18'.35$

Dec.(J2000) = $+23^{\circ}38'35''.40$

error box = $5''.70$

It is detected at 3.3σ and 3.5σ c.l. in the 0.3–10 keV energy range and above 3 keV, respectively.

➢ Source #2 is located at:

R.A.(J2000) = $02^{h}16^{m}21'.40$

Dec.(J2000) = $+23^{\circ}41'35''.10$

error box = $6''.00$

It is detected at 3.9σ c.l. in the 0.3–10 keV energy range and is not revealed above 3 keV.

➢ Source #3 is located at:

R.A.(J2000) = $02^{h}16^{m}27'.00$

Dec.(J2000) = $+23^{\circ}40'41''.60$

error box = $8''.90$

It is detected at 2.7σ c.l. in the 0.3–10 keV energy range and is not revealed above 3 keV.

Moreover, we note that in the region surrounding PBC_NEW_266 there is a bright source, which falls inside the 99% error circle of SWIFT J0216.3+2337 (source #4 in Figure 39), which is located at:

R.A.(J2000) = $02^h15^m58'.98$

Dec.(J2000) = $+23^\circ44'33''.26$

error box = $4''.78$

It is detected at 5.0σ c.l. in the 0.3–10 keV energy range and at 2.6σ c.l. above 3 keV.

We then extracted the XRT image above 3 keV (see Figure 40) to assess which of the X–ray detections might be the likely counterparts to the BAT high–energy emitter. As shown in the Figure, only two sources are still detected above 3 keV: source #1 and source #4.

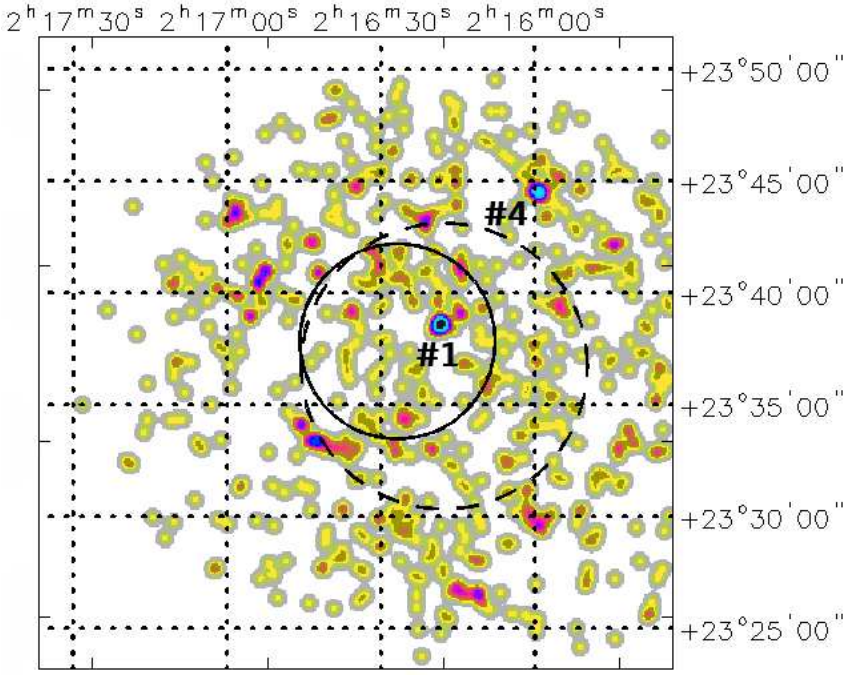

Figure 40: XRT image of the PBC_NEW_266 field above 3 keV.

Multi–wavelength counterparts to these XRT detections are:

➢ Source #1

- USNO–A2.0 1125–00727385 with magnitudes $B = 12.6$ and $R = 10.9$;
- 2MASS J02161829+2338336 with magnitudes $J = (14.889 \pm 0.101)$, $H = (14.246 \pm 0.126)$, and $K = (13.601 \pm 0.071)$;
- 2MASX J02161825+2338337 with magnitudes $J = (12.745 \pm 0.049)$, $H = (12.125 \pm 0.061)$, and $K = (11.791 \pm 0.079)$;

- AllWISE J021618.29+233833.7 with magnitudes $W1 = (11.855 \pm 0.022)$, $W2 = (10.611 \pm 0.021)$, $W3 = (7.658 \pm 0.020)$, $W4 = (5.040 \pm 0.033)$, and colours typical of an AGN ($W1 - W2 = 1.244$, $W2 - W3 = 2.953$);
- *Gaia* 1012020051582895 36 with magnitudes $G = (21.683 \pm 0.080)$, $BP = (18.255 \pm 0.073)$, and $RP = (16.649 \pm 0.025)$
  ($BP - RP = 1.606$);
- GALEX J021618.1+233832 with magnitudes $FUV = (19.012 \pm 0.120)$ and $NUV = (18.415 \pm 0.053)$;
- VLASS1QLCIR J021618.29+233833.8 with flux Ftot(2000–4000 MHz) $= (1.067 \pm 0.231)$ mJy;
- ILTJ021618.31+233833.5 with flux Ftot(144 MHz) = 5.372 mJy;
- RACS–MID J021618.3+233832 with flux Ftot(1367.5 MHz) = 2.5 mJy;
- RACS–HIGH J021618+23383 with flux Ftot(1655.5 MHz) = 1.3 mJy.

Due to the low quality of the data, we can only estimate a 2–10 keV flux of $\sim 3 \times 10^{-14}$ erg cm^{-2} s^{-1} by assuming a power law continuum (photon index frozen to 1.8) passing through Galactic absorption ($N_{\rm H(Gal)} = 6.33 \times 10^{20}$ cm^{-2}).

This source is associated with the spiral galaxy Z 483–13/LEDA 8671 at redshift $z = (0.031501 \pm 0.000023)$. Its properties (radio detection and near infrared colours) make it an AGN candidate; it is also characterised by a 21–cm line in emission (Haynes et al. 2018).

➢ Source #4

- USNO–B1.0 1137–0025769 with magnitudes $B2 = 20.38$ and $R1 = 20.11$;
- ILTJ021558.96+234433.1 with flux Ftot(144 MHz) = 1.767 mJy.

The fit of the X–ray spectrum is consistent with a power law continuum, passing through Galactic absorption ($N_{\rm H(Gal)} = 6.44 \times 10^{20}$ cm^{-2}), characterised by a flat photon index $\Gamma = (1.19^{+0.56}_{-0.68})$ and a 2–10 keV flux of $\sim 2.5 \times 10^{-13}$ erg cm^{-2} s^{-1}.

This source is most likely a background AGN at photometric redshift $z = 0.884$ (Duncan 2022).

It is difficult to discriminate between the two harder X–ray sources at this stage, being source #1 very weak but slightly harder than source #4, unless the closer object is a heavily absorbed AGN that emerges only at high energies.

PBC_NEW_269

Source position:

- R.A.(J2000) = $17^h29^m14'.12$
- Dec.(J2000) = $-53°31'18''.00$
- Positional uncertainty = $4'.66024$

One XRT observation available:

1. obscode: 00096689001
   observation date: 16/02/2023
   exposure: 2141 s

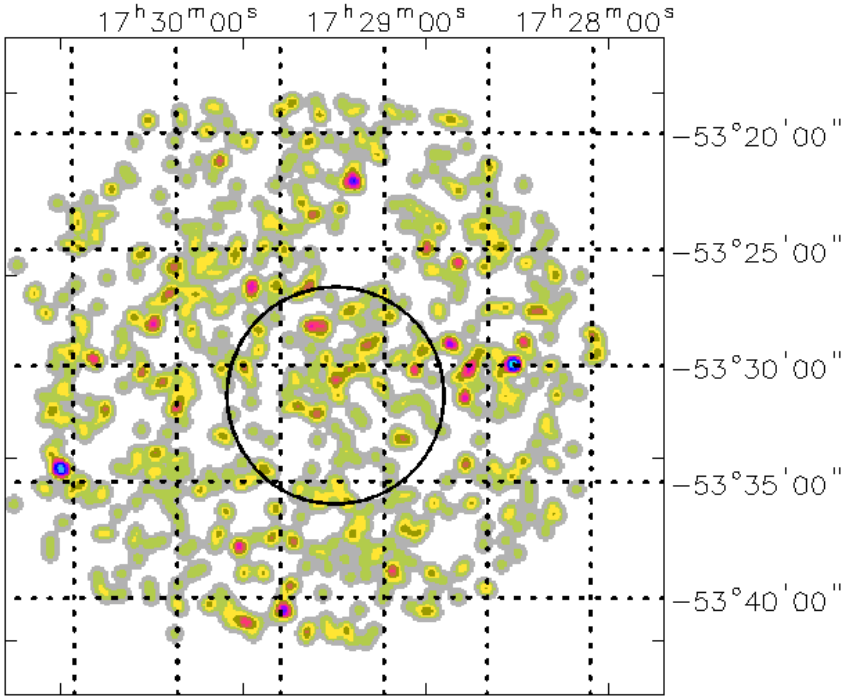

Figure 41: 0.3–10 keV XRT image of the PBC_NEW_269 field.

No X–ray source is detected by XRT within the region surrounding PBC_NEW_269 (see Figure 41).

However, within the BAT error circle we find two source belonging to the *eROSITA* All–Sky Survey Catalogue (eRASS1):

➢ 1eRASS J172914.2–533040 is located at:

R.A.(J2000) = $17^{h}29^{m}14'.21$

Dec.(J2000) = $-53^{\circ}30'40''.11$

F(0.2–2.3 keV) $\sim 8.9 \times 10^{-14}$ erg cm^{-2} s^{-1}.

➢ 1eRASS J172917.7–532956 is located at:

R.A.(J2000) = $17^{h}29^{m}17'.72$

Dec.(J2000) = $-53^{\circ}29'56''.23$

F(0.2–2.3 keV) $\sim 5 \times 10^{-14}$ erg cm^{-2} s^{-1}.

Both sources are still optically unclassified.

PBC_NEW_277

Source position:

- R.A.(J2000) = $16^h26^m41'.03$
- Dec.(J2000) = $+82°51'43''.00$
- Positional uncertainty = $4'.9449$

One XRT observation available:

1. obscode: 00096693001
   observation date: 21/02/2023
   exposure: 1800 s

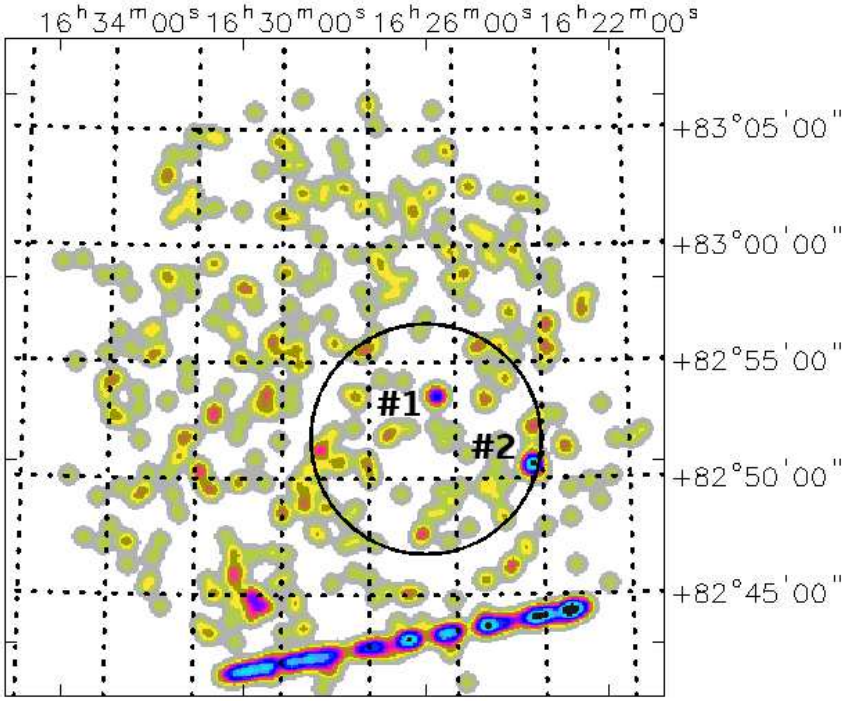

Figure 42: 0.3–10 keV XRT image of the PBC_NEW_277 field.

XRT detects two X–ray sources within the BAT positional uncertainty (see Figure 42):

➢ Source #1 is located at:

R.A.(J2000) = $16^h26^m21'.71$

Dec.(J2000) = $+82^{\circ}53'32''.80$

error box = $6''.0$

It is detected at 2.2σ c.l. in the 0.3–10 keV energy range; no detection is found above 3 keV.

Multi–wavelength counterparts to this XRT detection:

- AllWISE J162621.93+825328.0 with magnitudes $W1 = (16.392 \pm 0.045)$, $W2 = (15.482 \pm 0.060)$, $W3 = (12.354 \pm 0.211)$, $W4 = (9.200 \pm 0.000)$, and AGN colours ($W1 - W2 = 1.450$, $W2 - W3 = 3.128$);
- *Gaia* 1722867586092161280 with magnitudes $G = (20.727 \pm 0.024)$, $BP = (21.046 \pm 0.178)$, and $RP = (20.174 \pm 0.202)$
  ($BP - RP = 0.872$);
- GALEX J162622.1+825326 with magnitude $NUV = (22.637 \pm 0.403)$.

Due to the low quality of the XRT data, we can only estimate a 2–10 keV flux of $\sim 1 \times 10^{-13}$ erg cm^{-2} s^{-1} by assuming a power law continuum (photon index frozen to 1.8) passing through Galactic absorption ($N_{\rm H(Gal)} = 5.22 \times 10^{20}$ cm^{-2}).

This source is likely a QSO candidate (Souchay et al. 2024; Wu et al. 2023) at redshift $z = 1.207$ (photometric estimate from Duncan 2022).

➢ Source #2 is located at:

R.A.(J2000) = $16^{\rm h}24^{\rm m}11'.83$

Dec.(J2000) = $+82^{\circ}50'38''.40$

error box = $6''.00$

It is detected at 3.1σ c.l. in the 0.3–10 keV energy range and is not revealed above 3 keV.

Multi–wavelength counterparts to this XRT detection:

- USNO–B1.0 1728–0043157 with magnitudes $B1 = 20.72$, $B2 = 20.12$, and $R2 = 19.66$;
- AllWISE J162412.12+825033.2 with magnitudes $W1 = (15.231 \pm 0.028)$, $W2 = (14.548 \pm 0.033)$, $W3 = (11.587 \pm 0.123)$, $W4 = (8.823 \pm 0.245)$, and colours of an AGN candidate ($W1 - W2 = 0.683$, $W2 - W3 = 2.961$);
- *Gaia* 1722867684875675776 with magnitudes $G = (20.070 \pm 0.012)$, $BP = (20.150 \pm 0.089)$, and $RP = (19.582 \pm 0.076)$
  ($BP - RP = 0.567$).

Also in this case, because of the poor quality of the XRT data, we can only infer a 2–10 keV flux of $\sim 1.9 \times 10^{-13}$ erg cm^{-2} s^{-1} by assuming a power law continuum (photon index frozen to 1.8) passing through Galactic absorption ($N_{\rm H(Gal)} = 4.98 \times 10^{20}$ cm^{-2}).

Also this source is likely a QSO candidate (Souchay et al. 2024) and, in this case, Duncan (2022) provides a photometric redshift $z = 0.71$.

Both sources are weak in X–rays to be clearly associated with PBC_NEW_277, although, of the two, source #2 is slightly a more probable association.

PBC_NEW_287

Source position:

- R.A.(J2000) = $23^{h}13^{m}47'.54$
- Dec.(J2000) = $+23^{\circ}47'30''.30$
- Positional uncertainty = $4'.8185$

Two XRT observations available:

1. obscode: 00096698001
   observation date: 18/10/2022
   exposure: 1336 s
2. obscode: 00096698002
   observation date: 27/10/2022
   exposure: 434 s

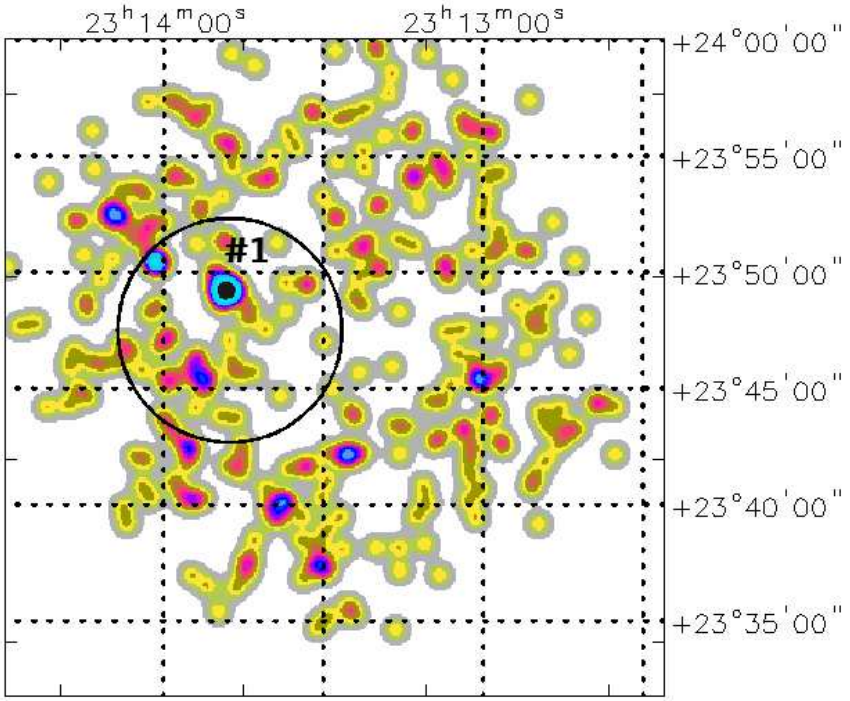

Figure 43: 0.3–10 keV XRT image of the PBC_NEW_287 field.

XRT detects only one X–ray source within the BAT positional uncertainty (see Figure 43), which is located at:

R.A.(J2000) = $23^{h}13^{m}48'.28$

Dec.(J2000) = $+23^{\circ}49'14''.05$

error box = $6''.52$

It is detected at 3.8σ and 3.1σ c.l. in the 0.3–10 keV energy range and above 3 keV, respectively.

Multi–wavelength counterparts to this XRT detection:

- USNO–A2.0 1125–19720938 with magnitudes $B = 12.7$ and $R = 11.3$;
- USNO–A2.0 1125–19720878 with magnitudes $B = 17.6$ and $R = 16.6$;
- 2MASS J23134830+2349140 with magnitudes $J = (13.989 \pm 0.048)$, $H = (13.287 \pm 0.061)$, and $K = (13.035 \pm 0.051)$;
- 2MASX J23134831+2349136 with magnitudes $J = (12.798 \pm 0.051)$, $H = (12.051 \pm 0.041)$, and $K = (11.985 \pm 0.083)$;
- AllWISE J231348.31+234914.0 with magnitudes $W1 = (11.685 \pm 0.022)$, $W2 = (11.159 \pm 0.021)$, $W3 = (7.469 \pm 0.018)$, $W4 = (4.799 \pm 0.027)$, and AGN colours ($W1 - W2 = 0.526$, $W2 - W3 = 3.690$);
- *Gaia* 2839452945822184960 with magnitudes $G = (17.906 \pm 0.014)$, $BP = (16.308 \pm 0.010)$, and $RP = (15.221 \pm 0.009)$
  ($BP - RP = 1.087$);
- GALEX J231348.3+234914 with magnitudes $FUV = (18.539 \pm 0.078)$ and $NUV = (17.975 \pm 0.0424)$;
- NVSS J231348+234913 with flux density $S(1.4\ \mathrm{GHz}) = (3.6 \pm 0.5)$ mJy;
- VLASS1QLCIR J231348.29+234913.8 with flux Ftot(2000–4000 MHz) $= (3.281 \pm 0.543)$ mJy;
- ILTJ231348.32+234914.3 with flux Ftot(144 MHz) = 13.568 mJy;
- RACS–MID J231348.3+234914 with flux Ftot(1367.5 MHz) = 4.57 mJy;
- RACS–HIGH J231348+23491 with flux Ftot(1665.5 MHz) = 3.29 mJy.

The low statistical quality of the data allows us to measure only a 2–10 keV flux of $\sim 1.7 \times 10^{-13}$ erg cm^{-2} s^{-1} by assuming a power law continuum (photon index frozen to 1.8) passing through Galactic absorption ($N_{\mathrm{H(Gal)}} = 5.85 \times 10^{20}$ cm^{-2}).

This source is associated with Mrk 317, classified as an AGN candidate in Simbad with redshift $z = (0.020708 \pm 0.000404)$. Interestingly, this galaxy might have undergone a transient event in its near nuclear region (Khamitov et al. 2023) due to the observation of proper motion.

PBC_NEW_306

Source position:

- R.A.(J2000) = $10^{h}26^{m}17'.85$
- Dec.(J2000) = $+45°34'20''.50$
- Positional uncertainty = $3'.8843$

Thirty XRT observations available:

1. obscode: 03111965001
   observation date: 04/06/2022
   exposure: 326 s
2. obscode: 03111965003
   observation date: 28/09/2022
   exposure: 323 s
3. obscode: 03111965005
   observation date: 01/10/2022
   exposure: 416 s
4. obscode: 03111965009
   observation date: 22/12/2022
   exposure: 183 s
5. obscode: 03111965011
   observation date: 08/02/2023
   exposure: 201 s
6. obscode: 03111965013
   observation date: 10/02/2023
   exposure: 196 s
7. obscode: 00096705001
   observation date: 27/02/2023
   exposure: 1642 s
8. obscode: 00096705002
   observation date: 27/02/2023
   exposure: 341 s
9. obscode: 03111965015
   observation date: 28/03/2023
   exposure: 303 s

10. obscode: 03111965017
    observation date: 20/05/2023
    exposure: 213 s

11. obscode: 03111965019
    observation date: 26/05/2023
    exposure: 1339 s

12. obscode: 03111965021
    observation date: 08/06/2023
    exposure: 627 s

13. obscode: 03111965023
    observation date: 19/09/2023
    exposure: 587 s

14. obscode: 03111965025
    observation date: 23/09/2023
    exposure: 216 s

15. obscode: 03111965027
    observation date: 24/09/2023
    exposure: 401 s

16. obscode: 03111965029
    observation date: 10/10/2023
    exposure: 148 s

17. obscode: 03111965031
    observation date: 29/10/2023
    exposure: 1494 s

18. obscode: 03111965033
    observation date: 02/11/2023
    exposure: 740 s

19. obscode: 03111965035
    observation date: 04/11/2023
    exposure: 366 s

20. obscode: 03111965037
    observation date: 05/11/2023
    exposure: 1474 s

21. obscode: 03111965039
    observation date: 08/11/2023
    exposure: 166 s

22. obscode: 03111965041
    observation date: 10/11/2023
    exposure: 765 s

23. obscode: 03111965043
    observation date: 13/11/2023
    exposure: 1101 s

24. obscode: 03111965045
    observation date: 14/11/2023
    exposure: 1264 s

25. obscode: 00098251002
    observation date: 20/06/2025
    exposure: 2716 s

26. obscode: 00098251003
    observation date: 20/09/2025
    exposure: 1242 s

27. obscode: 00098251004
    observation date: 21/09/2025
    exposure: 2396 s

28. obscode: 00098251005
    observation date: 24/09/2025
    exposure: 1185 s

29. obscode: 00098251006
    observation date: 11/11/2025
    exposure: 420 s

30. obscode: 00098251007
    observation date: 17/11/2025
    exposure: 1540 s

This source is also listed in the *Swift*/BAT 157–month catalogue as SWIFT J1026.3+4536, whose coordinates are:

- R.A.(J2000) = $10^{h}26^{m}20'.62$
- Dec.(J2000) = $+45^{\circ}35'57''.10$
- Positional uncertainty = $5'.40$

XRT detects three X–ray sources within the PBC_NEW_306 positional uncertainty, which also lie inside of the SWIFT J1026.3+4536 error circle (see Figure 44):

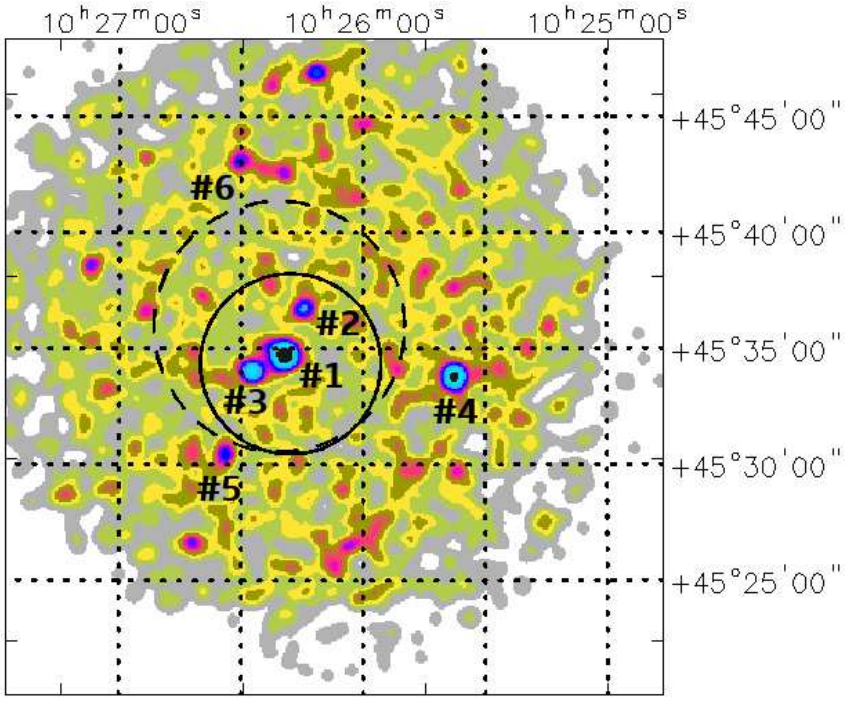

Figure 44: 0.3–10 keV XRT image of the PBC_NEW_306 field.

➢ Source #1 is located at:

R.A.(J2000) = $10^{h}26^{m}19'.21$

Dec.(J2000) = $+45°34'42''.70$

error box = $3''.89$

It is detected at 11.2σ and 7.2σ c.l. in the 0.3–10 keV energy range and above 3 keV, respectively.

➢ Source #2 is located at:

R.A.(J2000) = $10^{h}26^{m}14'.50$

Dec.(J2000) = $+45°36'43''.80$

error box = $6''.60$

It is detected at 5.0σ c.l. in the 0.3–10 keV energy range and is not revealed above 3 keV.

➢ Source #3 is located at:

R.A.(J2000) = $10^{h}26^{m}26'.80$

Dec.(J2000) = $+45^{\circ}34'01''.73$

error box = $4''.36$

It is detected at 6.6σ c.l. in the 0.3–10 keV energy range and is not revealed above 3 keV.

Nevertheless, there are other three detections that lie outside both the PBC_NEW_306 and SWIFT J1026.3+4536 positional uncertainties:

➢ Source #4 is located at:

R.A.(J2000) = $10^{h}25^{m}37'.43$

Dec.(J2000) = $+45^{\circ}33'46''.38$

error box = $4''.06$

It is detected at 7.8σ c.l. in the 0.3–10 keV energy range, but is not observed above 3 keV.

➢ Source #5 is located at:

R.A.(J2000) = $10^{h}26^{m}33'.45$

Dec.(J2000) = $+45^{\circ}30'25''.80$

error box = $6''.00$

It is detected at 4.1σ c.l. in the 0.3–10 keV energy range and is not revealed above 3 keV.

➢ Source #6 is located at:

R.A.(J2000) = $10^{h}26^{m}30'.78$

Dec.(J2000) = $+45^{\circ}43'00''.20$

error box = 6″.00

It is detected at 3.0σ c.l. in the 0.3–10 keV energy range; no detection is found above 3 keV.

We then extracted the XRT image above 3 keV (see Figure 45) to discriminate which of the X–ray detections might be the most likely counterpart to the BAT high–energy emitter. As shown in the Figure, only source #1 is still detected above 3 keV.

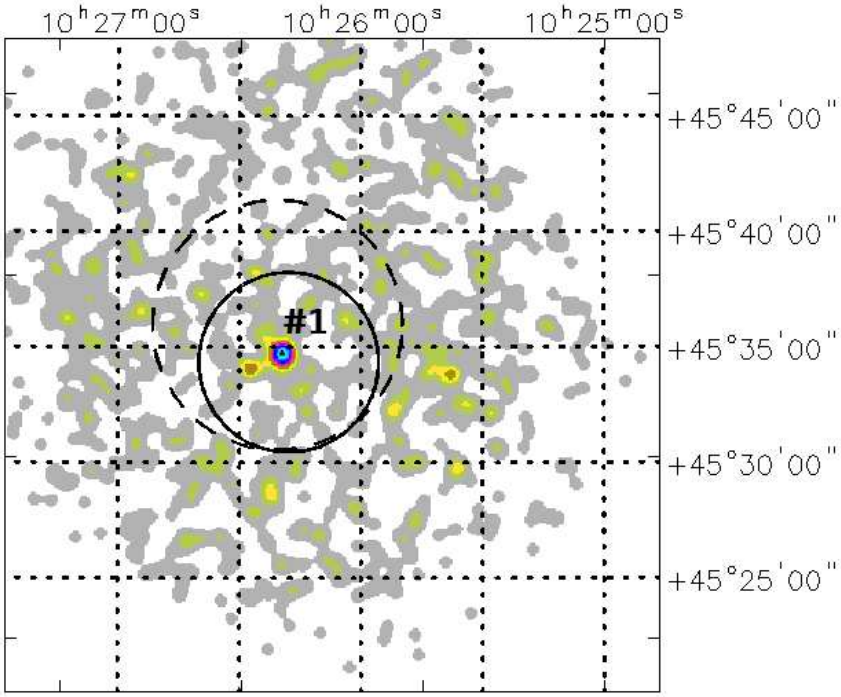

Figure 45: XRT image of the PBC_NEW_306 field above 3 keV.

Multi–wavelength counterparts to this XRT detection:

- USNO–A2.0 1350–07771796 with magnitudes $B = 11.6$ and $R = 10.1$;
- 2MASS J10261897+4534404 with magnitudes $J = (13.281 \pm 0.100)$, $H = (12.481 \pm 0.093)$, and $K = (12.068 \pm 0.067)$;
- 2MASX J10261903+4534400 with magnitudes $J = (11.867 \pm 0.024)$, $H = (11.100 \pm 0.030)$, and $K = (10.808 \pm 0.037)$;
- AllWISE J102618.99+453440.7 with magnitudes $W1 = (10.955 \pm 0.022)$, $W2 = (10.818 \pm 0.020)$, $W3 = (8.968 \pm 0.030)$, $W4 = (7.042 \pm 0.098)$, and colours that are not typical of an AGN ($W1 - W2 = 0.137$, $W2 - W3 = 1.850$);

- *Gaia* 833206376773096960 with magnitudes $G = (19.055 \pm 0.025)$, $BP = (16.368 \pm 0.024)$, and $RP = (14.805 \pm 0.010)$
  $(BP - RP = 1.563)$;
- NVSS 102619+453439 with flux density $S(1.4\ \mathrm{GHz}) = (8.5 \pm 0.5)$ mJy;
- FIRST J102619.0+453440 with flux density $S(1.4\ \mathrm{GHz}) = 8.82$ mJy;
- VLASS1QLCIR J102618.97+453440.4 with flux Ftot(2000–4000 MHz) $= (4.947 \pm 0.332)$ mJy;
- TGSSADR J102619.2+453439 with flux density $S(150\ \mathrm{MHz}) = (22.8 \pm 5.4)$ mJy;
- ILTJ102619.01+453440.4 with flux Ftot(144 MHz) = 28.32 mJy;
- RACS–MID J102618.9+453439 with flux Ftot(1367.5 MHz) = 7.16 mJy;
- RACS–HIGH J102618+45344 with flux Ftot(1655.5 MHz) = 5.31 mJy.

The residuals of the fit with a power law passing through Galactic absorption ($N_{\mathrm{H(Gal)}} = 1.52 \times 10^{20}\ \mathrm{cm}^{-2}$) suggest the presence of extra absorption. The addition of this component provides an intrinsic column density $N_{\mathrm{H(int)}} = \left(0.45^{+0.79}_{-0.40}\right) \times 10^{22}\ \mathrm{cm}^{-2}$; the photon index is $\Gamma = \left(1.61^{+0.98}_{-0.74}\right)$, while the 2–10 keV flux is $\sim 3.4 \times 10^{-13}\ \mathrm{erg\ cm}^{-2}\ \mathrm{s}^{-1}$.

This source is associated with LEDA 30651 at redshift $z = (0.02689 \pm 0.00019)$. The source is a strong radio emitter and variable at 1.4 GHz from comparison between NVSS and FIRST data sets (Ofek et al. 2011). It may be a type of galaxy characterised by weak emission lines, as often observed in Low–Ionization Nuclear Emission–line Regions (LINERs), due to its unusual *AllWISE* colours (see Dabhade et al. 2020 for a classification of the various AGN types on the basis of near–infrared colours). In others words, contrary to high–excitation/powerful emitting nuclei of active galaxies, its nuclear region may host a low–luminosity AGN.

PBC_NEW_320

Source position:

- R.A.(J2000) = $08^h11^m37'.73$
- Dec.(J2000) = $-11°46'18''.40$
- Positional uncertainty = $4'.9395$

One XRT observation available:

1. obscode: 000967110001
   observation date: 07/03/2023
   exposure: 22234 s

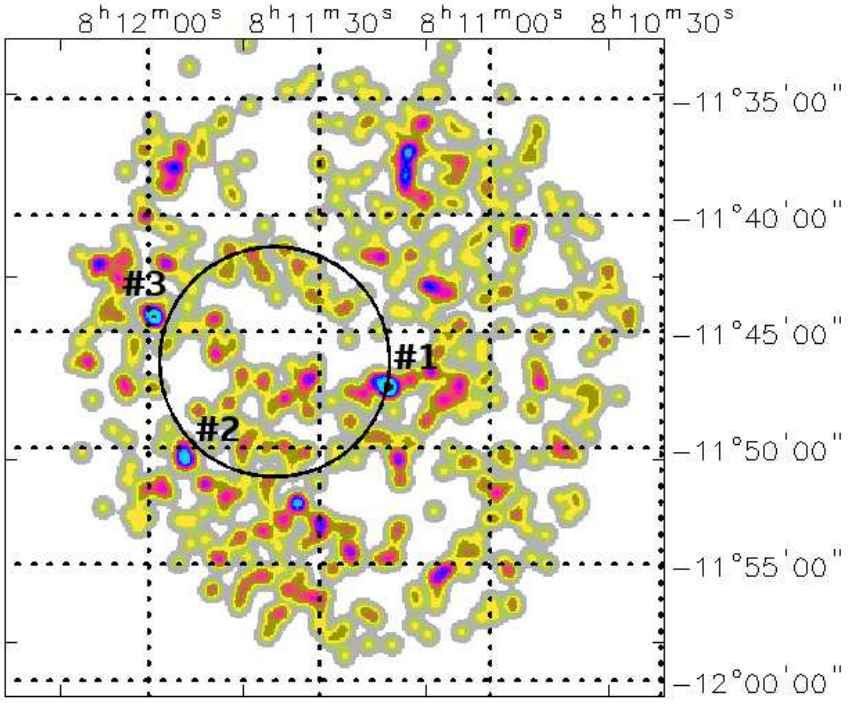

Figure 46: 0.3–10 keV XRT image of the PBC_NEW_320 field.

XRT detects three X–ray sources whose location is compatible with the BAT positional uncertainty (see Figure 46):

➢ Source #1 is located at the border of the BAT error circle at:

R.A.(J2000) = $08^{h}11^{m}17'.70$

Dec.(J2000) = $-11^{\circ}47'27''.20$

error box = $6''.0$

It is detected at 2.8σ c.l. in the 0.3–10 keV energy range; no detection is observed above 3 keV.

Multi–wavelength counterparts to this XRT detection:

- USNO–A2.0 0750–05880235 with magnitudes $B = 18.5$ and $R = 17.5$;
- 2MASS J08111774–1147299 with magnitudes $J = (16.552 \pm 0.135)$, $H = (15.669 \pm 0.000)$, and $K = (15.570 \pm 0.000)$;
- AllWISE J081117.71–114729.3 with magnitudes $W1 = (15.012 \pm 0.033)$, $W2 = (14.373 \pm 0.046)$, $W3 = (12.038 \pm 0.300)$, $W4 = (8.548 \pm 0.000)$, and AGN colours ($W1 - W2 = 0.639$, $W2 - W3 = 2.335$);
- *Gaia* 5727718225022761600 with magnitudes $G = (19.636 \pm 0.009)$, $BP = (20.045 \pm 0.064)$, and $RP = (19.102 \pm 0.062)$
  ($BP - RP = 0.944$);
- *Gaia* 5727718220733210240 with magnitudes $G = (17.839 \pm 0.030)$, $BP = (18.333 \pm 0.023)$, and $RP = (17.176 \pm 0.013)$
  ($BP - RP = 1.156$);
- GALEX J081117.5–114724 with magnitude $NUV = (21.244 \pm 0.367)$;
- NVSS J081117–114722 with flux density $S(1.4\ \mathrm{GHz}) = (4.5 \pm 0.6)$ mJy;
- VLASS1QLCIR J081117.63–114725.6 with flux Ftot(2000–4000 MHz) $= (1.836 \pm 0.148)$ mJy;
- RACS–MID J081117.6–114725 with flux Ftot(1367.5 MHz) = 2.63 mJy;
- RACS–HIGH J081117–11472 with flux Ftot(1655.5 MHz) = 2.53 mJy.

From the XRT data we can only infer, due to the low quality of the XRT data, a 2–10 keV flux of $\sim 1.7 \times 10^{-13}$ erg cm^{-2} s^{-1} by assuming a power law continuum (photon index frozen to 1.8) passing through Galactic absorption ($N_{\mathrm{H(Gal)}} = 9.05 \times 10^{20}$ cm^{-2}).

The source is likely an AGN candidate given its *AllWISE* colours and radio detection; it is also variable at 1.4 GHz from comparison of NVSS versus FIRST data (Ofek et al. 2011). Optically, it is classified as a QSO at redshift $z = 1.30$ (Flesch 2024).

➢ Source #2 is located just outside the BAT error circle at:

R.A.(J2000) = $08^{h}11^{m}53'.60$

Dec.(J2000) = $-11^{\circ}50'24''.20$

error box = $8''.30$

It is detected at 2.3σ c.l. in the 0.3–10 keV energy range and is not revealed above 3 keV.

Multi–wavelength counterparts to this XRT detection:

- USNO–B1.0 0781–0210077 with magnitudes $B1 = 19.58$, $B2 = 19.24$, and $R2 = 19.22$;
- AllWISE J081153.71–115027.1 with magnitudes $W1 = (15.194 \pm 0.037)$, $W2 = (13.949 \pm 0.038)$, $W3 = (10.938 \pm 0.128)$, $W4 = (8.401 \pm 0.273)$, and AGN colours ($W1 - W2 = 1.245$, $W2 - W3 = 3.011$);
- *Gaia* 5727705301467966720 with magnitudes $G = (18.905 \pm 0.005)$, $BP = (19.208 \pm 0.030)$, and $RP = (18.471 \pm 0.031)$
  ($BP - RP = 0.737$);
- GALEX J081153.7–115027 with magnitude $NUV = (20.804 \pm 0.241)$;
- 1eRASS J081153.4–115032 with flux F(0.2–2.3 keV) $\sim 1.3 \times 10^{-13}$ erg cm^{-2} s^{-1}.

From the X–ray data, also in this case, we can only infer a 2–10 keV flux of $\sim 5 \times 10^{-14}$ erg cm^{-2} s^{-1} by assuming a power law continuum (photon index frozen to 1.8) passing through Galactic absorption ($N_{\rm H(Gal)} = 9.28 \times 10^{20}$ cm^{-2}).

➢ Source #3 is located just outside the BAT error circle at:

R.A.(J2000) = $08^{\rm h}11^{\rm m}58'.80$

Dec.(J2000) = $-11^{\circ}44'23''.90$

error box = $6''.00$

It is detected at 2.7σ c.l. in the 0.3–10 keV energy range and is not revealed above 3 keV.

Multi–wavelength counterparts to this XRT detection:

- USNO–A2.0 0750–05895459 with magnitudes $B = 19.6$ and $R = 18.9$;
- AllWISE J081158.81–114426.3 with magnitudes $W1 = (14.734 \pm 0.031)$, $W2 = (13.768 \pm 0.035)$, $W3 = (10.813 \pm 0.114)$, $W4 = (8.000 \pm 0.239)$, and AGN colours ($W1 - W2 = 0.966$, $W2 - W3 = 2.955$);
- *Gaia* 5727719526399775744 with magnitudes $G = (19.526 \pm 0.007)$, $BP = (19.515 \pm 0.046)$, and $RP = (18.472 \pm 0.028)$
  ($BP - RP = 1.044$);

- GALEX J081158.8–114426 with magnitudes $FUV = (21.015 \pm 0.213)$ and $NUV = (20.722 \pm 0.177)$.

Also for this source the X–ray data allow us to estimate only a 2–10 keV flux of $\sim 1.2 \times 10^{-13}$ erg cm^{-2} s^{-1} by assuming a power law continuum (photon index frozen to 1.8) passing through Galactic absorption ($N_{\rm H(Gal)} = 9.12 \times 10^{20}$ cm^{-2}).

Both source #2 and #3 are likely background QSO, but we consider them as less likely associations than object #1 mainly due to the lack of radio detection.

PBC_NEW_330

Source position:

- R.A.(J2000) = $21^h35^m59'.69$
- Dec.(J2000) = $-16°17'20''.80$
- Positional uncertainty = $4'.5322$

Two XRT observations available:

1. obscode: 000966713001
   observation date: 30/03/2023
   exposure: 1618 s
2. obscode: 000966713002
   observation date: 01/04/2023
   exposure: 408 s

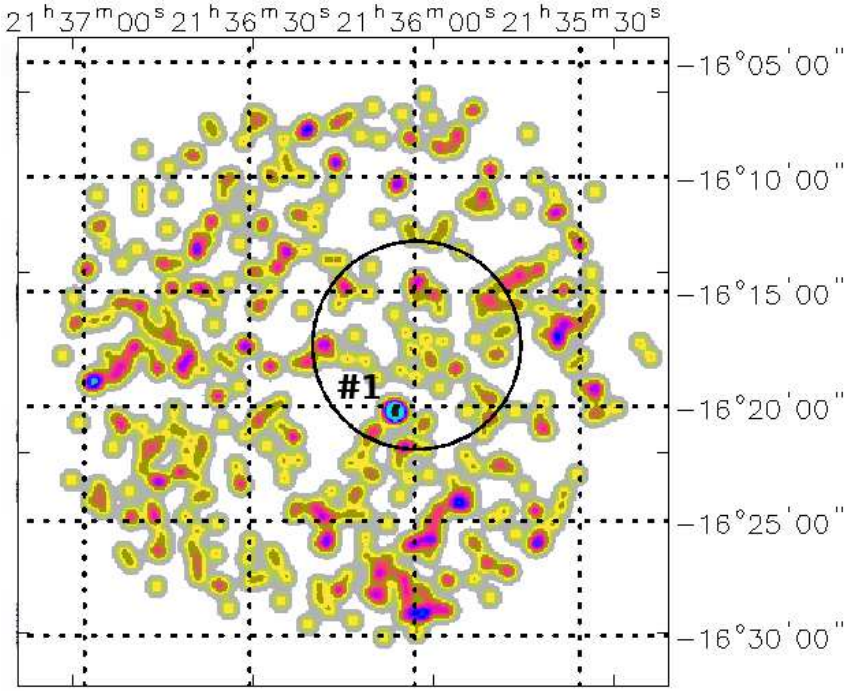

Figure 47: 0.3–10 keV XRT image of the PBC_NEW_330 field.

XRT detects only one X–ray source within the BAT positional uncertainty (see Figure 47):

R.A.(J2000) = $21^{\mathrm{h}}36^{\mathrm{m}}03'.40$

Dec.(J2000) = $-16°20'14''.50$

error box = $6''.00$

It is detected at 2.8σ c.l. in the 0.3–10 keV energy range; no detection is found above 3 keV.

Multi–wavelength counterparts to this XRT detection:

- USNO–A2.0 0675–36518201 with magnitudes $B = 18.5$ and $R = 18.9$;
- AllWISE J213603.27–162015.3 with magnitudes $W1 = (14.213 \pm 0.030)$, $W2 = (13.338 \pm 0.034)$, $W3 = (11.268 \pm 0.209)$, $W4 = (8.665 \pm 0.000)$, and typical colours of an active galaxy ($W1 - W2 = 0.875$, $W2 - W3 = 2.070$);
- *Gaia* 6841015319135385344 with magnitudes $G = (20.319 \pm 0.010)$, $BP = (20.316 \pm 0.106)$, and $RP = (19.436 \pm 0.075)$
  ($BP - RP = 0.880$).

From the XRT data we can only estimate, due to the low quality of the XRT data, a 2–10 keV flux of $\sim 1.7 \times 10^{-13}$ erg cm^{-2} s^{-1} by assuming a power law continuum (photon index frozen to 1.8) passing through Galactic absorption ($N_{\mathrm{H(Gal)}} = 4.82 \times 10^{20}$ cm^{-2}).

Although no radio emission is associated with this source, its *AllWISE* colours and its mentioning in various QSO catalogues, such as the "Catalogue of QSO candidates with *Gaia* EDR3" (Wu et al. 2023) and the "QSO candidates catalogue with APOP & *AllWISE* (QCC)" (Guo et al. 2018), make this object another AGN candidate; indeed, Fu et al. (2021) report a photometric redshift $z = 0.61$.

PBC_NEW_342

Source position:

- R.A.(J2000) = $07^h32^m56'.04$
- Dec.(J2000) = $+34°57'19''.00$
- Positional uncertainty = $4'.6479$

One XRT observation available:

1. obscode: 00096719001
   observation date: 14/03/2023
   exposure: 1951 s

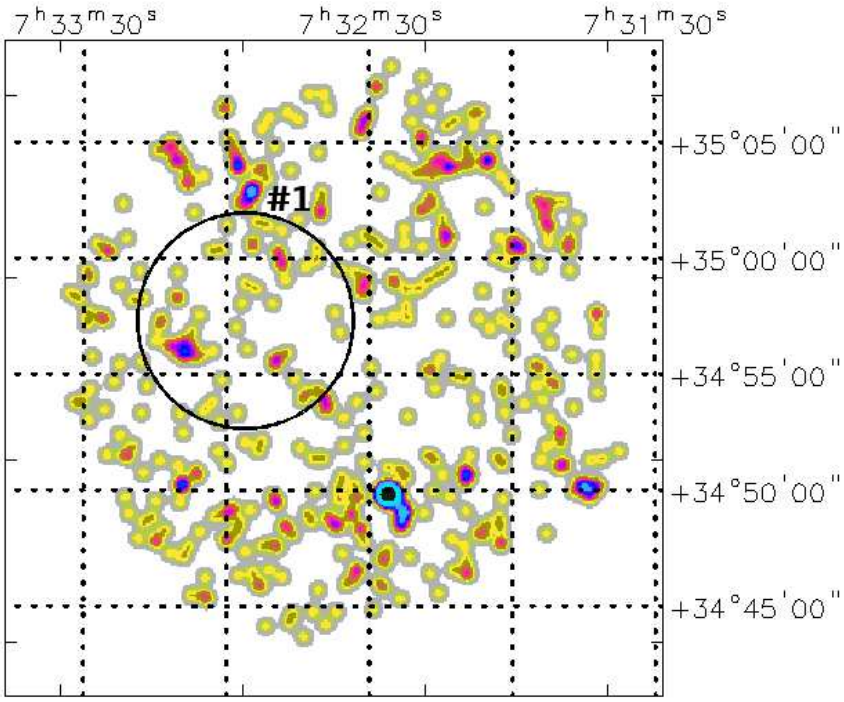

Figure 48: 0.3–10 keV XRT image of the PBC_NEW_342 field.

XRT detects one X–ray source just outside the BAT positional uncertainty (see Figure 48), which is located at:

R.A.(J2000) = $07^h32^m54'.70$

Dec.(J2000) = $+35^\circ 02' 54''.40$

error box = $6''.00$

It is detected at 2.3σ c.l. in the 0.3–10 keV energy range; no detection is found above 3 keV.

Multi–wavelength counterparts to this XRT detection:

- USNO–A2.0 1200–05692498 with magnitudes $B = 21.3$ and $R = 19.6$;
- USNO–A2.0 1200–05745486 with magnitudes $B = 19.7$ and $R = 17.5$;
- 2MASS J07325500+3502539 with magnitudes $J = (16.486 \pm 0.126)$, $H = (15.923 \pm 0.167)$, and $K = (15.425 \pm 0.195)$;
- 2MASS J07325423+3502554 with magnitudes $J = (16.336 \pm 0.109)$, $H = (15.369 \pm 0.112)$, and $K = (14.772 \pm 0.109)$;
- AllWISE J073254.22+350255.5 with magnitudes $W1 = (13.196 \pm 0.024)$, $W2 = (12.354 \pm 0.023)$, $W3 = (10.206 \pm 0.066)$, $W4 = (8.056 \pm 0.193)$, and colours of an active nucleus ($W1 - W2 = 0.842$, $W2 - W3 = 2.148$);
- *Gaia* 895372759910838528 with magnitudes $G = (19.256 \pm 0.004)$, $BP = (20.405 \pm 0.111)$, and $RP = (18.095 \pm 0.019)$
  ($BP - RP = 2.310$);
- *Gaia* 895372832926210944 with magnitudes $G = (19.078 \pm 0.014)$, $BP = (18.928 \pm 0.071)$, and $RP = (17.346 \pm 0.025)$
  ($BP - RP = 1.582$);
- ILTJ073254.25+350255.1 with flux Ftot(144 MHz) = 1.435 mJy.

The poor statistical quality of the data allows us to infer only a 2–10 keV flux of $\sim 1 \times 10^{-13}$ erg cm^{-2} s^{-1} by assuming a power law continuum (photon index frozen to 1.8) passing through Galactic absorption ($N_{\rm H(Gal)} = 5.36 \times 10^{20}$ cm^{-2}).

The source is clearly an AGN candidate, being a radio emitter and displaying *AllWISE* colours typical of an AGN. The photometric redshift is set in the range 0.13–0.23 (Duncan 2022; Fu et al. 2021, Saulder et al. 2023).

Bibliography

[1] Abdollahi S., Acero F., Baldini L., et al. 2022, ApJS, 260, 53

[2] Ahn C. P., Alexandroff R., Allende Prieto C., et al. 2012, ApJS, 203, 21

[3] Alam S., Albareti F. D., & Állende Prieto C. 2015, ApJS, 219, 12

[4] Assef R. J., Stern D., Noirot G., et al. 2018, ApJS, 234, 23

[5] Ballet J., Bruel P, Burnett T. H., & the *Fermi* Collaboration 2024, arXiv:2307.12546

[6] Barrows R. S., Comerford J. M., Stern D., & Assef R. J. 2021, ApJ, 922, 179

[7] Bianchi L., Herald J., Efremova B., et al. 2011, Ap&SS, 335, 161

[8] Boller T., Freyberg M. J., Trümper J, et al. 2016, A&A, 588, A103

[9] Cash W. 1979, ApJ, 228, 939

[10] Cavuoti S., Brescia M., D'Abrusco R., et al. 2012, MNRAS, 437, 968

[11] Chambers K. C., Magnier E. A., Metcalfe N., et al. 2016, arXiv:1612.05560

[12] Chenevez J., Brandt S., Kuulkers E., et al. 2011, ATel 3183

[13] Condon J. J., Cotton W. D., Greisen E. W., et al. 1998, AJ, 115, 1693

[14] Cutri R. M., Wright E. L., Conrow T., et al. 2013, `https://wise2.ipac.caltech.edu/docs/release/allwise/expsup/index.html`

[15] Dabhade, P., Mahato M., Bagchi J., et al. 2020, A&A, 642, A153

[16] D'Abrusco R., Álvarez Crespo N., Massaro F., et al. 2019, ApJS, 242, 4

[17] Dey A., Schlegel D. J., Lang D., et al. 2019, AJ, 157, 168

[18] Duchesne S. W., Ross K., Thomson A. J. M., et al. 2025, PASA, 42, e038

[19] Duchesne S. W., Grundy, J. A., Heald G. H., et al. 2024, PASA, 41, e003

[20] Duncan K. J. 2022, MNRAS, 512, 3662

[21] Edelson R. & Malkan M. 2012, ApJ, 751, 52

[22] Epchtein N., De Batz B., Copet E., et al. 1994, Astrophys Space Sci 217, 3 (1994)

[23] Farnes J. S., Gaensler B. M., & Carretti E. 2014, ApJS, 212, 15

[24] Flesch E. W. 2024, OJAp, 7, 6

[25] Fu Y., Wu X., Yang Q., et al. 2021, ApJS, 254,6

[26] Gaia Collaboration: Brown A. G. A., Vallenari A., Prusti T., et al. 2021, A&A, 649, A1

[27] Gavras P., Rimoldini L., Nienartowicz K., et al. 2023, A&A, 674, A22

[28] Gehrels N., Chincarini G., Giommi P., et al. 2004, ApJ, 611, 1005
[29] Gordon Y. A., Boyce M. M., O'Dea C. P., et al. 2021, ApJS, 255, 30
[30] Guo S., Qi Z., Liao S., et al. 2018, A&A, 618, A144
[31] Haynes M. P., Giovanelli R., Kent B. R., et al. 2018, ApJ, 861, 49
[32] Healey S. E., Romani R. W., Taylor G. B., et al. 2007, ApJS, 171, 61
[33] Helfand D. J., White R. L., & Becker R. H. 2015, ApJ, 801, 26
[34] Hill J. E., Burrows D. N., Nousek J. A., et al. 2004, Proc. SPIE, 5165, 217
[35] Hon W. J., Webster R. L., & Wolf C. 2025, MNRAS, 536, 3611
[36] Hughes A. C. N., Bailer–Jones C. A. L., & Jamal S. 2022, A&A, 668, A99
[37] Intema H. T., Jagannathan P., Mooley K. P., & Frail D. A., 2017, A&A, 598, A78
[38] Jones D. H., Read M. A., Saunders W., et al. 2009, MNRAS, 399, 683
[39] Kalberla P. M. W., Burton W. B., Hartmann D., et al. 2005, A&A, 440, 775
[40] Khamitov I. M., Bikmaev I. F., Gilfanov M. R., et al. 2023, Astron. Lett., 49, 271
[41] Lacy M., Baum S. A., Chandler C. J., et al. 2020, PASP, 132:035001
[42] Liao S., Qi Z., & Guo S. 2019, RAA 19, 29
[43] Lien A. Y., Krimm H., Markwardt C., et al. 2025, ApJ, 989, 161
[44] Mahony E. K., Croom S. M., Boyle B. J., et al. 2010, MNRAS, 401, 1151
[45] Malizia A., Bassani L., Landi R., et al., 2023, A&A, 671, A152
[46] McMahon R. G., Irwin M. J., & Maddox S. J. 2000, VizieR Online Data Catalog, p. I/267
[47] Merloni A., Lamer G., Liu T., et al. 2024, A&A, 682, A34
[48] Monet D. G., Levine S. E., Canzian B., et al. 2003, AJ, 125, 984
[49] Monet D. G. 1998, AAS, 30, 1427
[50] Ofek E. O., Frail D. A., & Breslauer B. 2011, ApJ, 740, 65
[51] Paliya V. S., Saikia D. J., Domínguez A., & Stalin C. S. 2024, ApJ, 976, 120
[52] Ross K., Hurley–Walker N., Galvin T. J., et al. 2024, PASA, 41, e054
[53] Saulder C., Howlett C., Douglass K. A., et al. 2023, MNRAS, 525, 1106
[54] Sazonov S., Burenin R., Filippova E., et al. 2024, A&A, 687, A183
[55] Saxton R. D., Read A. M., Esquej P., et al. 2008, A&A, 480, 611
[56] Schlafly E. F., Green G. M., Lang D., et al. 2018, ApJS, 234, 39
[57] Shimwell T. W., Hardcastle M. J., Tasse C., et al. 2022, A&A, 659, A1
[58] Skrutskie M. F., Cutri R. M., Stiening R., et al. 2006, AJ, 131, 1163
[59] Souchay J., Secrest, N., Sexton R., et al. 2024, A&A, 683, A112
[60] Stein Y., Vollmer B., Boch, T., et al. 2021, A&A, 655, A17
[61] Voges W., Aschenbach B., Boller Th., et al. 1999, A&A, 349, 389
[62] Wright E. L., Eisenhardt P. R. M., Mainzer A. K., et al. 2010, AJ, 140, 1868

[63] Wu Q., Liao S., Qi Z., et al. 2023, Res. Astron. Astrophys. 23 025006
[64] Zaw I., Chen Y., & Farrar G. R. 2019, ApJ, 872, 134
[65] Zou H., Zhang T., Zhou Z., et al. 2017, AJ, 153, 276